Technische Universität Dresden
Faculty of Forest, Geo and Hydro Sciences
Institute of Photogrammetry and Remote Sensing

Spectral Mixture Analysis for Monitoring and Mapping Desertification Processes in Semi-arid Areas in North Kordofan State, Sudan

The thesis is submitted for the degree of
Doctor of Natural Science (Dr.rer.nat.)

Manal Awad Khiry

Supervisors:

Prof. Dr. Elmar Csaplovics, Institute of Photogrammetry and Remote Sensing, TU Dresden, Germany
Prof .Dr. Jaochim Hill, Department of Remote Sensing, University of Trier, Germany
Prof .Dr. Marcus Nüsser, South Asia Institute, University of Heidelberg, Germany

Dresden, April 2007

Abstract

One of the most important recently issues facing Sudan as well as sub-Sahara Africa is the threat of continued land degradation and desertification, as result of climatic factors and human activities. Remote sensing and satellites imageries with temporal and synoptic view play a major role in developing a global and local operational capability for monitoring land degradation and desertification in dry lands as well as in Sudan. The process of desertification in central Sudan, especially in North Kordofan State has increased rapidly, and much effort has been devoted to define and study its causes and impacts. Taking advantages of the future hyperspectral imagery and developing methods such as spectral mixture analysis (SMA) are recently much recommended as most suitable methods for vegetation studies in arid and semi-arid areas. Therefore, this study is intending to improve the monitoring capability afforded by remote sensing to analyse and map the desertification processes in North Kordofan by using SMA technique. Three cloud free Landsat MSS, TM and ETM+ scenes covering the study area were selected for analysis. Imageries were acquired in January (dry season in the study area) in years 1976, 1988 and 2003, respectively. The three imageries for the study area were radiometrically and atmospherically calibrated and then converted from digital number (DN) into at-satellite reflectance. A linear mixture model (LMM) was adopted using endmembers derived from the image. Four endmembers, shade, green vegetation, salt and sand soils were selected. To identify the intrinsic dimensionality of the data the principle component analysis (PCA) was applied and the four endmembers were selected from the scatter plot of PC1, and PC2 of MSS, TM and ETM+ respectively. Fractions of endmembers and RMS error were computed. The study used the endmember fractions to conducted two methods for changes identification. Firstly, direct detection of change in fraction images between different years was analysed by use of visual interpretation in addition to statistical analysis. Secondly, change vector analysis (CVA) was applied to determine and analyse land cover change. To map and evaluate the soil erosion in the study area, eolain mapping index (EMI) was used to map the areas which are subjected to wind erosion hazard. Statistical measurements such as correlations coefficients, dynamics of change and analysis of variance (ANOVA) were also used. Mapping of the vulnerability of surface to wind erosion using EMI show the efficiency of multispectral data (MSS, TM and ETM+) for detecting the areas which affected with wind erosion in the study area. Interpretation of ancillary data and field observations verify the role of human impacts in the temporal change in both vegetation cover and sand soil. The findings of the study proved that SMA technique is powerful for characterisation and mapping of desertification processes in study area by providing direct measure of different land cover.

Application of multi-temporal remote sensing data on this study demonstrated that it is possible to detect and map desertification processes in the study area as well as in arid and semi-arid lands at relatively low cost. The study comes out with some valuable recommendations and comments which could contribute positively in reducing sand encroachments as well as land degradation and desertification processes in North Kordofan State.

Zusammenfassung

Fortschreitende Degradations- und Desertifikationsprozesse infolge klimatischer und anthropogener Einflüsse führen gegenwärtig zu den drängendsten Fragestellungen im Sudan und im sub-saharischen Afrika. Satellitengestützte Fernerkundung in synoptischer und temporaler Analyse spielen eine maßgebliche Rolle in der Entwicklung operationeller, global bis lokal einsetzbarer Werkzeuge für das Monitoring von Degradation und Desertifikation in Trockengebieten weltweit und im Sudan im speziellen. Das Vordringen der Wüste hat im westlichen Sudan insbesondere im Territorium der Provinz Nord-Kordofan stark zugenommen und großer Aufwand wurde darauf verwendet, Ursachen und Einflussfaktoren zu untersuchen. Zukünftig operationell verfügbare hyperspektrale Bilddaten und Methoden der spektralen Entmischung *spectral mixture analysis* (SMA) werden derzeit häufig als die am besten geeigneten Mittel für die Vegetationsanalyse in ariden und semi-ariden Gebieten empfohlen. Gegenstand der vorliegenden Studie ist es daher, die Leistungsfähigkeit fernerkundlichen Monitorings unter Anwendung des Verfahrens der spektralen Entmischung zu verbessern, um die Desertifikationsprozesse in Nord-Kordofan zu analysieren und zu kartieren. Drei wolkenfreie Satellitenbildszenen von Landsat MSS, TM und ETM+, die das Untersuchungsgebiet abdecken, wurden für die Analyse ausgewählt. Die Bilddaten wurden in der Trockenzeit im Januar 1976, 1988 sowie 2003 erfasst. Die drei Datensätze wurden radiometrisch und atmosphärisch korrigiert und daraufhin in Reflektanzwerte auf Satellitenebene umgerechnet. Mit Hilfe von aus den Bildern abgeleiteten spektralen Signaturen "reiner" Flächen (*endmember*) wurde ein *linear mixture model* (LMM) aufgestellt. Die vier Objektklassen Schatten, grüne Vegetation, Salz und Sandböden wurden als *endmember* ausgewählt. Mittels Hauptkomponententransformation (PCA) wurde die den Daten immanente Dimensionalität identifiziert und die vier *endmember* aus den Punktwolken der Komponenten PC1 und PC2 der MSS-, TM- und ETM+ -Daten bestimmt. *Endmember*-Anteile und RMS-Fehler wurden berechnet. In der vorliegenden Studie kommen die *endmember*-Anteile für zwei Methoden der Veränderungsanalyse zum Einsatz. Einerseits wurde die direkte Erfassung von Veränderungen in den *fraction images* zu verschiedenen Zeitpunkten mit Hilfe der visuellen Interpretation und zusätzlicher statistischer Analyse untersucht. Weiterhin wurde die Methode der *change vector analysis* (CVA) angewendet, um Veränderungen der Landbedeckung zu bestimmen und zu analysieren. Mit Hilfe des *Eolain Mapping Index* (EMI) wurden Gebiete kartiert, die einer besonderen Gefährdung durch Winderosion unterliegen. Statistische Messungen von Korrelation, Veränderungsdynamik sowie Varianz (*analysis of variance* - ANOVA) wurden ebenso einbezogen. Darüber hinaus

wurden Klimadaten und Felderhebungen kombiniert, um die Bearbeitung der Hauptzielsetzungen der vorliegenden Arbeit zu unterstützen. Die Anwendung des EMI zur Kartierung von Gefährdungsgebieten zufolge Winderosion zeigt, wie effizient multispektrale Daten (MSS, TM und ETM+) zur Kartierung dieser Flächen im Untersuchungsgebiet eingesetzt werden können. Die Interpretation ergänzender Daten und Geländebeobachtungen unterstreichen die Rolle menschlicher Einflüsse auf zeitabhängige Veränderungen von Vegetation und Sandböden. Die Ergebnisse der vorliegenden Studie beweisen, dass die spektrale Entmischung ein leistungsstarkes Verfahren zur Charakterisierung und Kartierung von Desertifikationsprozessen im Untersuchungsgebiet ist, da sie direkte Maßzahlen zur Bestimmung der Ausdehnung verschiedener Arten der Landbedeckung liefert. Die Anwendung multispektraler Fernerkundungsdaten hat gezeigt, dass es möglich ist, Desertifikationsprozesse im Untersuchungsgebiet im speziellen und in semi-ariden Gebieten im allgemeinen relativ preisgünstig zu erfassen und zu kartieren. Im Ergebnis dieser Studie können wertvolle Empfehlungen und Hinweise gegeben werden, welche einen positiven Beitrag zur Bekämpfung von Versandung, Degradation und Desertifikation im Nord-Kordofan leisten können.

TABLE OF CONTENTS

PART II: SPECRAL MIXTUER ANALYSIS AND DESERTIFICATION STUDIES IN ARID AND SEMI-ARID LANDS

CHAPTER 3: Theoretical background of Spectral Mixture Analysis (SMA)

CHAPTER 4: Views of desertification process in arid and semi-arid lands

PART III: RESEARCH APPROCHES AND MODELS ADOPTED FOR STUDY

CHAPTER 5: Research methodologies

PART IV : PRESENTATION AND DISCUSSION OF THE RESULTS

CHAPTER 6: Interpretation and analysis of fractions images

CHAPTER 7: Conclusions of findings and recommendations

LIST OF TABLES

LIST OF FIGURES

LIST OF ACRONYMS

ANOVA	Analysis Of Variance
AVIRIS	Airborne Visible /Infrared Imaging Spectrometer
CRC	Color Ratio Composite
CVA	Change Vector Analysis
DECARP	Sudan's Desert Encroachment Control and Rehabilitation Program
DN	Digital Number
EMI	Eolain Mapping Index
ENVI	The Environmental for Visualizing Images
ETM+	Enhanced Thematic Mapper
FAO	World Food and Agriculture Organization
FNC	Forest National Corporation
GIS	Geographic Information System
GPS	Global Position System
IFAD	The International Fund for Agriculture Development
IFOV	Instrumental Field Of View
LMM	Linear Mixture Model
LULC	Land Use/Land Cover
MESMA	Multi-Endmember Spectral Mixture Analysis
MODIS	Moderate Resolution Imaging Spectrometer
MSAVI	Modified Soil-Adjusted Vegetation Index
MSS	Multispectral Scanner
NDVI	Normalized Difference Vegetation Index
NIR	Near-Infrared
NOAA-AVHRP	National Oceanic and Atmospheric Administration-Advanced Very High Resolution Radiometer
NPV	Non-Photosynthetic Vegetation
PCA	Principle Component Analysis
R	Red band
RGB	Red Green Blue

RMS	Root Mean Square
SAVI	Soil-Adjusted Vegetation Index
SMA	Spectral Mixture Analysis
SRTM	Shuttle Radar Topography Mission
TM	Thematic Mapper
UN	United Nations
UNCCD	United Nations Convention on Desertification
UNEP	United Nations of Environmental Program
UTM	Universal Transverse Mercator
WEVI	Wind Erosion Vulnerability Image

Declaration

I, Manal Awad Khiry, hereby declare that the thesis entitled ***"Spectral Mixture Analysis for Monitoring and Mapping Desertification Processes in Semi-arid Areas in North Kordofan State, Sudan"*** is my own work. The major effort in this thesis is based on remote sensing data which I did during my field survey in Sudan beside the mentioned literature within the cited references in this work. It is my own responsibility to declare that it is not duplicated from any other pervious or presented work at any other institutions.

Manal Awad Khiry
Dresden, Germany
April 2007

Dedication

To my father Awad Khiry, from whom I have got to learn how life is
To my mother Sayeda Esmaeel, from whom I have got to know how love is
I dedicate this work with a great love and respect

Manal Awad Khiry

Acknowledgements

The positive contribution provided by many individuals and several institutions in the completion of this study is highly appreciated and accepted as well. With enormous indebtness to the Chair of Remote Sensing at the Institute of Photgrammetry and Remote Sensing, Dresden University of Technology, I am thankful to have such pleasant opportunity to do my PhD research.

First of all, let me express my endless gratitude to my supervisor, **Prof. Dr. Elmar Csaplovics**, who has patiently guided my thinking through the maze of the remote sensing science and its applications throughout my study program. He has friendly built up my competency and technical capability in remote sensing by granting me an unlimited access to his experience, precious time, valuable advices and moral support.

I am extremely grateful to the co-supervisor of this work, **Prof Dr. Jaochim Hill**, for his fruitful suggestion and valuable comments. I do appreciate his exerted efforts to facilitate this study. Particular thanks are due to the staff of Remote Sensing Department at the University of Trier, for their unlimited co-operation and support during the last stages of my study.

I would like also to thank the staff members of the following institutions in Sudan: Forests National Corporation (FNC); Ministry of Agriculture and Animal Wealth, North Kordofan State; Gum Arabic Research Center, University of Kordofan; Faculty of Forestry, University of Khartoum; and the Remote Sensing Center, University of Khartoum for their significant contribution to this work by availing me their resources during the field survey. I am gratefully indebted to “Wissenschaftliche Hilfskräfte der TU Dresden” for their generous financial support during the major efforts of this study. Special appreciation also for the “Gesellschaft der Freunde und Förderer der TU Dresden” for their valuable financial support during some periods of my work.

Thanks are extend to my Ph.D colleagues; Mohamed Salih Dafalla, Bedru Shrerfa, Mariam Akhter, Hassan Elnour for their spiritual encouragement and support. I am thankful to Dr. Tarig Elsheikh and Dr. Elrasheed Elkhadir at the University of Kordofan, for their support and advice during the analytical stage of this study. My sincere gratitude is also expanded to Dipl. Ing. Stefan Wagenknecht, Dipl. Ing Ralf Seiler and other colleagues at the Institute of Photogrammetry and Remote Sensing for their help and support whenever needed. Special

thanks to Mr. Abdel Sateer and his family at *Elbashiri* village for their hospitality and support during the field survey. Special note of thanks to *Haja* Fatima Makki (Dr. Tarig's mother) for her hospitality and courtesy during the field work. Exceptional grateful to Kathrin Babiker and our nice Sudanese community in Dresden for their spiritual support. Appreciations are also due to all colleagues, friends, many and many others who assisted me directly or indirectly through the course of my study. Finally, remarkable thankfulness is to my family, father, mother, sisters and lovely brothers for their unlimited spiritual and moral support.

Manal Awad Khiry
Dresden, Germany
April 2007

PART I

DESERTIFICATION PROCESSES AND STUDY AREA

CHAPTER 1: DESERTIFICATION IN ARID AND SEMI-ARID LANDS

1.1 Introduction

Arid and semi-arid lands cover approximately one third of the continental surface of the earth. They include the deserts and their semi-arid and sub-humid dry margins and the subtropical Mediterranean latitudes. Because of the vast area covered these lands play a major role in energy balance and hydrologic, carbon and nutrient cycles. The dryland areas are characterised by irregularity and shortage of rainfall, prolonged dry seasons, high temperature and high evaporation. Such variation in climatic factors makes drylands more fragile and prone to land degradation and desertification.

The terms degradation and desertification are sometimes used interchangeably even if the two terminologies are distinct. To appreciate their meaning it is necessary to give sound definition. Desertification, as previously defined, means land degradation in arid, semi-arid and dry sub-humid areas resulting from various factors including climatic variations and human activities (UNEP, 1993; Darkoh, 1995). Land degradation can be considered in terms of the loss of actual or potential productivity or utility as a result of natural or anthropogenic factors. It is the decline in land quality or reduction in its productivity. In the context of productivity, land degradation results from a mismatch between land quality and land use (Beinroth *et al*., 1994). Mechanisms that initiate land degradation include physical, chemical, and biological processes (Lal, 1994). These processes include water erosion, wind erosion and sedimentation, long-term reduction in diversity of natural vegetation and salinization. Thus, the two terminologies are the same as far as drylands are concerned. Combined pressure from human and climatic variations of these regions resulted in high and serious land degradation and desertification, especially in the tropics. In tropical arid and semi arid regions loss of plant cover seems to be related to poor soils and aridity, which prevail throughout short as well as long periods of drought and thus permit very limited recovery of natural vegetation.

According to UN (1991), 70 percent (3,600 million ha) of the drylands are already in some stage of degradation associated with enormous direct loss in income and indirect economic and social costs for the people affected. The vulnerable areas exist in Africa, Asia, America, Australia, and Mediterranean countries. These facts have led to the ratification of the UN Convention to Combat Desertification (UNCCD, 1994) by almost 180 nations worldwide. In particular, it emphasises the need to assess land degradation and desertification processes, since the knowledge on the current status of land degradation or the magnitude of the

potential hazard is incomplete and fragmented for the most parts of the world. Monitoring of the environment in these areas is considered as a very important task in the context of global climatic change and worldwide desertification dynamics. Ideally, remote sensing should play a major role in developing a global operational capability for monitoring land degradation and desertification in drylands. Remote sensing has long been suggested as a time and cost-efficient method for monitoring change in desert environments. In this capacity, it can serve both to enhance monitoring efforts as well as provide valuable information on dry land degradation in specific areas.

1.2 Desertification and arid lands in Sudan

Sudan is the largest country in Africa covering an area of over 2.5 million square kilometres. It is occupying 8% of the African continent, extending over 2000 kilometres from latitude of 3°35' N in the equatorial zone to latitude of 21°55' N in the Sahara desert (Figure 1.1).

Sudan is characterised by a wide range of rain fall zones from nil rain falls in the North to 1500 mm/ annum in the South, associated with different ecological regions, from the desert in the North to high rain-fall woodlands savannas in the South. Classification of the vegetation of Sudan, as firstly published by Harrison and Jackson (1958), is primarily intended to follow an ecological terms, based on the floristic composition of the vegetation. However, as the features of the vegetation in Sudan depend largely on rainfall and soil types, the divisions of the vegetation correspond to changes in rainfall and soil. The arid drylands (with an average annual rainfall less than 75 mm and the semi-arid drylands with annual rainfall from 75mm to 300mm) cover approximately 60% of the country (1.5 million square kilometres), thus constituting the largest area of drylands in Africa. The dry land is faced with serious environmental and socio-economic problems such as drought, deforestation, desertification, poverty, famine and migration.

Fig 1.1: Location of Sudan and North Kordofan State (Developed by the author 2006) www.unsudaing.org.

One of the most important problems facing Sudan as well as North Africa is the threat of continued drought and desertification resulting in destruction of natural resources, agricultural lands and in political and social disturbances. Desertification has been defined as the phenomenon of environmental degradation which converts land into desert-like conditions unfit for man and animals. The assumption that desert encroachment is a manifestation of major geological climatically changes is still subject to considerable scientific debate. Most scientists seem to agree that weather fluctuation or cyclic drought of one or more years and land misuses are the actual causes of desertification particularly in arid regions such as is the case in Sudan. This fact most probably led Sudan's soil conservation committee (1994) to conclude that soil degradation and desertification which has occurred is mainly attributed to general land misuses rather than to major climatic changes.

The region affected by drought and desertification in Sudan lies between the latitudes 12° N and 18° N and covers the country from the east to west. Severe desertification occurs along the Nile north of Khartoum stretching to the Egyptian border between latitudes 17° N to 20° N. Characteristics of this region are its instability, fragility and high resilience landscape prone to human and livestock disturbance. In Sudan the most destructive effects of human activities which are leading to natural resources degradation and causing desertification result from droughts, coupled mainly with the extended rainfed farming on marginal lands, overgrazing, wood cutting, deforestation, uprooting of shrubs and burning of grasslands and forest shrubs. It may ultimately be concluded that a combination of factors involving fragile ecosystems developed under harsh climatic condition and human activities which are increasing in irreversible magnitude are the actual causes of desertification in Sudan (DACARP, 1976). Recently, the problems of desertification and drought in Sudan are a worldwide concern and specific attention was paid to discussing and combating these impacts particularly in the central part of the country which is severely hit by desertification. The implication of severe drought conditions of 1984 resulted in serious ecological and socio-economic problems such as migration to urban areas, deterioration of forest cover, reduction of agricultural production, and famine and lack of adequate food supply.

1.3 Problem statement and rationale for study

The process of desertification in central Sudan, especially in North Kordofan, has increased rapidly and much effort has been devoted to define and study its causes and impacts. North Kordofan is a region which is characterised by a fragile ecosystem having considerable contribution to Gum Arabic production in the country. The greater part of the area is semi-arid with a small portion of rainfall ranges between 75-300 mm annually. The region endures intensive land-use pressures and is highly sensitive to climate fluctuations. Various practices in these regions, such as changes in fire regimes, removal of vegetation and over-grazing by cattle and sheep have been linked to many recognised causes of land degradation and desertification. Most of populations spread in rural areas either as settled or practicing a nomadic life. The increasing of human population and livestock, continued with the demands of enlarging areas of traditional farming lead to soil and vegetation deterioration. The trend of clearance of trees for growing annual cash crops coupled with the low and erratic rainfall are the main causes of desertification in the region. The impact of desertification and its causes in North Kordofan were described in several reports during the 1970s following the 1964-1974 Sahelian droughts. It is evident that the southern boundary of the desert has shifted south by an average of about 90-100 km in the last 17 years particularly in North Kordofan and also in the study area.

According to Baumer (1979) and Lampery (1975), the desert is continuing to move southwards at a rate of 5-6 km per year. The studies stated also that desertification is spreading in other areas including the adjacent low rainfall Savanna and that desert encroachment in these areas is mainly a man made phenomenon caused by the misuse of land.

Sand encroachment has moved rapidly ahead of the southern boundary of the desert and accumulating sand over the formerly consolidated sand soils. This has led to destruction of all vegetation except the trees of *Acacia tortilis* and *Balantites aegyptica* and a small number of dune adapted shrubs. The mobile dunes are moving southwards with the prevailing wind and are becoming an increasingly serious threat to agricultural lands and several villages in the *Elbashiri* and *Bara* areas of the *Kherian* region. Due to this, degradation was sustained round many watering points creating desert nuclei which soon converged to form desertified pockets. This situation left clear marks on the study area and led to reduction in surface water, migration of nomadic population to southern parts of the region and to low yield of crops. Currently, conditions have very much deteriorated. The effect is total destruction of the eco-

system which induces economic and social disturbance. It is argued that due to the economical, social and environmental value of this area, spatial and temporal analysis of desertification is recommended. Although, studies at local and regional scale have been made for monitoring this problem, still there is less quantitative spatial information about the dynamics of desertification processes. Because vegetation is often linked to both causes and consequences of land degradation in the study area, most of the studies tried to explain the observed change in Normalized Vegetation Index (NDVI) by using the capabilities of Landsat and NOAA earth observation satellite in semi-arid areas in Kordofan. A group of researchers from Lund University integrated investigations on desertification using advanced equipments for digital image analysis combined with conventional geographical methods and rainfall data and arrived at more convincing factors leading to spread aridity in North Kordofan (Hellden, 1978 and 1988; Olsson, 1985; and Ahlcrona, 1988). Yagoub *et al*. (1994) studied the assessment of biomass and soil potential in North Kordofan using NDVI indices. Their study concluded that the land degradation and ecological imbalance in this region are associated with the combined adverse effects of rainfall and mismanagement of lands.

Tobias (2004) tried to explain the environmental change in Kordofan by studying the NOAA-NDVI changes on local and regional scale in semi-arid areas. The study concluded that it is difficult to explain the observed trend in NOAA-NDVI between 1982 and 1999 on the local scale, based on the data that have been used. Elmqvist (2004) analysed land use change in northern Kordofan during the period of 1969-2002 by using recent and historical high resolution satellite data such as Corona and IKONOS. The study highlighted the state of land cover changes in the region of interest and it pointed out that the population increase was much higher than the increase in cropland areas during 1969-2002. As result of the above mentioned efforts in monitoring desertification in study area, they are mostly concentrated more on the vegetation parameters together with the relation with rainfall. However, vegetation indices are likely to underestimate live biomass in desert, are intensive to non-photosynthetic vegetation and sensitive to soil colour. Monitoring of land degradation in such areas needs more and high advanced techniques. Especially, the study area endures intensive land use pressures, and the vegetation cover is more heterogeneity and is highly sensitive to climate fluctuations. This spatial complexity and heterogeneous as well as limitation of spatial resolution of the data reduce reliability of traditional remote sensing approaches to produce accurate results of monitoring. Taking advantages of the future hyperspectral imagery and analysis methods such as spectral mixture analysis (SMA) is recently much recommended as most suitable method for vegetation studies in such areas. Therefore, this study is intending to

improve the monitoring capability afforded by remote sensing to analyse and understand the phenomenon of desertification in the study area by using SMA technique. Accordingly, this study tries to explore and assess the dynamics of desertification processes affecting the study area by using multiple analysis approaches. In order to monitor and map the desertification processes the following questions were addressed by this study:

Firstly, what are the main causes of desertification in the study area? and to what extent the desert encroachment is increasing? and in which directions?

Secondly, is SMA technique in combination with multispectral data (MSS, TM, and ETM+), providing an efficient tool for detecting and mapping desertification processes in the study area and if yes, what are the major outcomes as well as limitations in using such technique in monitoring and mapping land degradation processes in semi-arid areas?

In this way of thinking, the study tried to combine remote sensing data, climatic data and field data to enlighten the nature and consequences of desertification processes in the study area.

1.4 Objectives of study

1. Reviewing the role of human activities and other factors as main causes of desertification in the study area.
2. Assessing and evaluating the efficiency of spectral mixture analysis (SMA) as a tool for detecting and monitoring desertification processes in the study area.
3. Mapping land degradation in the study area by using SMA and Eolain Mapping Index (EMI).
4. Developing recommendations on the basis of the obtained results for monitoring desertification processes in the study area in particular as well as in arid regions in general.

1.5 Structure of study

The study comprises four parts including seven chapters. The first part as an introductory one is devoted to the problem statement and rationale for the study, objectives and introduction to the study area. Part 2 reviews the theoretical and empirical background of the spectral mixture analysis (SMA). It summarizes the challenges and opportunities of the application of this method in monitoring desertification in arid lands. Part 3 focuses on the methodological aspects of the study with special emphasis on the analysis, and interpretation, classification of images, together with the field observations. The presentation and discussion of results are presented in part 4, which summarize, conclude, recommends and highlights the main limitations of the study.

CHAPTER 2: INTRODUCTION TO STUDY AREA

2.1 Location

North Kordofan State is located in central Sudan. It is bordered by Northern State to the north, Khartoum to the northeast, White Nile State to the east, North Darfur to the northwest, West Kordofan to the west and Southwest and South Kordofan to the south. The total population of North Kordofan was estimated at 1,554,000 persons in 2003 (67.08% rural). North Kordofan is divided into five localities and 17 administrative units. The localities are: *Skeikan, Bara, UmRuwaba, Sodari* and *Gebret el Skeikh*. The study area covers the two provinces *Bara* and part of *Sodari* with an area of about 31107.122 square kilometres between latitudes 13º33' and 15º21' N and longitude 29º01' and 30º33' E. (Figure 2.1).

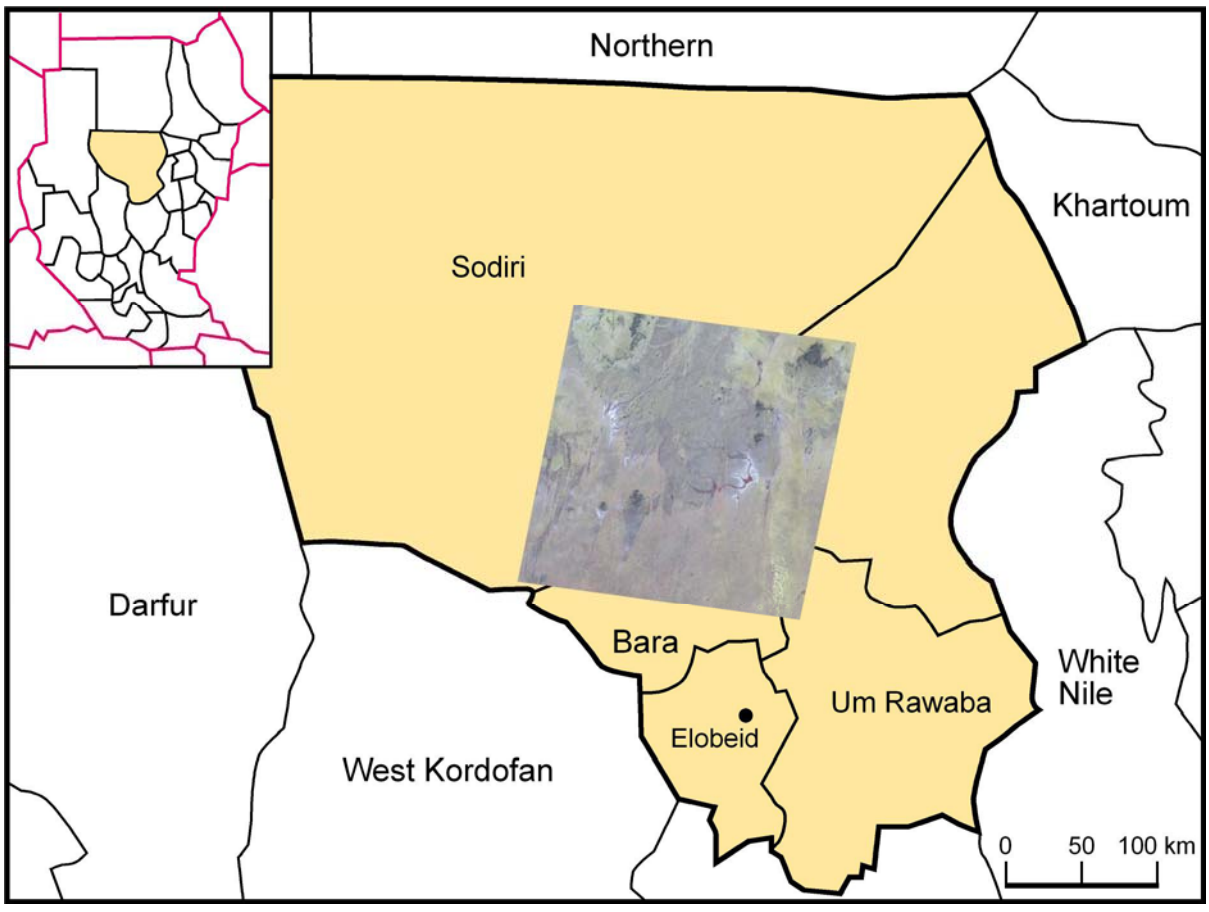

Fig 2.1: Location of study area (Developed by Kathrin Babiker 2006)

2.2 Topography and drainage

North Kordofan is generally characterised by gently undulating plains of low relief with an average altitude ranging from 350 to 500 m. This plain is mostly covered with sand dunes and its monotony is often protruded by isolated hills or clusters of hills in form of inselbergs e.g. *Jbel. Abu. Sinun* (820m) and *Jbel. Umm Shgerira* (846m). The study area lies mainly within a sand belt forming a narrow strip across with intrusion of clay soils in isolated spots heavier *vertisols* around seasonal water courses. Hills appear as chains extending along the north, west and south boundaries and in the centre of the study area. Stabilized and disturbed sand dunes are covering most of the northern and eastern part of the study area. The study area lies within the drainage system of the river Nile basin. Most of the water courses (*Wadis*[1]*)* in the study area are ephemeral streams which flow during a short period after the rainy season. Particularly, little or no runoff reaches the Nile as they end up in the desert before joining the river.

2.3 Climate

The study area lies within the dominantly prevailing arid and/or semi-arid –desert climate with limited and seasonal rains. The mean annual rainfall ranges from less than 100mm in the north to about 350mm in the south. Four seasons are recognised: the rainy season (locally called *kharif)* from May to October with peak rains in August, the harvest season (*Darat*) to early December with low humidity and night low temperatures, the cold season (*shita*) from December to mid-February with moderate temperature and comfortable humidity and the hot dry season (*seif)* with prevalent north –easterly winds to mid May. Rainfall precipitates in short high intensity storms of over six months from May through October, with concentration of 80 to 90% in July, August and September (Figure 2.2). Rainfall shows a great variability both in time and space (Hulme, 2001). The length of the rainy season depends to a large extent on the latitude (Olsson, 1985). The mean annual isotherm is 27° C with extreme temperatures ranging between 10°C to 46° C. Mean relative humidity ranges from 20% in winter to 75% during August, in the middle of the rainy season. The prevailing winds in the study area blow from north east during winter and from south west during summer. Wind action is more pronounced in the northern part than in southern part of the study area. Winds

[1] Water courses in the rainy season small and narrow

have medium speed generally with less than 3 meters/second, but are quite capable of moving sands from sand dunes when soils are exposed.

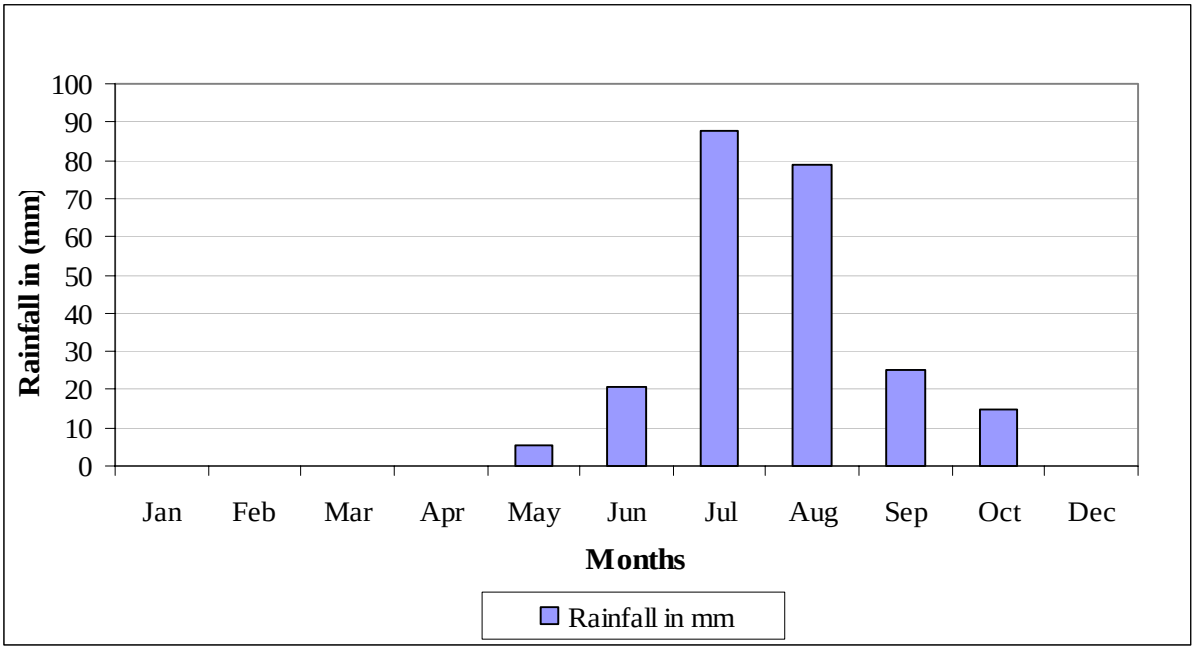

Fig 2.2: Mean monthly rainfall in the study area based on data from (1960-1990)
(Source: Meteorological Station *Elobeid,* 2003)

2.4 Soils

The soils of the study area are various, with sand dominating. Mobile whitish sand is found in forms of sheets and dunes (qoz[2]), while slightly lateritic brown sand is found in areas with sandstone. Basement clay depressions covered by clay soils are found between the dunes. There are also some rocky outcrops, mainly in the northern part. Although sandy soils are deficient in organic matter, nitrogen, phosphorus and other elements they sustain more cropping pressure. This is because the sandy soils are very easy to cultivate and it suits the production of many crops such as groundnuts, millet, sorghum and sesame. The problem with the sandy soils is that they lose their fertility in very short time and when stripped of their plant cover they became very easily eroded and desertified.

[2] Stabilised sand dunes

2.5 Vegetation

The study area is sparsely vegetated as a result of the low amount of rainfall. The vegetation is exposed to extreme conditions and must survive drought, which can stretch over several years with little or no rain at all (Schmidt and Karnieli, 2000). The study area falls in the semi-desert or sand ecological zone with a single rainy season. There is usually a short growth period followed by dry season with a great reduction in the amount of green plant materials. In the eastern part of the study area vegetation is sparse dominate by *Acacia tortilis, Maerua crassifolia* and *Leptadena pyrotechnica* (Figures 2.3 and 2.4). According to the Kordofan Resource Inventory, the study area is located within Zone 1 which encompasses the whole of *Bara* province and part of *Um Ruwaba* province. The sandy range land cover with scattered upper storey vegetation characterised by grasses such as *Cenchurs ciliaris, Chloris gayana, Eragrostis* spp., *Panicum turgidum, Cyprus mundtii, Dactyloctenium aegyptium* and *Aristida* spp. In the western part the vegetation is higher and denser. The common trees and shrubs are *Adansonia digitata, Acacia senegal, Acacia mellifera, Acacia tortili*s, *Calotropis procera,* and *Cadaba farinosa.* Trees and shrubs are disturbed alternatively with open grassland (Figures 2.5 and 2.6). From the field observations it is clear that vegetation cover in the western part is denser and the grass cover is dominated. This is due to firstly, shortage of the ground water in this part which leads to reduction and or limitation of grazing pressure. Secondly, the most and dominant practice of people in this part is tapping of Gum Arabic, which represents the main income in the study area. Accordingly, it is well observed that the pressure of human activities is lower and the vegetation is more or less constant.

Fig 2.3: Sparse vegetation between the sand dunes in the eastern part of study area
(Photograph by the author, *Elbashiri* village in northern part of *Bara,* July 2004, rainy season)

Fig 2.4: Vegetation cover in *Wadis* (clay pockets), vegetation is denser and dominated by *Acacia tortilis* (Photograph by the author, northern part of *Bara,* July 2004, rainy season)

Fig 2.5: Western part of the study area with denser vegetation, *Acacia senegal* is dominating and the ground is covered with grass (Photograph by the author, western part of *Bara*, Jan 2004, dry season)

Fig 2.6: Grasses areas in the western part of the study area, grasses are denser and the tree cover is lower (Gum Arabic area) (Photograph by the author, eastern part of *Elmazrub*, Jan 2004, dry season)

2.7 Water resources

The sources of water in north Kordofan can be itemised as rainfall, surface water and ground water. The study area suffers from an acute annual deficit in its water balance. Most of the rain water falls between July and September in form of heavy storms of short duration. The potential evapotranspiration exceeds the total precipitation by some 1400 mm/annum. The greater part of this deficit occurs during the dry season. Variability in time and space of the amount of annual precipitation in the northern Kordofan is quite remarkable. The recent drought which struck the Sahelian ecological zone has resulted in a general decrease of some 30% of the total amount of annual precipitation. The lower amount of rainfall has increased the risks of crop cultivation and has obliged local inhabitants to increase their areas under rainfed cultivation. This in turn, has led to the successive deterioration of natural vegetation and subsequently induced desertification. Because of the torrential nature of the rainfall in north Kordofan a good part of the rain water flow as surface runoff. Surface runoff either cuts its own courses forming *Khors*[3] and *Wadis*[4] or accumulates in natural depressions forming *Turda*[5] and *Fula*[6] or is gathered in artificial excavations forming *Hafirs*[7]. There are no perennial streams in the study area. Runoff from rains forms a number of seasonal streams scattered within the study area with irregular, short duration flows in rainy season for a few days. The dependency of human and livestock population of northern Kordofan on surface water resources was almost complete before the drilling of the first tube well in 1912 at *Um Ruwaba*. This dependency drastically diminished with the establishment of Rural Water and Development Corporation Programme drilling tube in most of the favourable areas in north Kordofan. Ground water is an important source of water in northern Kordofan. Most of the human and livestock population in the study area depend on ground water (Figure 2.7) for their living and only a few agricultural schemes use ground water resources for supplementary irrigation purposes. The main physical constrains limiting development of water resources in the study area are: low and erratic rainfall combined with high temperature and low humidity which implies high evaporation losses and high water requirements, short stream flow season comprising high sporadic, short duration floods, high rates of infiltration in sandy soils and evaporation. Despite many efforts to improve the rural water supply, the water shortages

[3] Water courses in the rainy season with larger depth than *Wadis*
[4] Water courses in the rainy season small and narrow
[5] Natural depression used to collect surface water to supply villages for long time
[6] Natural depression used to collect surface water to supply villages for short time (6months)
[7] Man mad depression for collecting surface water

remain a chronic problem in northern Kordofan State. Table (2.1) shows improved water sources in the north Kordofan as estimated by UN (2003).

Table 2.1: Population using improved water sources in North Kordofan State

Main sources	**Percentage**
Pipe into dwelling	23.9
Pipe in yard or plot	7.5
Public tap	18.2
Tube well/borehole with pump	19.0
Protected dug well	2.1
Protected spring	9.8
Rain water collection	19.5
Total	**100**

Source: (UN, 2003)

(a) (b)

Fig 2.7: Ground water resources for human and livestock in the study area (a) Protected dug well and (b) woody container made by local people for animal drinking (Photograph by the author, Jan 2004)

2.8 Patterns of land use

Most of the population in rural areas are either settlers or nomads. Their main occupations are livestock raising and traditional farming (Figure 2.8). Rainfall and its distribution are key determinants of practising agriculture. In the north part of the study area the tribes of *Kababish*, *Hawaweer* and *Kawahle* are dominant. They raise animals and grow crops in marginal land where rainfall is very erratic and the risk of agricultural failure is greatest. But in the south part of the study area the rainfed farming is carried out on *qoz* and clay soils, with preference for the high infiltration rates and ease of cultivation of the sandy soils. The main crops in *qoz* soil are millet and sesame, as well as sorghum and groundnut in the clay soils. Due to increase of livestock pressure and human population, coupled with climatic element of low and erratic rainfall, the study area has been facing the clearance of trees in favour of annual cash cropping. The land use practices have changed significantly according to rotation systems length from short periods of cultivation (4-5 years) to more or less continuous cultivation over the last three to four decades. Whenever the yields of crops become low, the farmer responds by enlarging the area. This is especially the case when the type of farming is tied to cash economy. This situation left clear marks in the southern part of the study area. Crop yields have decreased mainly due to a marked decline of rainfall, but to some extent also due to the abandonment of fallow periods (Olsson and Ardö, 2002). In addition to cultivating crops, people also tap indigenous *Acacia senegal* trees for Gum Arabic production. Gum tapping as an important source of income especially in the western part of the study area starts in October every year. The most common types of livestock in the area are sheep, goats, camels and cattle. These animals are not only raised for food but also for marketing purposes. Livestock in the study area act like insurance against possible crop failure. Before the drought of 1984, cattle were much more common in the area. Farmers used to adapt themselves against adverseable conditions by raising drought tolerant livestock, such as camels and goats. Ground water is only permanent source of water in northern Kordofan for human and livestock water supply and mini-irrigation projects. Ground water availability has always been a determinant factor in population distribution in the study area. This is very clear in the southern part of the study area, where population is more concentrate than in the northern part. Therefore, degradation was sustained round the many watering points creating desert nuclei which soon converged to form desertified pockets, such as one around the *Elbashiri* area.

(a) (b)

Fig 2.8: Land use in the study area (a) livestock raising in northern part of *Bara* and (b) rainfed agriculture in southern part of *Bara* (Photograph by the author, Jan 2004)

2.9 Drought periods in the study area

During the last three decades north Kordofan has experienced catastrophic and frequent drought periods with far-reaching consequences on agricultural and pastoral system, regional economy, traditional family livelihood and environment. The drought of 1984 was the most recent devastating one. Much has been written on these past droughts which distressed the Kordofan environment describing how the local population tried to cope with this situation. A severe drought is defined as covering two or more consecutive years in which rainfall is below the drought threshold. Severe droughts have occurred twice in the study area, especially in *Bara* province. It has been observed since the late 1960s (Figure 2.9).

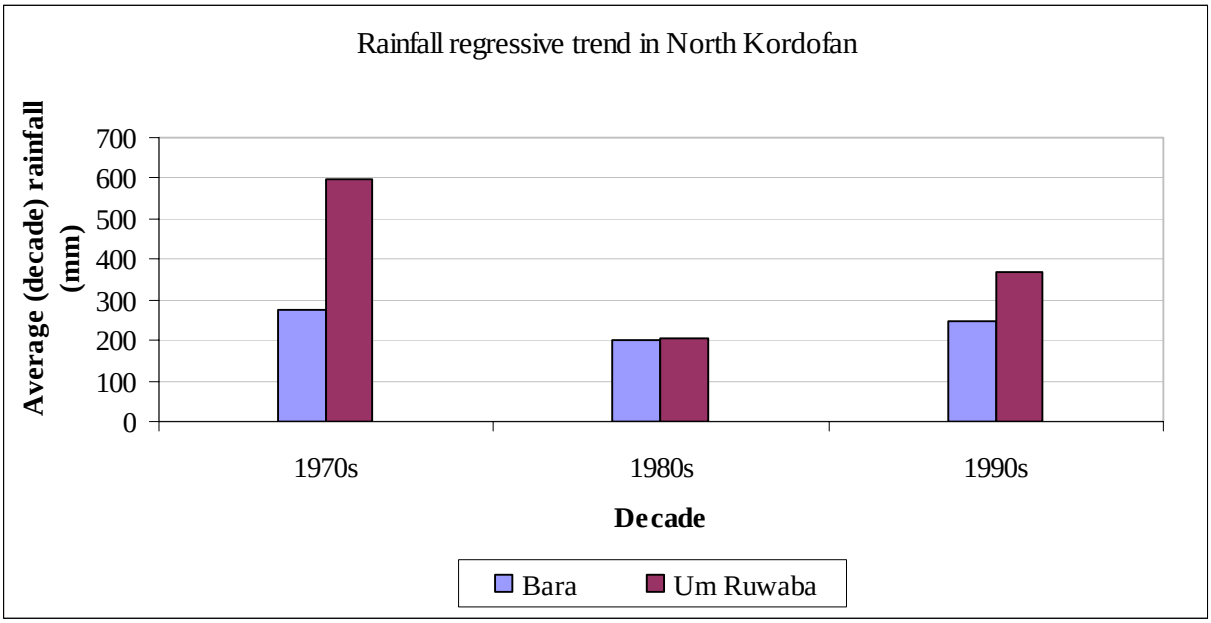

Fig 2.9: Drought periods in the study area (IFAD, 2004)

The droughts of the 1970s and 1980s triggered short cycles of famines in the study area and these effects most vulnerable area farmers in traditional rainfed sector in the study area. Severity of drought depends on the variability of rainfall both amount and frequency. Soil moisture in the study area is only supplied through rainfall. The capacity of the soil to absorb and retain moisture determines how much rain water will be available for cropping. Therefore, the high seasonality of rainfalls in this region with long dry seasons (6-8 months) results in drastic changes in land covers and thus contributes in desertification processes.

PART II

SPECRAL MIXTURE ANALYSIS AND DESERTIFICATION STUDIES IN ARID AND SEMI-ARID LANDS

CHAPTER 3: THEORETICAL BACKGROUND OF SPECTRAL MIXTURE ANALYSIS (SMA)

3.1 Overview

The importance of remote sensing in monitoring and mapping degradation and desertification in arid and semi-arid regions is widely recognised and well developed in a wide variety of fields. The developments in satellite technologies as well as remotely sensed image acquisition and analysis offer effective opportunities for monitoring land cover change in such areas. Remotely sensed imagery provides an attractive source of land cover data however, this source stores a lot of spatial detail. In this sense, spatial resolution is important in scaling the observations. Particularly, each pixel within an image provides only single measurement of spectral response for an area consisting of multiple surface components. How the spectral properties of these components combine and how the link between properties of the surface and multispectral remotely sensed data can be described must be clearly understood. Usually, mapping land use and land cover has been accomplished using traditional classification techniques, e.g. supervised and unsupervised classification. When properly applied, these methods have been successful with individual image data sets. However, because of different atmospheric, illumination and instrumental effects, it is difficult to obtain consistent classes within these approaches between images taken at different times. Sub-pixel classification in terms of SMA is based on and influenced by the spectral reflection properties of the observed materials. This section of the thesis introduces and discusses the problematic of the spectral behaviour of specific materials and of SMA for application to remotely sensed data, with some attention of using this technique in desertification studies in arid lands.

3.2 Spectral characteristics of features on the earth surface

Remote sensing involves the recording of reflected or emitted electromagnetic radiation at or from earth's surface by sensors on board an aircraft or a satellite. Electromagnetic energy can be transmitted, absorbed, scattered or reflected in the interaction process with the matter trains. Different features on the earth surface respond differently to incoming electromagnetic radiation. The type and condition of the feature determine the proportions of the energy reflected, absorbed and transmitted in particular wavelengths. Figure (3.1) shows typical reflectance curves for three basic types of earth features. These are healthy green vegetation, dry soil and clear water.

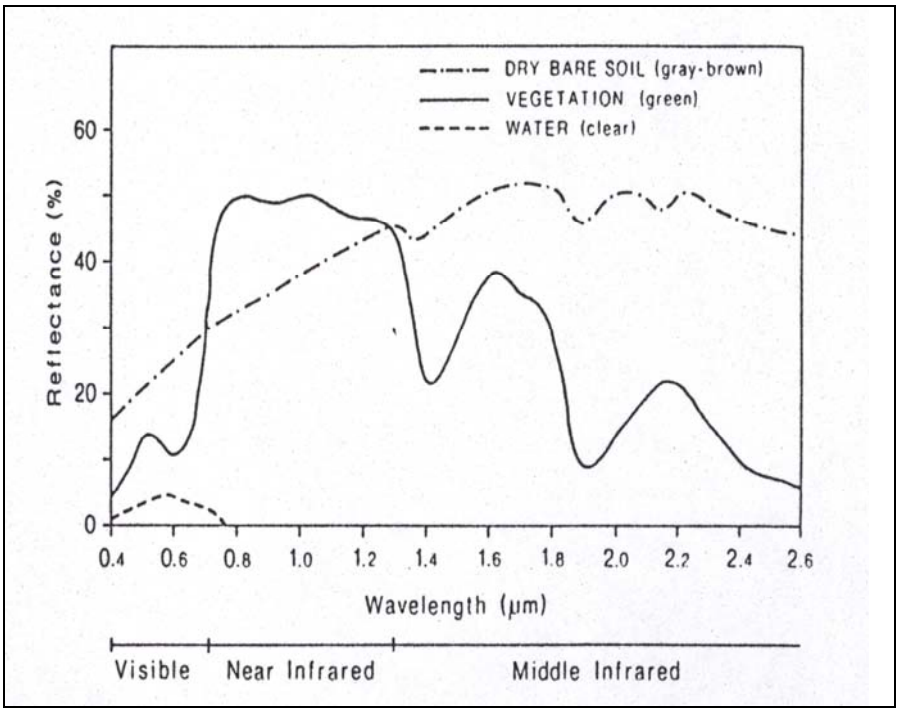

Fig 3.1: Spectral reflectance curve for vegetation, soil and water (Lillesand and Kiefer, 2000)

Generally, there is a relation between objects and their reflectance in different wavelengths or bands. This important property of objects makes it possible to identify different characters of surface substances and allows for separation by analysis of their spectral signatures. For example in the visible range healthy vegetation shows high absorption in blue and red bands and high reflectance in green and near-infrared bands. Meanwhile, soils illustrate less reflectance in the near-infrared band. Figure (3.1) demonstrates that the soil reflectivity increases approximately in a linear function with the wavelength. There are minimum dips centred at about 1.9 µm and 2.25 µm owing to absorption bands of water thus to moisture content. These water absorption bands are almost unnoticeable in very dry soils and sand. Reflection, absorption and transmission of vegetation canopy are dependent upon the leaves pigmentation, physiological structure and water content. Pigment of the plant absorbs the visible light in the red wavelengths. The most important pigment, chlorophyll absorbs highly at wavelength of 0.43-0.44 µm and 0.65-0.66 µm. The absorption of plant leaves in the red allows for photosynthesis and amounts 70% to 90% of the incoming radiation (Campbell, 1996). The reflectance of healthy vegetation varies with soil type, sun angle and sensing angle, vegetation cover and non-vegetation components.

The most common combination of spectral bands of remotely sensed imagery for estimating green vegetation cover is the vegetation index, which employs the red (R) and infrared (NIR) wavelengths, e.g. the Normalized Difference Vegetation Index (NDVI= NIR-R/NIR+R). Some studies of semi-arid vegetation canopies have successfully used these vegetation indices for land use classification, but also for biomass estimation (Kennedy, 1989). Meanwhile, other studies documented that the vegetation index and classification techniques which have been primarily used to map vegetation in sparsely vegetated areas, such as arid areas, have shown lower performance (Tucker and Miller, 1977; Elvidge and Lyon, 1985; Huete *et al*., 1985; Ustin *et al.,* 1986a; Tueller and Oleson, 1989). Arid and semi-arid regions consist of complex mosaics of vegetation cover, structure and phenology. Furthermore, arid regions endure intensive land use pressures and are highly sensitive to climate fluctuations. Vegetation cover in these areas is dominated by sparsely distributed shrubs and grasses. This sparse distribution of vegetation cover, together with the open canopies of shrubs, affects spectral reflectance. Soils in arid regions differ widely in their spectral response. This depends on soil colour, mineralogy, textures, presence of sand and rocks, surface roughness and various other factors. The variability of soil reflectance as well as of spectral interaction between the sparsely distributed plant canopies and soils in surfaces in such regions make the measurement of plant cover in arid and semi-arid regions more complicated. Furthermore, remote sensing of arid regions is difficult and needs innovative techniques (Pickup *et al*., 1993; Ray, 1995). The spatial complexity of arid regions restricts the use of traditional remote sensing approaches. This is mainly because the changes in geographical location often do not indicate structural or functional variations. Although studies at the global scale have documented changes in ecosystem in arid lands, there has been a shortage of global ecological information on dry lands. Accordingly, many other means of mapping and monitoring the changes in arid regions have been developed. One of the most promising is SMA.

3.3 Spectral Mixture Analysis (SMA)

Spectral Mixture Analysis (SMA) is a promising technique developed from the efforts of earth and planetary scientists (Adams *et al*., 1986; Smith *et al.*, 1990a; Ustin *et al.*, 1993). Land covers types (e.g. soil, vegetation and water in Figure 3.1) have shown characteristics patterns of reflectance within wavelengths across the electromagnetic spectrum. In reality, surfaces of land cover types are often composed of a variety of mixtures of materials and the distinction between them especially from space is not so clear. Mixed pixels have been

recognised as a problem affecting the effective use of remotely sensed data in Land Use and Land Cover (LULC) classification and change detection (Cracknell, 1998; Fisher, 1997). Fisher (1997) summarised four causes for mixed pixel problem as follows: boundaries between two or more map units, the intergraded between central concepts mapping units, linear sub-pixel and small sub-pixel objects. When a sensor observes a ground unit referring to a pixel which is composed of mixed types of surface, the reflectance spectra produced will not match any pure spectra (Figure 3.2). For example a pixel composed of both soil and vegetation will have a spectral response which depends on combination of the general soil and vegetation spectra. When mixed pixels occur, pure spectral responses confuse with the pure responses of other features, leading to the problem of composite signatures (Campbell, 2002). The aim of SMA is to identify primary spectral contributions within each pixel (Adams *et al.*, 1993). It provides a means for determining relative abundance of land cover materials present in any pixel based on the spectral characteristics of the materials (ENVI[1], 2002). The conceptual model used to develop SMA relies on the fact that most pixels in scenes are mixtures of a few specific ground cover units or endmembers, especially in arid areas and mixed land use environments. If pure spectra of spectrally distinct primary land cover materials (e.g., vegetation, water and soil) can be found in a scene, a data set can be converted to fractions of pre-defined land cover for each pixel (Huete, 1986; Smith *et al.*, 1990a and 1990b; Adams, 1993). SMA based on assumption that spectra of materials as covered by an instrumental IFOV[2] combine linearly with proportions given by their relative abundances. A combined spectrum thus can be decomposed into a linear mixture of its "spectral endmembers" that is the spectra of distinct materials within the IFOV (Figure 3.3).

[1] [1] ENVI refers to the software of Environmental for Visualization Image

[2] IFOV refers to Instrumental Field of View, means a measure of the spatial resolution of a remotely sensed image

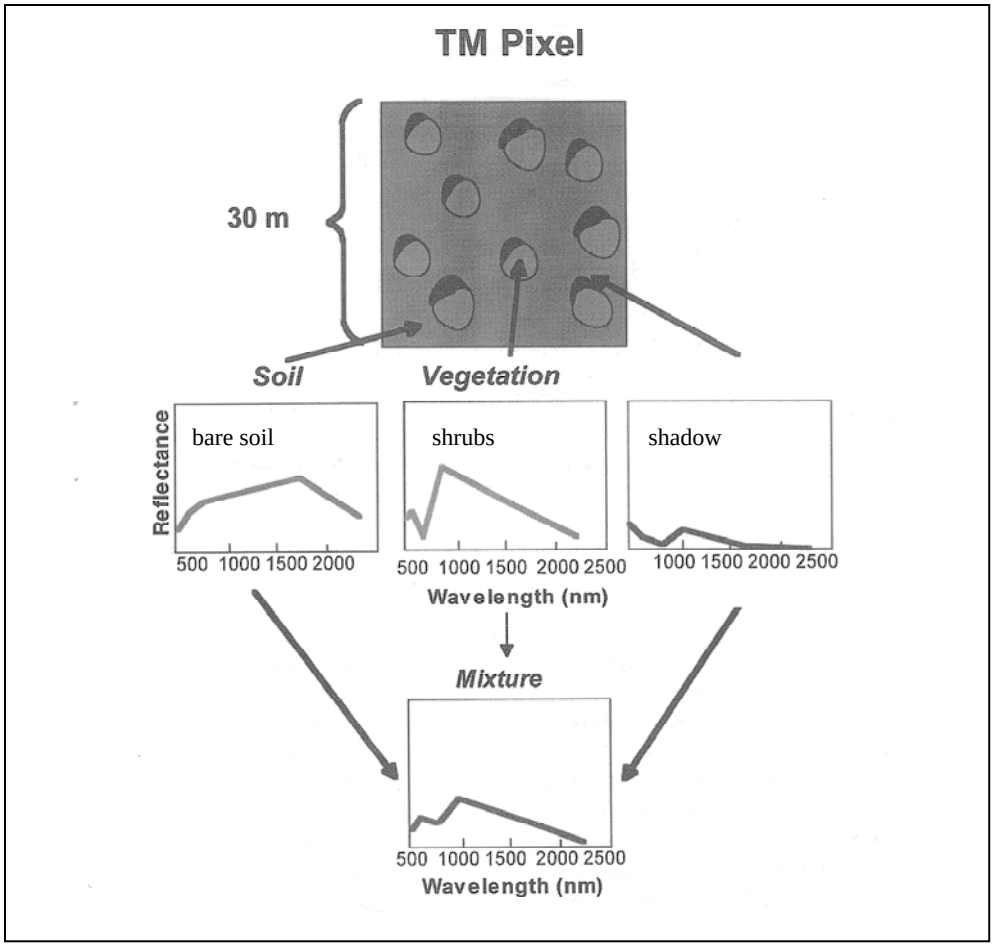

Fig 3.2: Mixed spectra in a 30*30 m of TM pixel consisting of shrubs, shadow and bare soil (Roberts *et al*., 1999)

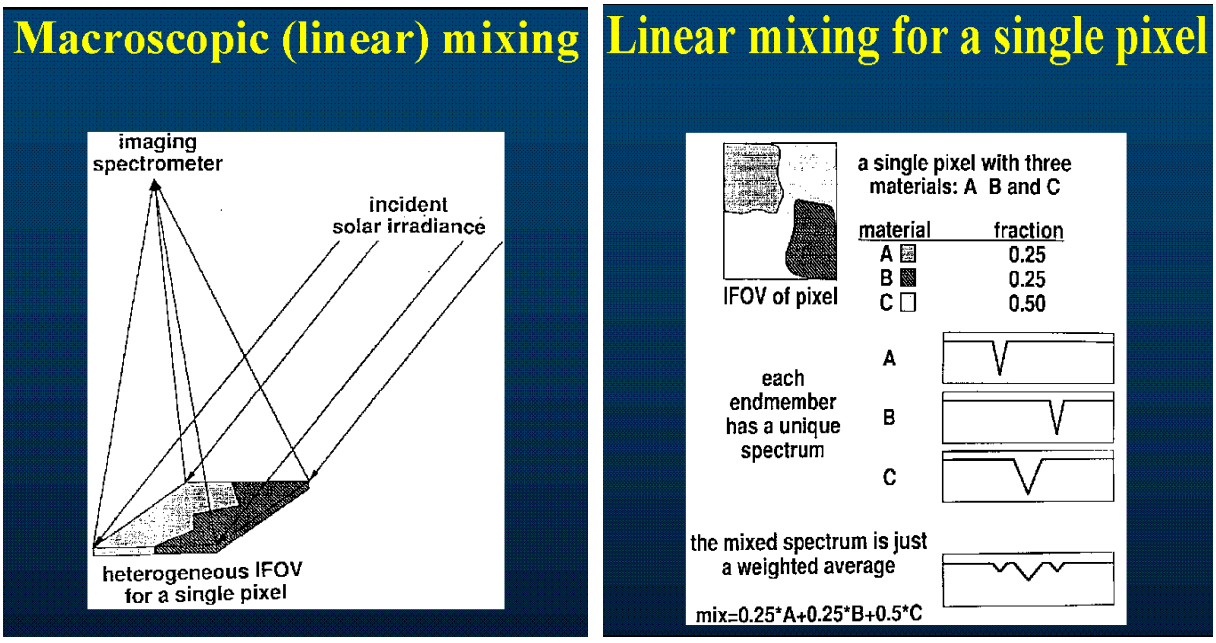

Fig 3.3: Linear spectral mixture of material for a single pixel in instrumental IFOV (ENVI, 2002)

SMA involves firstly, the definition of a set of pure spectra for selected land cover materials, which is often referred to as endmembers. Endmembers can be identified using either (a) libraries of known spectra collected with a spectrometer in the field or in the laboratory, (b) libraries of known spectra from previous SMA studies or (c) spectrally pure or "extreme" pixels identified within the images being analysed. Most applications of SMA will use the third option because libraries of field-collected endmember spectra are rare, field spectrometers are expensive and not readily available to researchers. The empirical portion of this study used this third option. Secondly, a linear mixture model has to be developed which assumes that areas of endmembers that is pre-defined primary land cover are arranged in spatially district areas in each pixel and can therefore be extracted through the application of specific algorithms (Eq, 1). Each pixel is modelled as a spatial mixture of endmember spectra to determine the physical abundance of land cover types in each area. Specifically, the following equations are solved for each pixel over each band in all data sets of the study:

$$DN = \sum Fi * DNi + Ei \quad (1)$$

$$\sum Fi = 1 \quad (2)$$

$$RMSE = \sqrt{\sum Ei^2} \quad (3)$$

DN is the brightness value of a given pixel for a specific wavelength or band. *Fi* is the fractional abundance of a particular endmember. *DNi* is the intensity of the image endmember at each particular wavelength or band. *Ei* is the error of the fit for each particular band. There is one equation for each band. Provided that the number of endmembers is less than the number of bands, this system of equations can be solved using a least square inversion (Eq, 2). The sum of these endmember fractions is considered to equal 1. Therefore, the fraction of cover for each endmember image should be between 0 and 1. The third equation is the total root mean square error for all bands used in the analysis (Elmore *et al*., 2000).

The SMA result can be expressed by the percentage coverage of each defined ground cover material or endmember in each pixel. This method has the advantage of deriving not only vegetation data, but land cover fraction for all the endmembers used as well. Additionally, the data is generated into a physically based measure and can therefore easily be integrated into studies as measures of percent active vegetation cover rather than indexed relative measures. Elmore *et al*. (2000) found percent live cover estimates using SMA to be accurate within 4.0% and change in percent live cover to have a precision of 3.8%. SMA has been extensively applied to characterisation of surface materials on the Moon and Mars (Adams *et al.*, 1986; Mustard and Head, 1996; Pinet *et al*., 2000; Bell *et al*., 2002). It has been also used in monitoring urban environments (Phinn *et al*., 2002; Small, 2002), measuring water turbidity (Kameyama *et al*., 2001), and mapping land degradation (Metternicht and Fermont, 1998; Haboudance *et a*l., 2002). SMA, as a tool for vegetation cover analysis receives much attention in last decades. Since SMA can be used to provide a full spectrum measurement of vegetation response, SMA fractions are more robust than traditional vegetation indices (Elmore *et al*., 2000; Peddle *et al*., 2001; Riano *et al*., 2002). Fractions model by SMA have been linked to biophysical vegetation components in boreal forest and Savannah ecosystems (Hall *et al*., 1995; Asner *et al*., 1998; Peddle *et al*., 1999; Peddle *et al*., 2001).Vegetation fractions produced by SMA have been used to describe fractional vegetation cover (Cross *et al.*, 1991), land cover change (Elmore *et al*., 2000; Roberts *et al*., 2002; Rogan *et al*., 2002), seasonal changes in vegetation (Roberts *et al*., 1997a; Garcia and Ustin, 2001) and regeneration after disturbance (Raino *et al*., 2002). Roberts *et al*. (1998) introduce multiple endmembers spectral mixture analysis (MESMA) is a technique for identifying materials in a hyperspectral image using endmembers from a spectral library. MESMA has been applied in variety of environments for vegetation and geological analysis. Roberts *et al*. (1997b; 1998; 2003) and Dennison *et al*. (2000) used MESMA to map vegetation species and land cover types in the Southern California chaparral. Painter *et al.*, (1998; 2003) mapped snow grain size in the Sierra Nevada of California using a MESMA approach. It has been also used to map the lunar surface composition (Li and Mustard 2003). While Okin *et al*. (2001) assessed vegetation cover in semi- arid environments in California.

Despite all the research efforts, there are limitations of the utility and accuracy in using SMA. In addition to being limited in the total number of possible endmembers, SMA also is limited by the type of endmembers which can be used, especially when using multispectral data (Adams *et al.*, 1993; Roberts *et al*., 1993). Endmembers must be spectrally distinct from one to another and generally account for the dominant land cover and spectral characteristics of

the scene. Generally research is limited to land cover classes such as vegetation, soil, sand, and shade when using multispectral satellite imagery. Additionally, SMA requires a good deal of processing capabilities and expertise in order to find pure spectra of appropriate endmembers in the scene. However, it is important to emphasise the advantage of additional datasets provide by the assessment of endmember surface cover which is generated using SMA. These data allow for extraction of more information from imagery than applying only vegetation index calculation. SMA has thus for several reasons reliable potential versus the traditional image analysis techniques in studies of environmental changes. Schweik *et al*. (1999) summarised these reasons in five points as follows:

Firstly, like multispectral classification and PCA, SMA uses all the information (bands) of multispectral image. Secondly, unlike traditional classification methods SMA is an independent image. As mentioned before SMA endmembers can be identified from image data, field data, or laboratory inventories or from endmember fraction libraries (Bateson and Curtiss, 1996). Therefore, time series or multiple geographic location SMA fraction coverage is more readily comparable than the products from classification based on DNs. Thirdly, endmember fraction coverage represents physical properties of landscape based on surface reflectance values. Fourthly, endmember fraction imagery is more appropriate for analysis of physical landscapes exhibiting a high degree of continuously varying land cover, such as most forested areas. Fifthly, and perhaps most important, is the fact that SMA provides the spectral data in terms of multiple endmember fraction coverage and not as a single pixel classification, hence allowing a more detailed analysis of pixel contents (Adams *et al*., 1993). It is thus clear that applying SMA and the producing of endmembers fraction images allow for more detailed analysis of individual spectral content of pixel. This is important for satellite imagery with relatively high spatial resolution such as Landsat TM, but becomes especially important when using coarse resolution sensor system such as Landsat MSS which is also used in this study.

3.4 SMA for monitoring arid and semi-arid regions

Arid and semi-arid regions are ones of the most active areas of environmental research (UNEP, 1992). A key characteristic of most arid ecosystems is that the relation between vegetation dynamics and environmental variations in climate, soils and human disturbances (Westoby *et al*., 1989). Like everywhere, many arid ecosystems plant community structure is tightly coupled with the spatial distribution of soil and water resources (Schlesinger *et al*., 1990; Ludwig and Tongway (1995). Another key characteristic of arid and semi-arid

ecosystems is that they often strongly affected by both fluctuations and directional changes in climate and disturbance regimes including grazing, fire and cultivation activity (Archer, 1994; Le Houerou, 1996; Weltzin *et al*., 1997). As a result, arid and semi-arid ecosystems are commonly viewed as highly susceptible to degradation. Remote sensing has been suggested for long time as a cost-efficient method for monitoring change in arid environments. In this capacity, there are many efforts in the development of different remotely sensed methods for monitoring and providing information on dry land degradation. There are several factors affecting accurate retrieval of vegetation parameters in arid regions using remote sensing. The most important one is the fact that vegetation cover in these areas is low and the contribution of vegetation to the area averaged reflectance of a pixel is small. Furthermore, because of their low organic matter content, soils in desert areas tend to be bright and mineralogically heterogeneous. All these factors have a tendency to hide out the spectral contributions of vegetation in individual pixels (Huete *et al*., 1985; Huete and Jackson, 1987; Smith *et al*., 1990; Escafaded and Huete, 1991; Huete and Tucker, 1991). The dominance of soil spectra in arid regions also requires more using of remotely sensed image analysis which allows these underlying soil spectra to vary across an image. For example, sparse distribution of vegetation cover in the study area has shown that soil spectra are dominant rather than vegetation covers (Figure 3.4).

Fig 3.4: Example of distribution of sparse vegetation covers of *Acacia tortilis* in arid and semi-arid region of North Kordofan, study area (Photograph by the author, northern part of *Bara*, Jan 2004)

The problem of mapping vegetation cover in such areas, as well as in most of arid regions, is that the plant canopies are typically small and do not reach the spatial scale of Landsat – related satellite image pixels. In addition the vegetation cover is compound by the fact that senescent material can be a major component of the total surface cover. Non-Photosynthetic Vegetation (NPV), whether in form of dead shrubs and leafless deciduous plants during dry season, or senescent annuals plays an important role in both the biotic and non biotic dynamics of land cover in this regions. Furthermore, the bright soils with open vegetation canopies in these areas increase the potential of non-linear mixing due to multiple scattering of light rays (Huete, 1988; Roberts *et al*., 1993; Ray and Murray, 1996).

Many common methods for estimating vegetation cover, such as most vegetation indices, are insensitive to the presence of NPV. Therefore, vegetation indices may not be used as a proxy for total vegetation cover in a situation when NPV is a significant component of surface cover, particularly in cases when NPV does not coincide in space or time with green vegetation. Numerous studies have shown that mixture modelling can be used to estimate vegetation cover (Smith, 1990; Reborts *et al*., 1993). Gracia-Haro *et al*., (1996) have shown that mixture modelling is less sensitive than NDVI to soil background effects. Furthermore, Adams (1995) proved that it is possible to map the proportions of both green and non-photosynthetic vegetation (NPV) using mixture modelling. SMA has been widely used in studies of vegetation cover in arid regions and appears to be the most promising method to determine information about soil surface type, vegetation cover and even vegetation canopy characteristics.

In contrast, the quantitative detection of sparse vegetation in remotely sensed imagery and hence in many arid and semi-arid areas world wide remains problematic. Nevertheless the unique capabilities of imaging spectrometers have proven useful for SMA in a variety of different land cover types. There are few investigators have examined the usefulness of hyperspectral data in quantitative detection of vegetation with low coverage (Chen *et al.*, 1998).

3.5 Multispectral and hyperspectral remote sensing in SMA

As discussed in previous paragraphs, multispectral and hyperspectral data have been widely used in studies of land degradation in arid and semiarid regions. Both data became more widely available and contribute to greater extent to the understanding of the dynamics of dry land and degradation processes. Compared to aerial imagery, spaceborne data offer a number of advantages which are necessary for a system that will be used for change detection, despite their still rather coarse resolutions (e.g. Landsat TM, 30*30m). These advantages are the regular repeat coverage data collection from the same geographic area at the same time of day, maintenance of the same scale and viewing angel, recording reflected radiant flux in consistent and useful spectral regions and lower costs compared to other methods (Jensen, 1986). At the same time, these data are facing the same challenges which tackle all remote sensing in dry lands. Multispectral sensors collect data in a few broad spectral bands which cover important regions of the reflective solar spectrum (about 350 μm to 2500μm). Because these sensors provide data in multiple bands, the ground resolution is degraded and total number of pixels per line for these sensors is less. Therefore, the spatial resolution for these multispectral sensors is usually poorer. Given sufficient spatial resolution and sensor performance, a hyperspectral sensor provides information using reflectance measurements over the 0.4-2.5μm region. Hyperspectral sensors also known as imaging spectrometers which provide data in a large number of narrow and contiguous bands that cover the entire reflected solar spectrum. These sensors typically provide data in very narrow bands (such as Earth Observer 1Hyperion instrument or the Airborne Visible /Infrared Imaging Spectrometer (AVIRIS) or with large pixel size such as the Moderate Resolution Imaging Spectrometer (MODIS) instrument. The precise spectral information contained in hyperspectral image enables better characterisation and identification of targets. Hyperspectral images have potential applications in agriculture (e.g. monitoring type, identify health, moisture status and maturity of crops) and coastal management (e.g. monitoring of concentrate phytoplankton's and pollution). Important considerations in using SMA with either multispectral or hyperspectral data refer firstly, to the spatial coverage desired and secondly to the ability to convert an image into meaningful units. In arid regions, Garcia *et al*. (1996) have applied SMA field spectrometer in detection of vegetation and concluded that SMA is less sensitive to soil background than NDVI. McGwire *et al*. (2000) have shown the use of SMA with multiple soil endmembers is significantly better suited for quantifying sparse vegetation cover in a desert than NDVI, the soil-adjusted vegetation index (SAVI) , or the modified –SAVI (MSAVI). As with multispectral data, SMA appears to be a more robust alternative to

vegetation indices when considering hyperspectral data. SMA is particularly amenable for use with hyperspectral data with the number of useful bands much higher than the number of model endmembers. The unique capabilities of imaging spectrometers have proven to be useful for SMA in detection of variety of different land cover types with significant plant cover. Roberts *et al*. (1993; 1997b; 1998) used linear mixture analysis of AVIRIS data to map green vegetation, non-photosynthetic vegetation and soils in the Jasper Ridge Biological Preserve in the Santa Monica Mountains. Okin *et al*. (2001b) showed that even using hyperspectral data under best case assumptions for noise and intra-species variability, discrimination of different vegetation types using SMA and other techniques was nearly impossible when cover was below 30%. They stated that soil surface type, on the other hand, can be reliably retrieved when applying multiple endmember SMA (MESMA).

3.6 Capabilities of SMA compared to other classification methods

Remotely sensed data is to produce a classification map of the identifiable or meaningful features or classes of land cover in a scene (Jasinski, 1996). As a result, the main product is a thematic map with topics such as geology or vegetation types. In this field remotely sensed image classification is a process in which pixels or the basic units of an image are assigned to classes. By comparing pixels to one another and to those with known identity, it is possible to assemble groups of similar pixels into classes which match the categorisation predefined by various users of groups. Numerous methods of image classification exist and classification has formed an important part of not only remote sensing, but also of the fields of image analysis and pattern recognition. In some instances, the classification itself may form the object of analysis and serve as the final product. In other instances, the classification may form only an intermediate step towards the analysis, such as land degradation studies, landscape modelling, costal zone management, resource management, and other environmental monitoring applications. Therefore, image classification represents one of the most important tools for analysing digital images. Accordingly, the selection of specific classification technique to be employed can have a substantial effect on the results, whether the classification is used as a final product or as one of several analytical procedures applied to derive information from an image for further analysis. The traditional method for inferring characteristics about vegetation cover from satellite data is to classify each pixel into a specific land cover class based on a predefined classification scheme. An alternative is to use the mixed pixel method or spectral mixture analysis (SMA). This method recognises that a

reflectance value of a single pixel is typically made up of a number of various spectral types such as soil, water and vegetation (Atkinson *et al.,* 1997). The results of land cover information can be used in conservation and biodiversity assessment, land resource management and extrapolation of results of more studies of human dimensions of global change (Townshend *et al*., 1994). In order to set the stability and capabilities of SMA for technique compare to other classification techniques, basic information concerning classification methods were defined in next paragraphs.

Image classification is defined as the process of creating thematic maps from satellite imagery (DeFries *et al*., 1999). The objective of image classification is to classify each pixel of an image into land cover categories. In the case of crisp or *hard classification*, each pixel is assigned to only one class. However, in fuzzy or *soft classification*, such as in SMA, a pixel is associated with many land cover classes. In general, classification techniques may be categorised by the training process into supervised or unsupervised classification. Supervised classification procedures tend to require considerable interaction with the analyst, who must guide the classification by identifying areas on the image which are known to belong to each category of interest. These areas are referred to as training sites. In general, supervised classification methods have many advantages relative to unsupervised classification. Firstly, the analyst has control of a selected menu of informational categories adapted to a specific purpose and to geographic region (Campbell, 1996). This control is essential if it is the specific task to compare one classification with another of the same scene at different dates, or if the classification must be compatible with those of adjacent regions. Secondly, supervised classification is associated with specific areas of known identity as a result of selecting training areas. Finally, serious classification errors are detectable by field verification to determine whether they have been correctly classified. On the other hand, supervised classification has numerous disadvantages. The analyst imposes a classification structure upon the data based on predefined classes instead of finding natural classes in an image. Furthermore, the defined classes may not match the classes which may exist in the data. In supervised classification, training sites and classes are based primarily on the information categories and only secondarily on spectral properties. Another source of error is the selection of training data, since these samples of pixels may not be representative of conditions encountered throughout the image. Moreover, supervised classification is not able to recognise the specific or unique categories which are not represented in training data due to the small areas they occupy on the image or simply because they are not known to the analyst. Unsupervised classification involves the process of automatically segmenting an

image into spectral classes based on the natural groupings found within the data set. The objective is to group multi-band spectral response patterns into clusters which are statically separable. In supervised classification, any individual pixel is compared to each discrete cluster to select the one which it is closest in terms of spectral values. The two most frequently used grouping algorithms are K-means and ISODATA cluster algorithms. These two statistical routines for grouping similar pixels together are iterative procedures. Advantages of unsupervised classification can be summarised into three key points. Firstly, no extensive prior knowledge of the region of interest is required. Compared to supervised classification, where detailed knowledge of the area is necessary required to select training sites. Secondly, the opportunity of human error is minimised. Finally, unique classes are recognised as distinct units in unsupervised classification.

Since unsupervised classification identifies spectrally homogenous classes within the data, such classes do not necessarily correspond to the informational categories which are of interest to the analyst. In summary, unsupervised classification tends to be involving a large extent of generalisation in that the spectral clusters only roughly match some of the actual classes. Unlike supervised and unsupervised image classification, SMA did not rely on the detection or identification of pixel clusters with similar reflectance spectra. Rather, it is possible to consider each pixel individually and assess the presence and proportion of selected endmembers. The fraction images produced by SMA refer to a pixel- by pixel measure of the percentage composition of each endmember in the spectral mixing model. The SMA technique is able to generate more accurate estimates of the endmember classes and appeared to be an effective means of mapping vegetation cover. Since supervised and unsupervised methods are based on predefined classification schemes classifying entire pixels, this causes an erro which often produces too high or low estimates of land cover classes due to the inability to distinguish sub-pixel covers. From these facts it is clear that the application of SMA and the production of endmembers fraction images for land cover classification allow for a more detailed analysis of individual pixels in the image. Thus, it can maintain higher accuracy in classification and provide more realistic representation of landscape, as opposed to the patchy and discrete nature of traditional classification techniques.

CHAPTER 4: VIEWS OF DESERTIFICATION PROCESSES IN ARID AND SEMI-ARID LANDS

4.1 Introduction

The interactions between people and environment at the beginning of the 21st century are more complicated, intensive and extensive than ever before (Babaev, 1999). Land degradation and desertification in dry lands have been suggested to be the most pressing of current environmental problems (Stocking, 1995). Nearly two decades ago the United Nations (1980) announced that desertification had affected some 35 million km^2 of land globally and that overall 35% of the earth's land surface was at risk of undergoing similar changes. Based on this fact, many assumptions have been made about the nature and character of desertification processes in the arid regions. With over one hundred published definitions, desertification has been interpreted as both environmental process and as a state of the environment. Many of the published definitions treat desertification as a collective term for environment degrading processes which are enhanced by both direct and indirect anthropogenic action. Some authors, such as Graetz (1991) mostly ignoring the relationship to climate and reviewed desertification as the extension of desert-like condition to areas where they should not occur climatically. Meanwhile, the view of desertification as an image of the "advancing desert" with the living environment is not an accurate presentation of the situation (Nicholson, 1994a). In another view other authors, such as Williams and Balling (1996) have presented desertification as the outcome of late 20th century population growth resulting in increased human pressure on marginal dry land environments. More recently, proposes and more encompassing definition of desertification is reviewed with special emphasis on the relationship between human activities and climate change in dry lands. Puigdefabregas (1995) and Warren (1996) define desertification as land degradation in arid, semi- arid and dry sub humid areas resulting from various factors, including climate variation and human activities. The vulnerability of land to desertification is mainly due to the climate, the relief, the state of soil and natural vegetation, and the ways in which these two resources are used. Scientists, politicians and even environmental journalists are strongly focussing on analysis and discussion all the national and local level efforts for monitoring and compacting desertification. Application of high and low spatial resolution satellite imageries, such as SPOT or Landsat imagery, combined with NOAA data and ground information using global position system (GPS) are used effectively in such context. These methods make it possible to observe, evaluate and monitoring both the biophysical as well as socioeconomic aspect of desertification.

4.1.1 Causes and consequences of desertification in arid lands

The complexity of causes of desertification and diversity of its effects make it difficult to evaluate its magnitude with any degree of accuracy. Estimates of the areas affected or threatened by desertification are matter of controversy. The different notions in terms of the time scale are also a matter of disagreement among scientists. Despite the modernisation of observation methods using satellite imagery and of data analysis using computers, there are still uncertainties at the global, regional and national level about the causes, extent and the seriousness of desertification. Reviewing the causes and consequences of desertification return back to the main fact that desertification is the outcome of the interaction between human land use activities and the dynamics of the environment. Based on this fact, there are a number of reasons and factors that can be identified as main causes of desertification, especially in the past 20 years. Recognising these factors provide a useful background to the consideration of the role of human dimensions in the desertification processes. The human dimension of desertification means that a definition of the problem must have relevance to human needs, especially in dry lands, where ecosystems are extremely vulnerable to over-exploitation and inappropriate land use. Finkel (1986) points out how the semi- arid Mediterranean uplands have been suffered long and severe human pressures. Dry lands usually respond quickly to climatic fluctuations, and people have learned to protect these resources with some strategies such as shifting agricultural and nomadic herding. However, in recent decades these strategies have become less practical, and nowadays economical and social pressure, ignorance, political instability and drought, can lead to over-cultivation, deforestation, over-grazing and bad irrigation practices, which all lead to desertification. Thus desertification is the result of climate variations associated with unsustainable land use (Yagub *et al.,* 1994).

The problem of desertification in arid and semi-arid areas has a long history through the past centuries. It has been an overlap of long-term changes in climate and human activities. Rising of population growth and increasing in consumption of the very limit resources leading to sever degradation of vegetation, soil and water resources, which compose the natural resources of human existence (Warren, 1996). Desertification has consequences at the global level, primarily because of the influence on carbon exchange. The amount of carbon stored in vegetation in dry zones, averaging about 30 tones per hectare, decreases when the vegetation is depleted or disappears. Another consequence of desertification at both regional and global levels is the reduction in biodiversity, as it contributes to destruction of habitats of animal and

vegetal species and micro-organisms. Lastly desertification directly reduces the world's fresh water reserves. It has a direct impact on river flow and level of ground water tables.

4.1.2 Desertification and climate

All definitions of desertification traced back climate variation to direct causal factors and implicitly link climate changes to the extent of desertification. Since arid and semi- arid areas are extremely fragile and very response to climate fluctuations, determining the precise contribution of climate variations to desertification is not an easy matter. Climate changes are both a consequence and cause of desertification. The reduction of the natural grass and woody vegetation cover in dry areas affects the topsoil temperature and the air humidity and consequently influences the movements of atmospheric masses and rainfall. Furthermore, the drying of the soils and the reduction of soil cover encourage wind erosion. Through cycles of drought years and climate changes can contribute to the advance of desertification. Droughts occur frequently in the areas affected by desertification and are generally a feature of their natural climate. The relations between desertification and drought on the one hand, and human influence on the other, are complex. Human influence can also hasten desertification and aggravate the negative consequences on climate. But the degradation of land due to desertification has serious compounding effect on drought and thereby reduces the chances of local people to cope with difficult periods. Although desertification is usually associated with drought, it is quite common for land degradation to occur without change in rainfall. The Sahel region seems to have undergone decline of rainfall since the late 1960s. Between 1961 and 1998, episodes of drought have inflicted Sudan with varying severity. This period witnessed two droughts during 1967-1973 and 1980-1984. The later being the more sever. The drought of 1980-1984 highlighted the basic problems which have been long ignored. By the 1980s, researchers have challenged the emphasis on human impact and produced several Sahelian studies which utilise precipitation and agricultural statistics in the combination with remote sensing information. Olsson (1985) and Ahlcrona (1988) conclude that climate was the driving force behind the degradation. Meanwhile, climate change exacerbates desertification through the alternation of spatial and temporal pattern in temperature, rainfall, solar isolation, and winds. Conversely, desertification aggravates climate change through the release of CO_2 from cleared and dead vegetation and through the reduction of carbon sequestration potential of desertified land.

4.1.3 Desertification and human interactions

Discussion of human impact in desertification processes in arid and semi-arid lands has been for long time major issue of many of scientific arguments. The resilience of dry lands is usually low and this why dry lands are particularly susceptible to degradation (Blum, 1998). Like the neo-Malthusian theorem, population increase and associated human activities in regions with arid, semi-arid or dry sub-humid climate put pressure on natural ecosystems. This exploitation of natural resources, including the natural vegetation resources and land and water resources, causes serious soil erosion that has led to desertification of these regions. Cultivation, grazing and wood gathering practices have been cited in the definitions as major causes and contributors to the desertification processes in arid, semi-arid and sub-humid areas. Traditional rainfed cropping systems have been breaking down not only in Sudan, but in most of Sahel countries. Over-cultivation of marginal lands for cash crops and the consequent crowding of increasing number of livestock on to smaller areas of pasture has caused both crop and livestock productivity to fall and soil erosion to increase. Rainfed farmers in arid and semi-arid areas such as in the study area, usually keep some animals grazing on follow and on communal village grazing lands. The relatively limit areas of such pasture means a considerable amount of degradation.

According to the IIED/IES report (1990), the main factors contributing to degradation of natural resources in Sudan are as follows:

1. Misused of natural resources could be considered as most important cause of degradation. Major forms of resources mismanagement in the Savannah belt of Sudan have been experienced.
2. Expansion in cultivated acreage and conversion of forests and woodlands, especially beyond the agronomic boundary, into cereal cultivation.
3. Misuse of the rangelands by pastoral nomadic systems, resulting from improper management increase in livestock population and unbalanced distributions of animals.
4. Over-cutting of trees for fuel wood and other purpose, leading to an irreversible devastation of the tree cover in many areas.

Theses human activities are often cited as major causes of land degradation and desertification processes in Sudan as well as arid region in general.

PART III

RESEARCH APPROACHES AND MODELS ADOPTED FOR THE STUDY

CHAPTER 5: Research methodologies

5.1 Overview

The processing in this research work composes of multiple analyses and an integrated model approach. In order to achieve the objectives of the study, spectral mixture analysis (SMA) together with the eolain mapping index (EMI) were used. Figure (5.1) shows the main processes in gathering and analysing the remotely sensed data as well as field observations and climatic data. Data in form of satellite imagery of the study area were analyzed qualitatively by visual interpretation and qualitatively using Spectral Mixture Analysis and other indices. In order to identify changes in different land cover in the study area change detection was adopted using change vector analysis (CVA) method. Furthermore, some statistical analyses such as correlations, dynamics of change and on way analysis of variance (ANOVA) were also used. The combination of both statistical analyses and spectral change detection techniques was applied.

5.2 Data acquisition and preprocessing

Three cloud free Landsat MSS, TM and ETM+ scenes covering the study area were selected for analysis. These images data were acquired in January, the dry season in the study area in 1976, 1988 and 2003, respectively. MSS image consists of four bands. The characteristics of this image compared to the others are low in terms of spatial ground resolution and band widths (Figures 5.2a, 5.2b, 5.2c and Table 5.1). Multispectral sensors collect data in a few spectral bands which cover important regions of the reflected solar spectrum (about 350 to 2500μm). Because these sensors provide data in multiple bands, the ground resolution is degraded and total number of pixels per line for these sensors is less than that of panchromatic sensors. This is due to both the decreased light energy available in each band as well as bandwidths. Therefore, the spectral resolution for spaceborne multispectral sensors is usually poorer than for panchromatic sensors. Multispectral sensors have been used effectively in studies of land degradation in arid and semi-arid lands.

Table 5.1: The main characteristics of the imagery used in the study

Instrument	**MSS**	**TM**	**ETM+**
Landsat	Landsat 2	Landsat 4	Landsat 7
Acquisition date	14 Jan 1976	20 Jan 1988	13 Jan 2003
Path / row no	188/50	175/50	175/50
Spectral bands((μm)	4 bands 1. 0.5-0.6 (green) 2. 0.6-0.7 (red) 3. 0.7-0-0.8 (near-infrared) 4. 0.8-1.1 (near-infrared)	7 bands 1. 0.45-0.52 (blue) 2. 0.52.0.60 (green) 3. 0.63-0.69 (red) 4. 0.76-0.90 (near-infrared) 5. 1.55-1.75 (mid-infrared) 6.10-4-12.5 (thermal) 7. 2.08- 2.35 (mid-infrared) 2.0	9 bands same as TM , except : - Optical bands - Thermal - Panchromatic
Ground resolution	79m*79m	30m*30m	30m*30m
Dynamic range (bit)	7 bit	8 bit	8 bit

TM and ETM+ imagery was acquired in seven and nine bands respectively, they covering the visible, near and middle infrared region of the electromagnetic spectrum. The utility of Landsat imagery for studying environmental changes in arid region has long been suggested as a time and cost-efficient method. There are several justifications for the use of MSS and TM imagery in studies concerning human dimensions of environmental change, and many of these reasons are directly associated with scale issues discussed as follows:

Firstly, both the MSS and TM data cover abroad spatial extent. Each individual scene of Landsat sensors covers an IFOV on area of approximately 185*185 kilometres. Furthermore, since the launch of Landsat 1 in 1972, the terrestrial surface of the earth between 81° N and 81° S latitudes has been subject to image acquisition (Campbell, 1996). Secondly, the data archive covers a relatively long temporal sequence of more than 25 years[1]. For example, MSS technology began in 1972 and after 10 years later TM started. Although this cumulative period may be short in terms of the history of humanity, the time period covers a temporal range to capture a variety of the man-induced changes in arid lands. Thirdly, the MSS and Landsat instruments provide a reasonably high degree of spectral resolution when compared

[1] The data used in the study cover 30 years (1976, 1988 and 2003)

to other remotely sensed data platforms such as aerial photographs, SPOT , or IRS satellites data hence they have better spatial resolution. MSS provides bands, each sensitive to different portions of the electromagnetic spectrum. As table 5.1 shows MSS band1 collects EM radiation at visible green wavelengths (0.5μm-0.6μm) band2 responds to light at visible red portion of the spectrum (0.6μm-0.7μm), and both band 3 and band4 different portions of near-infrared wavelengths (0.7μm-0.8μm and 0.8μm-1.1μm, respectively).TM data provide better spectral resolution employing seven bands with sensors collecting additional data from the mid-infrared and thermal regions of the electromagnetic spectrum. Although other technologies such as National and Oceanic and Atmospheric Administration (NOAA), Advanced Very High-Resolution Radiometer (AVHRR) or hyper-spectral instruments such as the Air-borne Visible/Infrared Imaging Spectrometer (AVIRIS) provide even better resolution than Landsat data do (Campbell, 1996; Verbyla, 1995), the MSS instrument nevertheless provides adequate data in terms of multitemporal radiometric data for analysis and studies of land use history in arid regions. Fourthly, the temporal samplings of the Landsat MSS and TM systems are relatively high. Location coverage repetition frequency was 18 days for Landsat 1, 2 and 3 and 16 days for Landsat 4 and 5. These revisits provide probably adequate data for addressing many important human–induced processes. As the previous discussion indicates, there are ample reasons to consider the use of Landsat MSS and TM for studies relating human decision making and action to land cover change. In this study using of Landsat MSS 1976 adds a significant extension of the temporal coverage of the image data used. For many aspects of change analysis, this adds trial time frame may be more vital. However, the relative poor spatial resolution provided by MSS data is one significant limitation in this study.

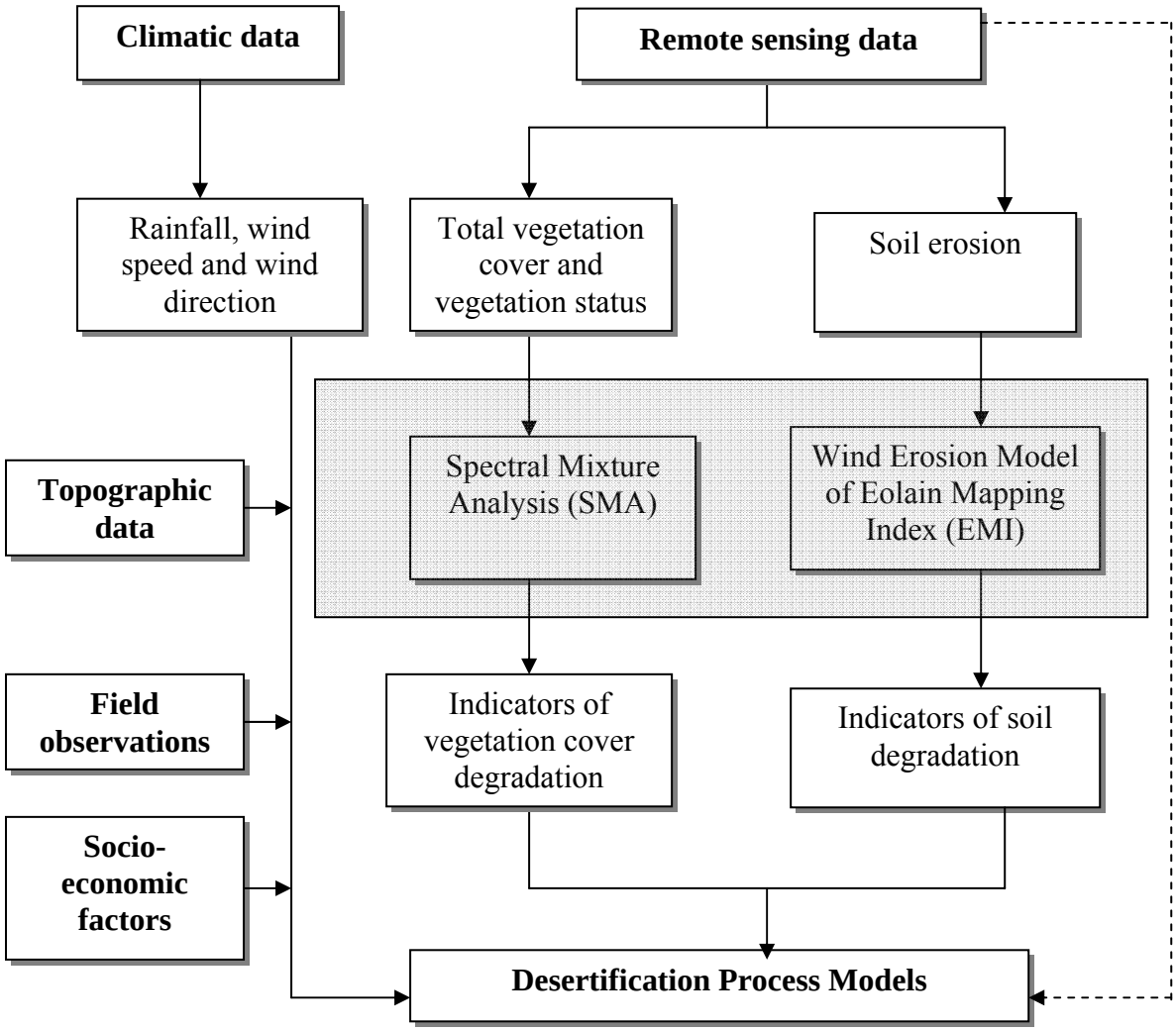

Fig 5.1: Conceptual framework of the methodology (Developed by the author 2006)

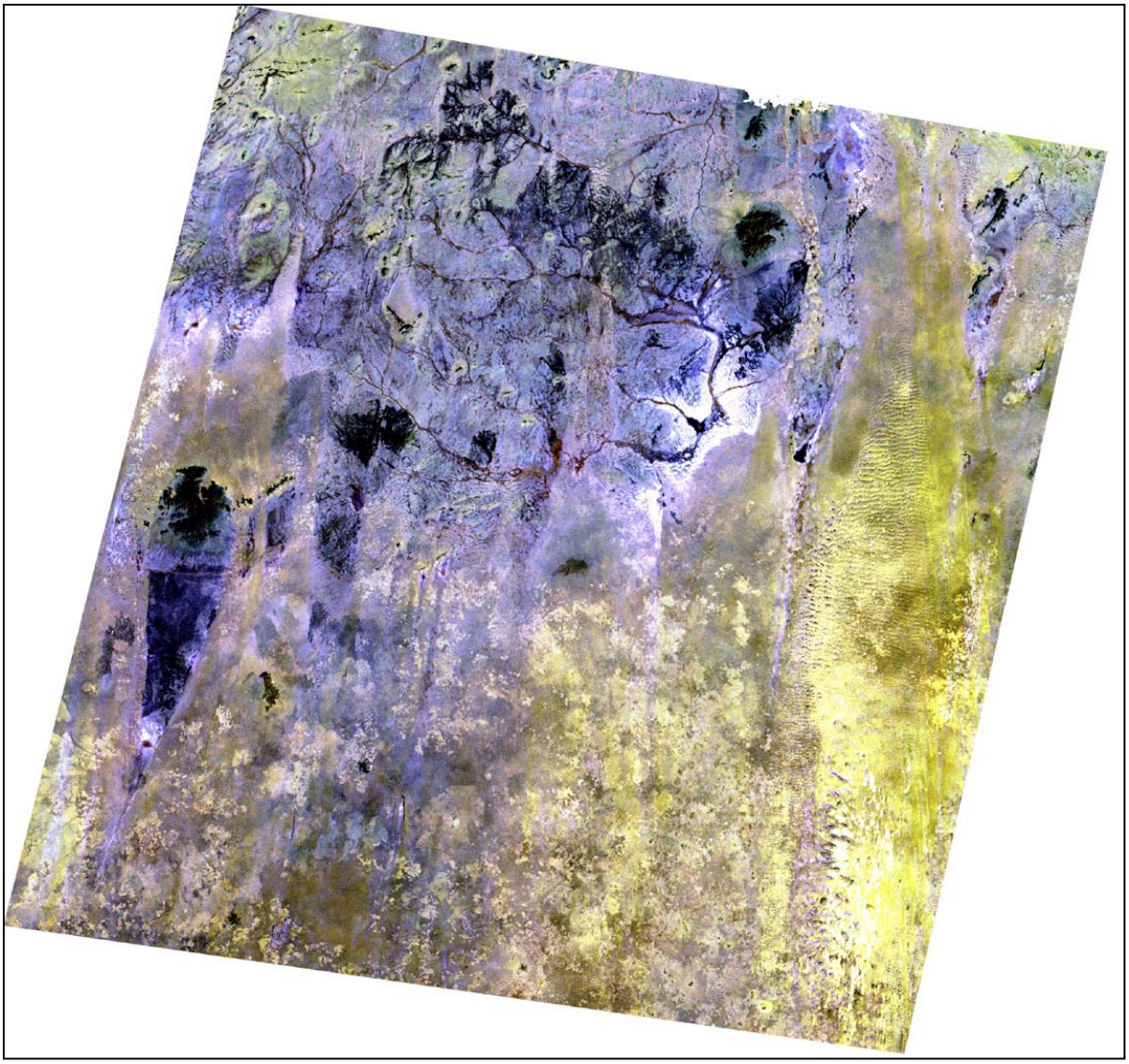

Fig 5.2a: Landsat 1 Multispectral Scanner MSS image, date of acquisition 14 January 1976[2]

[2] Refer to table (5.1) for more description of the image

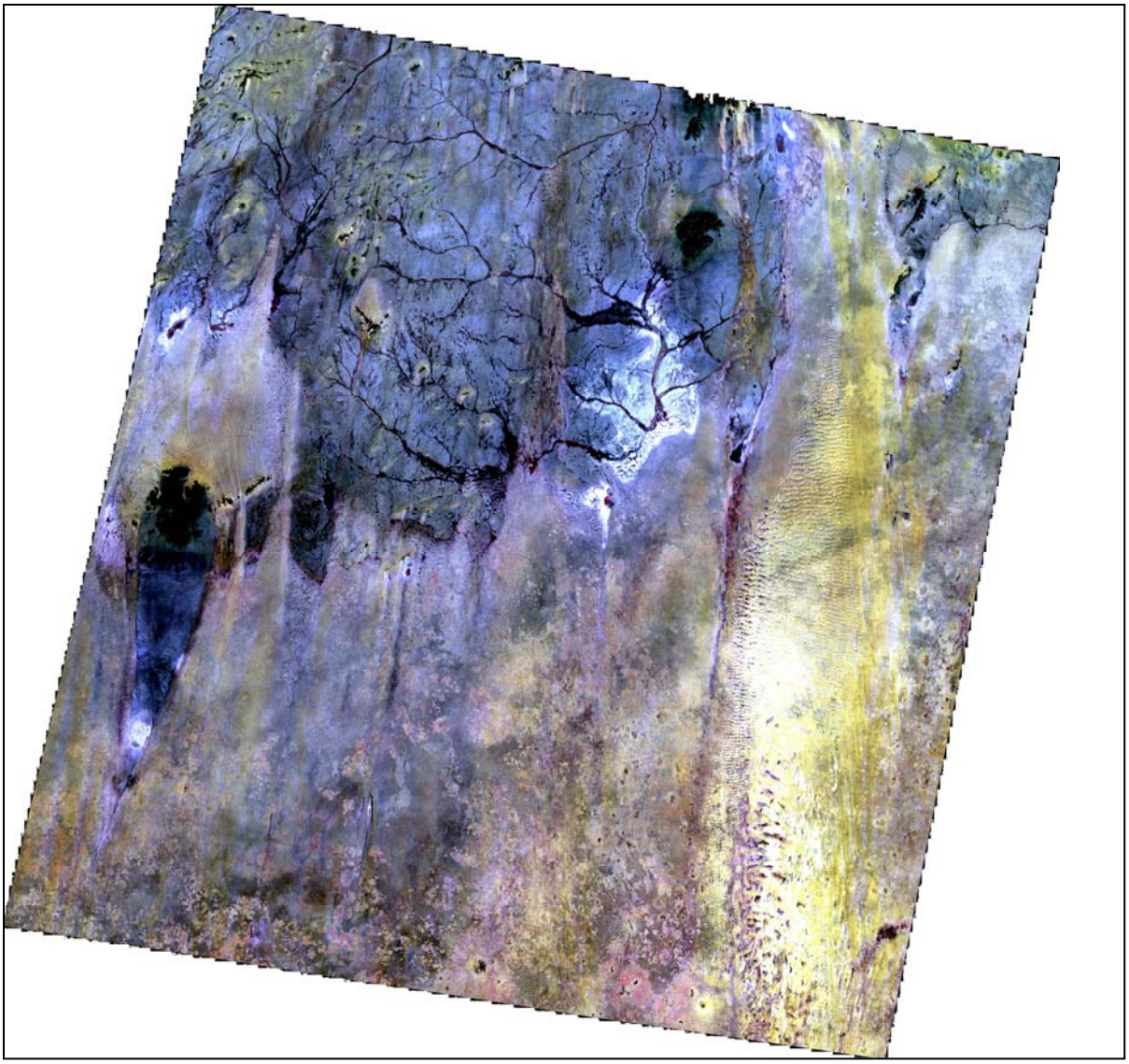

Fig 5.2b: Landsat 4 Thematic Mapper TM 1988 image, date of acquisition 20 January 1988[3]

[3] Refer to table (5.1) for more description of the image

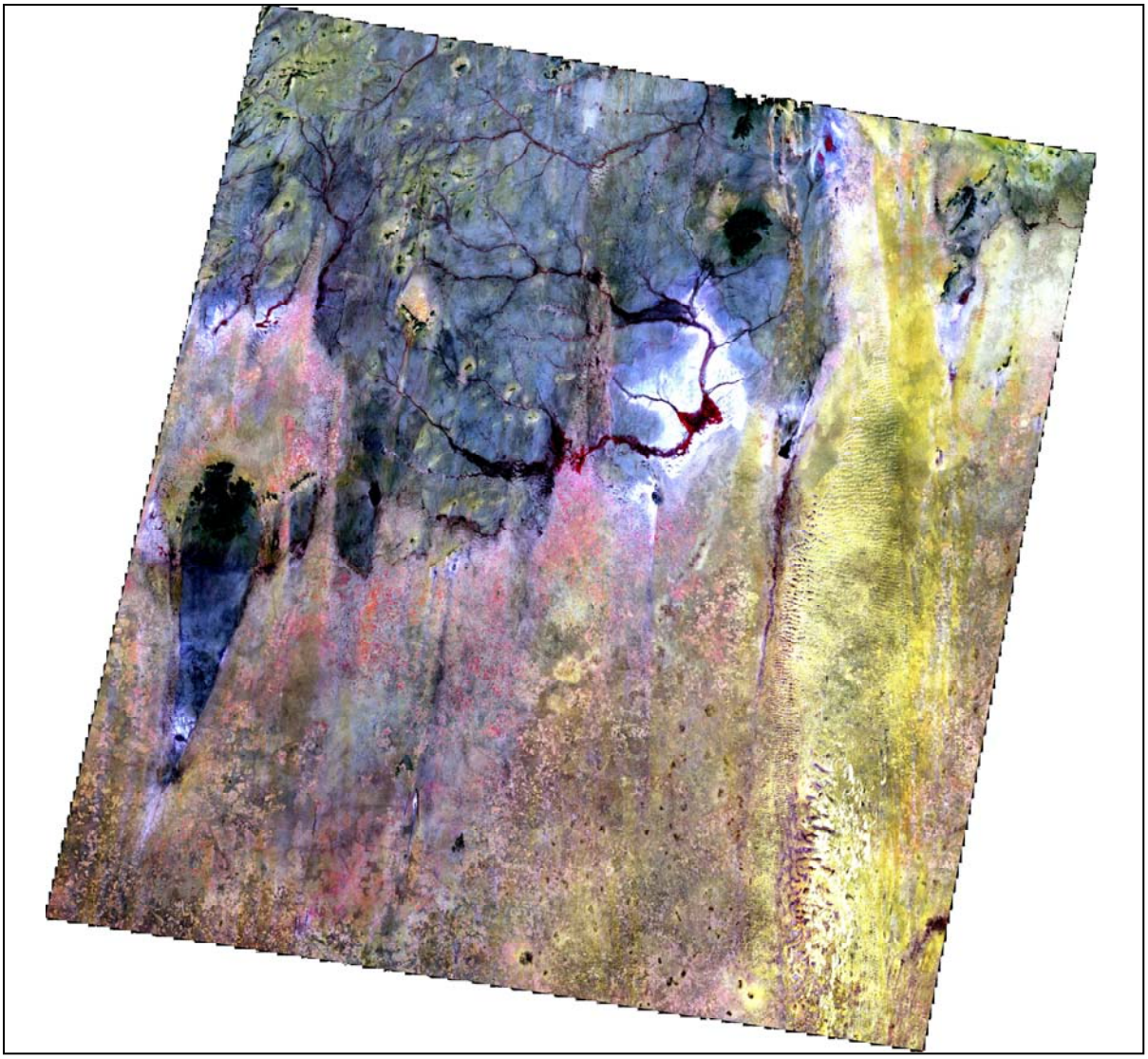

Fig 5.2c: Landsat 7, Enhanced Thematic Mapper ETM+, date of acquisition 13 January 2003[4]

[4] Refer to table (5.1) for more description of the image

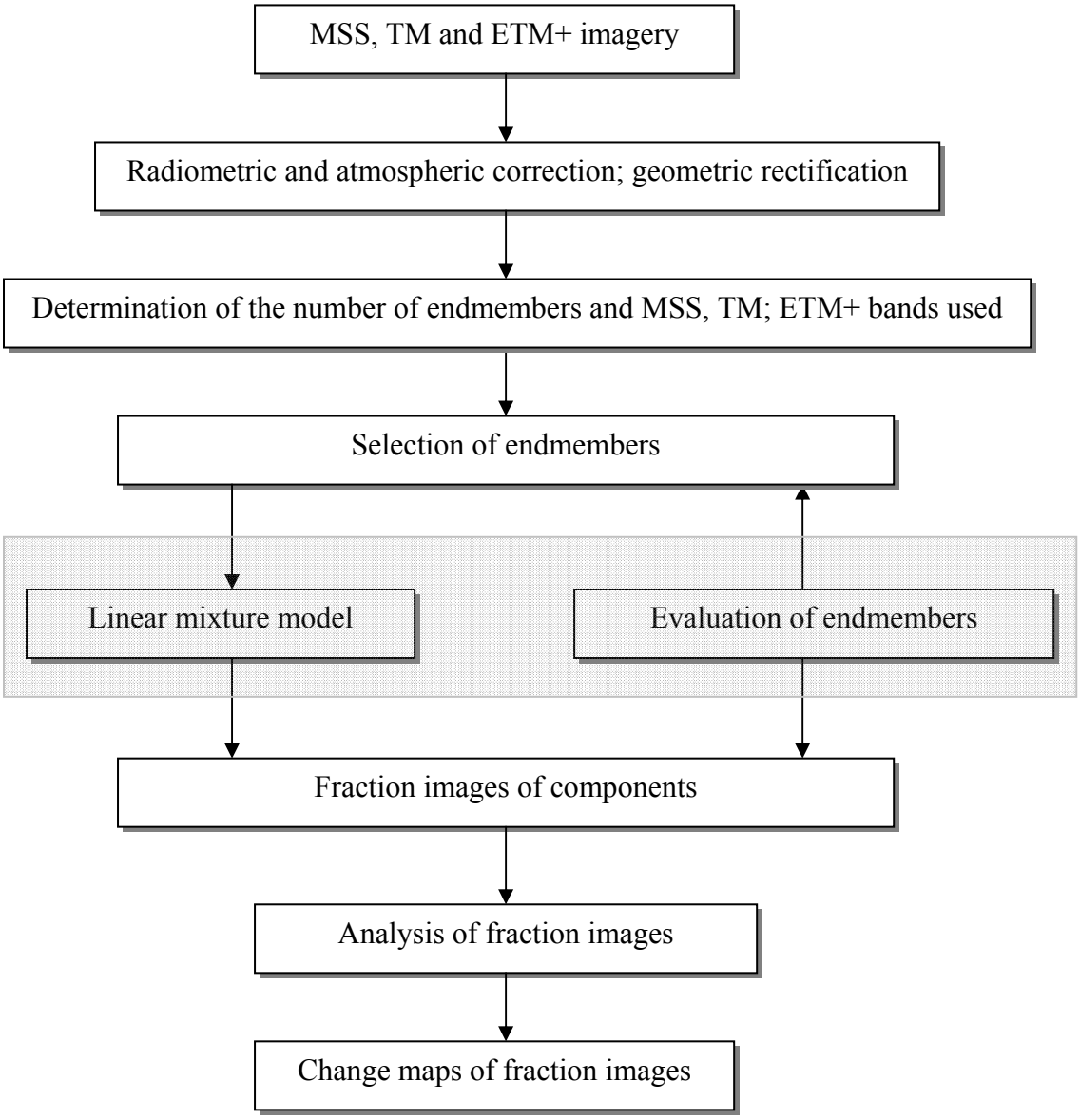

Fig 5.3: Flow chart for the methodology of process of multiple spectral analyses

5.3 Image processing

In remote sensing digital image processing historically is important due to two principle areas of application. Firstly, the improvement of the spectral information for visual interpretation and secondly, the processing of image data for computer assisted classification. The whole task of digital image processing revolves around increasing spectral separability of the object features in the image. Accordingly, the two images, MSS 1976 and TM 1988, were geometrically co-registered to the rectified ETM+ 2003 data (UTM north zone 35). Georeferencing was provided by selecting and applying ground control points (GCPs). Nearest-neighbour re-sampling technique was used. The root mean square (RMS) error of georeferencing is approximate 0.5 pixels. Subsets of the study area were selected. To apply the Spectral Mixture Analysis the conversion of digital number (DN) into reflectance radiance was required. The conversion process to transform reflectance spectra of materials from reflectance into relative radiance firstly requires a conversion of the DN to quantitative physical values such reflectance radiance. For each of the six bands the at-satellite radiances L [W m^{-2} sr^{-1} μm^{-1}] were calculated using the equations (1), (2) and (3) for MSS, TM and ETM+ respectively.

$$L_\lambda = GAIN.\ DN_\lambda + BIAS_\lambda \quad (1)$$

$$L_\lambda = \frac{LMAX_\lambda - LMIN_\lambda}{QCALMAX - QCALMIN}\ .\ QCAL - QCALMIN - LMIN \quad (2)$$

Where:

λ	= ETM + /TM band number
L	= spectral radiance at the sensor aperture in watts
GAIN	= rescaled gain (contained in the product header)
BIAS	= rescaled bias (contained in the product header)
QCAL	= the quantized calibrated pixel value in DN
LMIN	= the spectral radiance that is scaled to QCALMIN
LMAX	= the spectral radiance that is quantized to QCALMAX
QCALMIN	= the minimum quantized calibrated pixel value
QCALMAX	= the maximum quantized calibrated pixel value

At –satellite reflectance is given by equation (3):

$$\rho\lambda = \frac{\pi \cdot L\lambda \cdot d2}{ESUN\lambda \cdot \sin(\theta)} \quad (3)$$

Where:

P = unitless at- satellite reflectance
D = earth- sun distance in astronomical units
ESUN = mean solar exoatmspheric irradiances (band specific) in W m μm
θ = solar zenith angle in degrees
Lλ = spectral radiance in W m μm

For image interpretation, it is required to work with reflectance values instead of DN values. It is known that Landsat MSS, TM and ETM imagery has a specific range of measured radiance however each band is converted into values from 0 to 255 DN. Thus the calibration of each band is different. Therefore, if bands are rationed within a single scene, which is usually the case for spectral un-mixing, the resulting values can quantitatively be incorrect.

5.4 Spectral Mixture Analysis (SMA)

In order to assess the land cover types in the study area the application of multitemporal spectral mixture analysis was adopted. This method involves images pre-processing, image endmembers selection, image fraction production, classification of SMA fractions and finally interpretation of the fraction images (Figure 3.3).The aim of SMA is to estimate how each ground pixel is divided up among different cover types. The results are the series of images, each giving a map of the concentration of different cover type across the scene (Settle and Darke, 1993). Before these proportions can be calculated a set of spectra is defined called "image endmembers", representing the spectral reflectance of the different cover types. Different approaches have been used to define these endmembers (Smith *et al*., 1990; Boardam, 1993; Roberts *et al*., 1993; Boardam *et al.*, 1995; Basteson and Curtiss, 1996). There is variety of methods used to determine endmembers either by using image endmember selection in the image or by spectral libraries derived from field measurement with field spectrometer (field endmember). The study used image endmembers because they can be obtained easily and they represent spectra measured at the same scale as image data (Robert *et*

al., 1998).Thus the study relied exclusively upon image endmembers extracted independently from the images. The image endmembers were derived from the extreme of the image feature space, assumed to present the purest pixels in the images (Robert *et al*., 1998; Mustard and Sunshine, 1999). The four endmembers salt soil, green vegetation, sand soil and shade were defined. .The second step in SMA is to estimate for each pixel the abundance of each general endmembers by applying a linear mixing equation (Adams *et al*., 1993; ENVI, 2002). The general mathematic model of the Linear Mixing Model (LMM) can be expressed as:

$$DN_{i} = \sum_{K}^{n} EM_{ik} f_{ik} + \varepsilon_{i} \quad (4)$$

$$\sum_{K}^{n} f_{ik} = 1 \quad (5)$$

Where:

DN_i relative radiance in band i for each pixel

EM_{ik} relative radiance in band i for each endmembers k

f_{ik} fraction of each image endmembers k calculated band by band

k each of n endmembers

ε_i reminder between measured and modelled DN (band residuals)

Since the spectral compositions of pixel are assumed to be percentages, the mixing proportions are assumed to sum to one. Generally, the number of endmembers should be less than or equal to the number of bands used. A number band plus one (i+1) is possible on condition that a constrained method is used. This means that the fraction of the determined endmembers for each pixel in image sums to 100 percent. Unconstrained means that an endmember fraction may be less than zero or greater than 100 percent per pixel. This physically impossible fraction is useful as diagnostics for the adequacy of the model. If an endmember fraction greater than 100 percent occurs the pixel has spectra similar to that of the particular endmember, but with higher reflectance. A negative value of fraction indicates that an endmember is unnecessary to model the reflectance of a particular pixel. Usually the unconstrained method is used to optimise the endmember composition. Images classified with inappropriate endmembers will show insufficient results. Theoretically, it is possible to get the endmember fraction by unconstrained analysis in range of fraction value between 0 and 100 percent. This would require that the basic main surface materials of the image and their pure signature can be found. Based on that assumption, the unconstrained analysis technique is judged to be more exact than the constrained one. Unmodeled portions of the bands are

expressed as residual terms ε_i at $band_i$. The accuracy of the model is assessed either as error in fraction residuals or as the root mean square error (RMSE) across the bands. The residuals are calculated from the differences between the original DN of pixels and the modelled DN. To estimate the accuracy of the computed endmember fraction an error image is computed using the formula for the RMSE for an n-band image:

$$\text{RMSE} = \sqrt{1/n.\sum_{i=1}^{n}(\varepsilon_i)^2} \quad (6)$$

The overall of the model was judged to be accurate if band residuals or RMS errors have low value and if the fraction was not lower than 0 or larger than1. Pixels having high RMS values and/or fractions lower 0 or larger than 1 indicated an unmodelled compositional variability in the scene.

In order to develop high quality fraction images different transformations can be used (Cochrane and Souza, 1998; Van der Meer and de Jong, 2000). It is also necessary to understand the structure (or topology) of the mixing space in images. Therefore, band ratio Colour Ratio Composite (CRC) and Principal Component Analysis (PCA) were conducted and used interactively for the analysis.

5.5 Ratio analysis

In order to identify the different land cover types in the images the Colour Ratio Composite (CRC) has been created using the standard band ratio of MSS 1976, TM 1988 and ETM+ 2003. The main aim of this method is to get around the limitations of relatively broad spectral bands in Landsat images 1976, 1988 and 2003 by using ratios of bands to determine relative spectral slope between bands, thus the approximate shape of the spectral signature for each pixel. Common TM band ratios include: band5/band7 for the clay soil and carbonates, band3/band1 for iron oxide and band2/band4 for vegetation (ENVI, 2002). The combination of 5/7, 3/1 and 2/4 (RGB) results in an image which clays/carbonates are distinguish by magenta, sandy soils as green and vegetation as red as it shown in Figure 5.4.

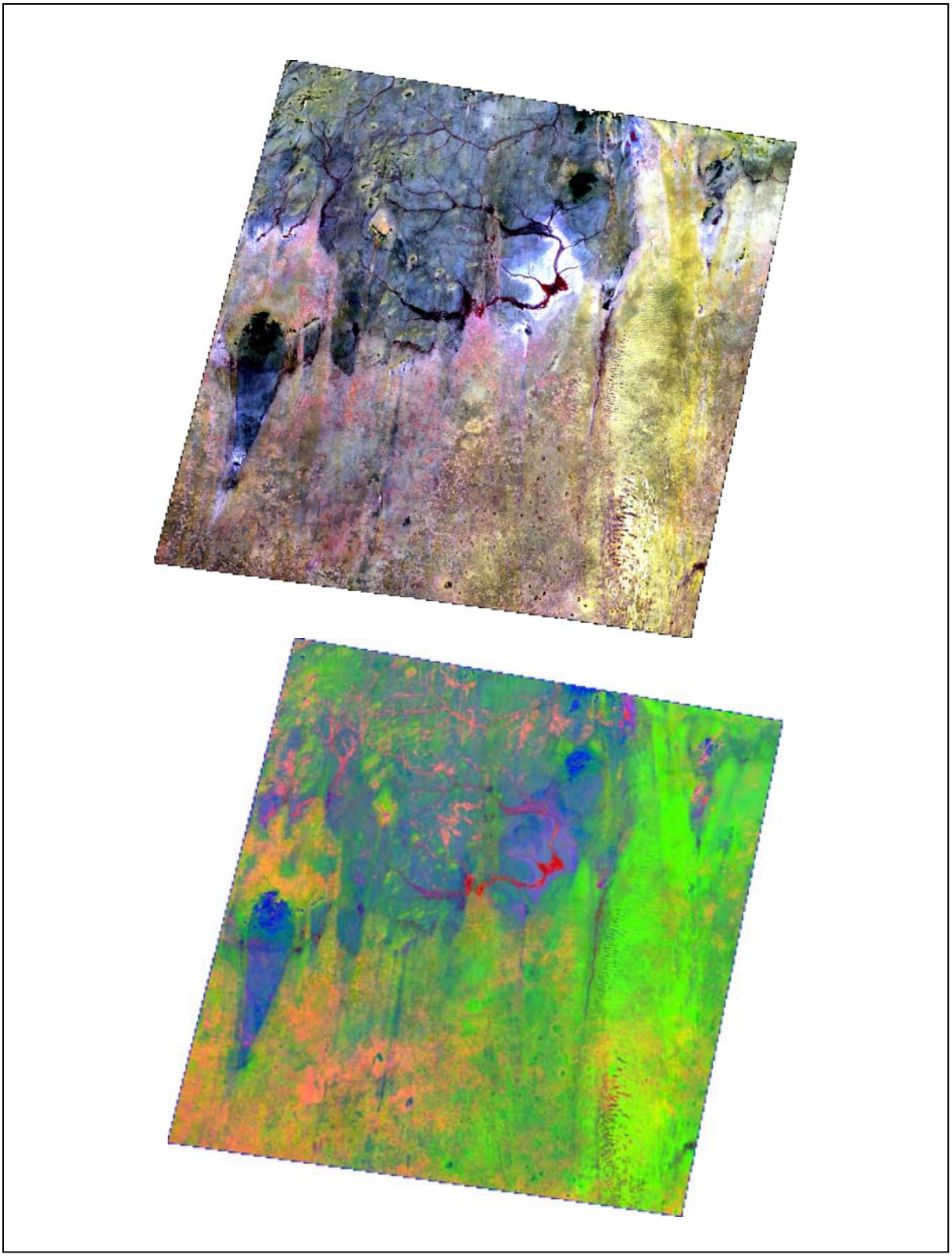

Fig 5.4: Colour Ratio Composite (CRC) of ETM+ 2003 image of the study area

5.6 Principal Component Analysis (PCA)

Principal Component Analysis (PCA) is applied to the three images MSS1976, TM1988 and ETM+2003 to quantify the dimensionality and topology of the spectral mixing space of the images. The principal component rotation minimises the correlations among dimensions so that the resulting principal component bands (PCs) represent orthogonal components of diminishing variance. The accompanying eigenvalue distribution provides a quantitive estimate of the variance partition between the signals versus the noise dominated principal components of the image. By using hyperspectral sensors this partition and number of signal dominated components can form the basis of estimated a n-dimensionality of the image (Green and Boardman, 2000; Price, 1997). The broad band sensors like ETM+ the number of distinguishable spectral dimensions is generally less than the true number of spectrally distinct endmembers and hence than the inherent dimensionality. All components will contain some signal in the form of a spatially coherent structure (Small, 2004). The multidimensional feature space of the low order principal components therefore provides a spectral mixing space which can be used to show the individual spectra as combination of spectral endmembers (Boardman, 1993; Johnson *et al*., 1985). The mixing space could be represented by scatterplots of the unrotated bands. Using scatter plots of PCs gives an "optimal" projection of the mixing space because the PC rotation provides an ordering scheme with respect to the variance bands. This means that two or three PCs can often present a first order representation of the mixing space which contains the majority of image variance. In the case of Landsat TM data, over 90% of spectral variability is mapped into PC1 and PC2, thus areas of spectral endmembers can usually be selected from scatter plots of PC1 and PC2. The process of selecting endmembers on based of principle component scatter plots illustrated in Figure (5.5). In this analysis the eigenvalues, eigenvectors and principal components are derived from a covariance -based rotation. PCA images and scatter plots were used to examine unique areas and to investigate the possibility of deriving un-mixing endmembers from the data. The four endmembers salt soil, green vegetation, sand soil and shade were selected. Figures 5.6 and 5.7 show the sand and salt soil and spatial distribution of vegetation cover in the study area.

ETM+2003

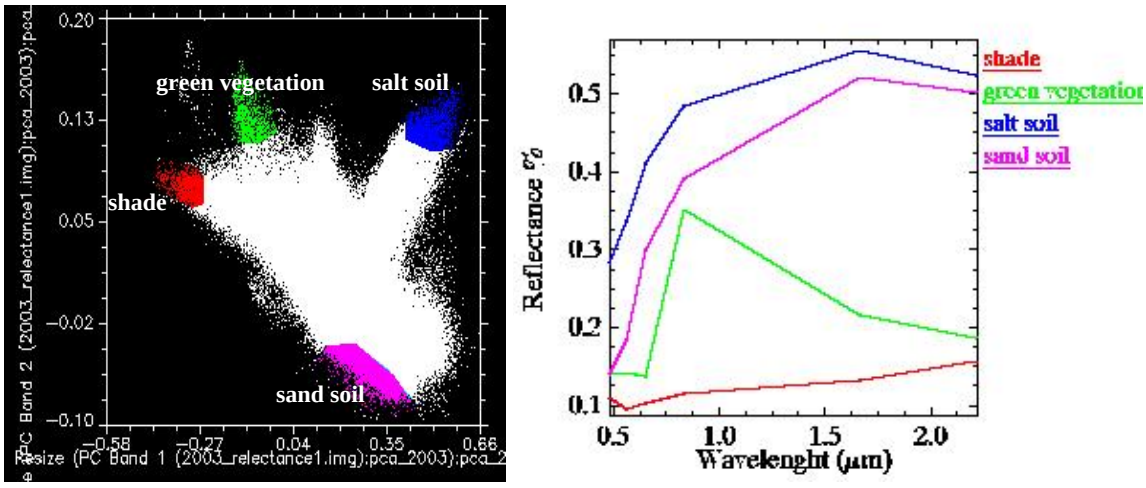

TM 1988

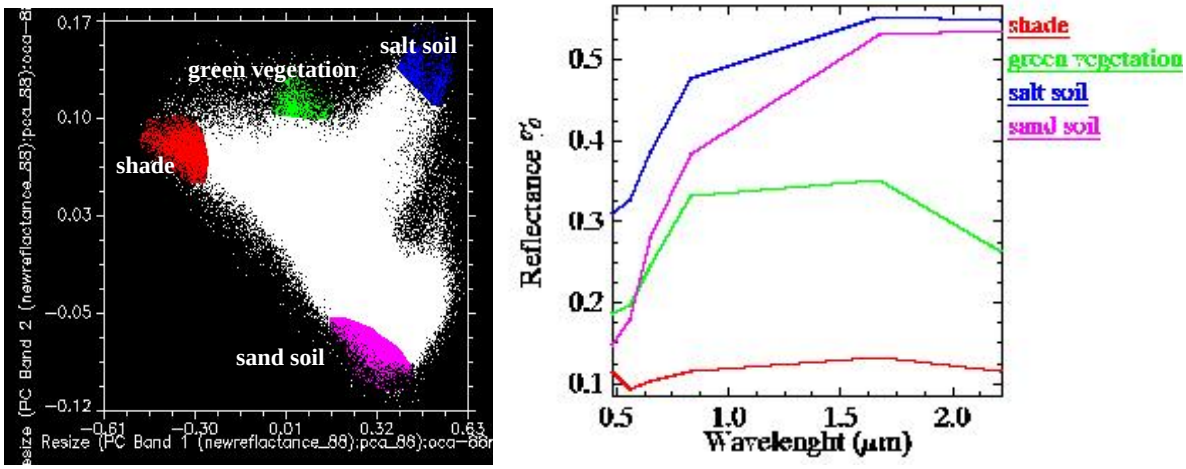

MSS 1976

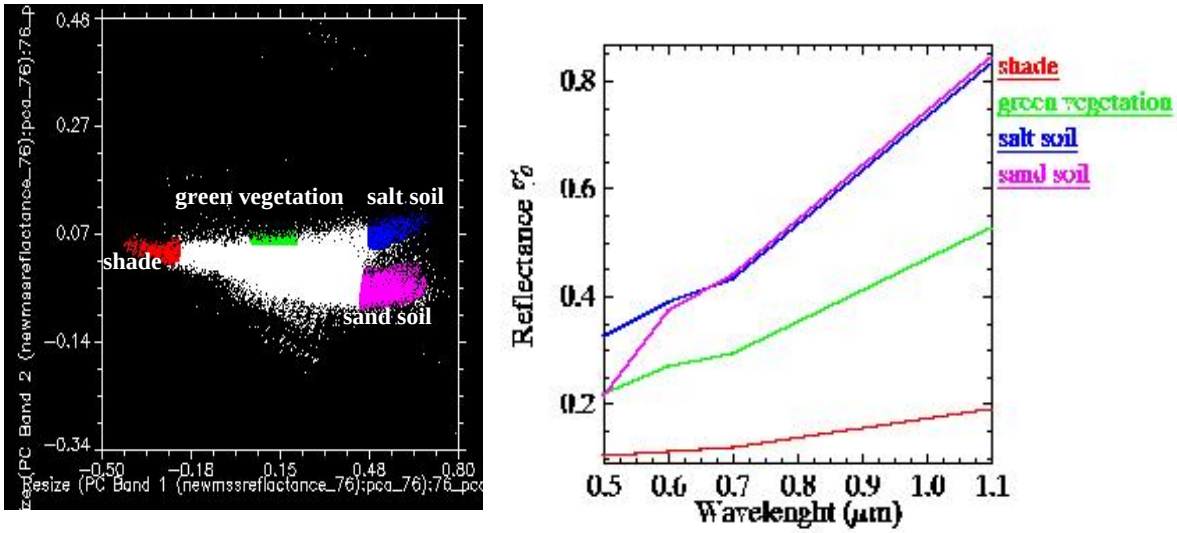

Fig 5.5: Scatter plot of PC1 vs. PC2 of ETM+2003, TM 1988 and MSS 1976 and the spectral reflectance of selected endmembers used in analysis *(Spectral band used for ETM and TM are 1, 2, 3, 4, 5, and 7 and for MSS are 1, 2,3and 4)*

(a) (b)

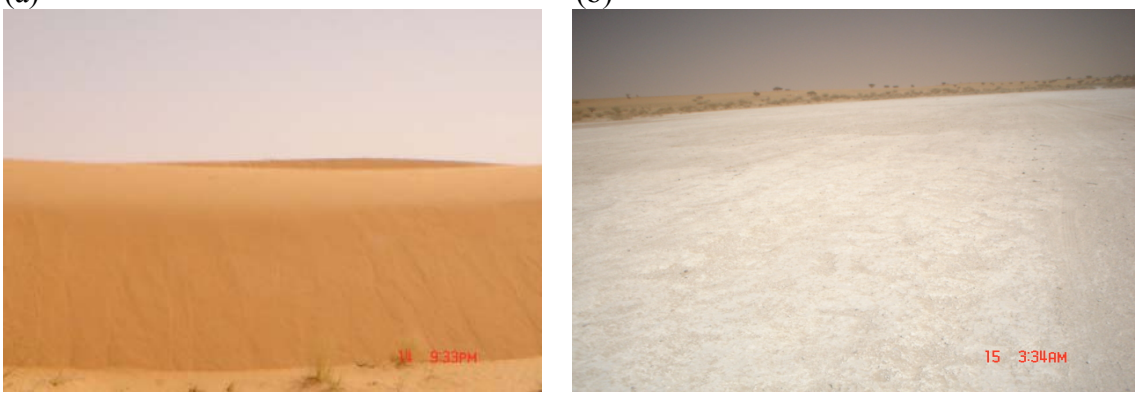

Fig 5.6: Different soil types in the study area (a) sandy soils in southern part (b) salt soils in *ELgaa* area in northern part (Photograph by the author, Jan 2004)

(a) (b)

Fig 5.7: Spatial distribution of vegetation covers in study area (a) vegetated sand dunes in *Elbashiri* area (b) mixed shrubs land in *Bara* (Photograph by the author, Jan 2004)

5.7 Eolain Mapping Index (EMI)

In order to analyse and evaluate the wind erosion in the study area the Eolain Mapping Index (EMI) was generated. EMI is a simple model which has been developed to generate an image that emphasized areas with low vegetation density and high soils reflectance. Many factors influence vulnerability of wind erosion. Two critical factors related to the amount of vegetation cover and soil surface type. For the purpose of detecting and mapping theses critical factors, the spatial and spectral resolution of remotely sensed images are more important than temporal resolution. A simple model has been developed using multispectral imagery to generate a wind erosion vulnerability image (WEVI) that is directly related to the amount of vegetation cover and surface characteristics. Generally, the out put image shows

the areas where the (e.g. amount of vegetation cover/ density and general surface soil type) are occur simultaneously. The image product shows various shades of yellow colour indicating levels of low vegetation density and high soils reflectance and serves as a guide to estimate the relative level of erosion potential/ vulnerability by wind. MSS, TM and ETM+ were used respectively to generate this model. The index used the red and near-infrared (R/NIR) spectral bands from the Landsat images to generate an image that emphasizes areas with a low percentage cover/density and/or high surface-soil reflectance. The near-infrared and red spectral bands), along with the ratio of the red to near-infrared bands (NIR, R and R/NIR) are used as the red, green and blue (RGB) components to make colour composite respectively.

5.8 Change detection analysis

There are many well developed techniques for land cover change detection using digital remotely sensed imagery. The nature of digital data allows for greater comparative capabilities of multi temporal analysis in comparison to traditional mapping methods. Change detection analysis approaches can be broadly divided into either post -classification change methods or pre-classification spectral change. In this study the pre-classification spectral change detection was applied. Using image endmembers, the study conducted two methods for changes identification. The first approach focused on the analysis of change in endmembers fractions images, by providing a direct measure of changes of different land cover in the study area. The second approach was the Change Vector Analysis (CVA).

5.8.1 Change in fraction image

According to Adams *et al.,* (1995), change can be identified explicitly either as change in endmember fractions or as change in classes as defined by endmember fractions. The study used the former approach which provides a direct measure of change. Change between the different dates (1976, 1988 and 2003) was identified using a standard RGB composite and loading fractions for salt soil, sand and shade as red, green and blue respectively for the different dates. Visual interpretation for the three dates was conducted and interpretation of different land covers was conducted.

5.8.2 Change Vector Analysis (CVA)

Change Vector Analysis (CVA) is an effective approach for detecting and characterising land cover change. Processing and analysing is applied to multi-spectral/multi-temporal data layers. CVA was introduced by Engvall *et al*. (1977) and Malila, (1980). The vector describing the direction and magnitude of change from the first to second date is a spectral change vector (Figure 5.8). This time trajectory is represented as a vector in multidimensional measurement space.

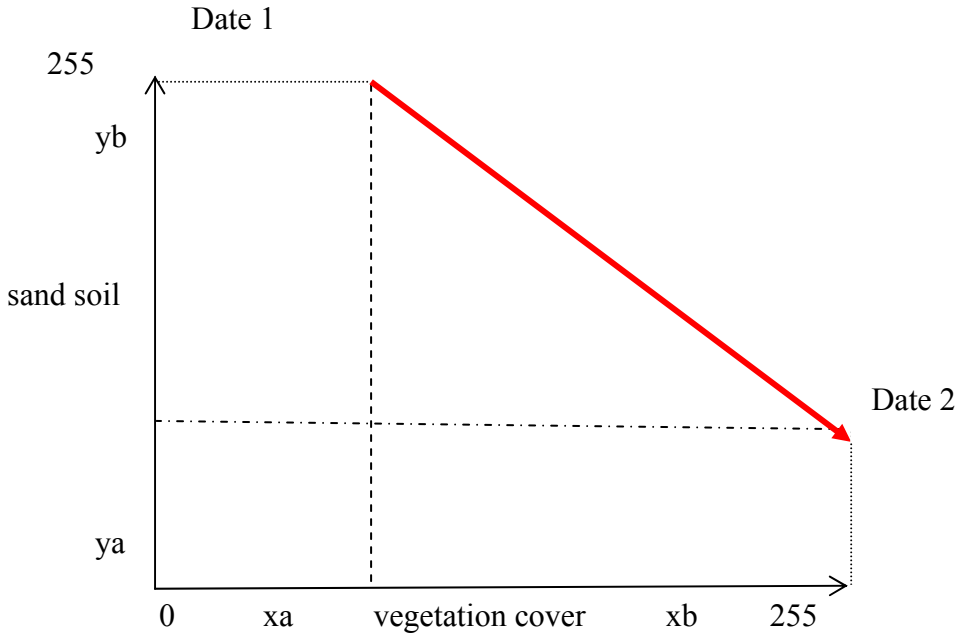

Fig 5.8: Change vector obtained from the variation position of the same pixel in bi-temporal data

The length of the change vector indicates the magnitude of change, while its direction indicates the nature of the change (Lambin and Strahler, 1994a). In this study the magnitude of vectors was calculated among spectral changes between the endmember fractions images of dates 1976/1988 and 1988/2003 respectively. Fraction of vegetation was placed along the X-axis and the fraction of sand soil placed along the Y-axis (Figure 5.9). The magnitude of the vector was calculated from the Euclidean Distance and represented the difference between the pixel values of the fraction images for sand soil and vegetation cover respectively between the dates 1976/1988 and 1988/2003 .It is shown in equation (7) as follows:

$$R = \sqrt{(y_b - y_a)^2 + (x_b - x_a)^2 + \ldots\ldots} \quad (7)$$

Where:

R Euclidean Distance

y_a fraction value of sand soil from date 2

y_b fraction value of sand soil from date 1

x_a fraction value of vegetation cover from date 2

x_b fraction value of vegetation cover from date 1

Change direction is measured as the angle of the change vector from pixel measurement at time 1 to the corresponding pixel measurement at time 2 (Figure 5.9).

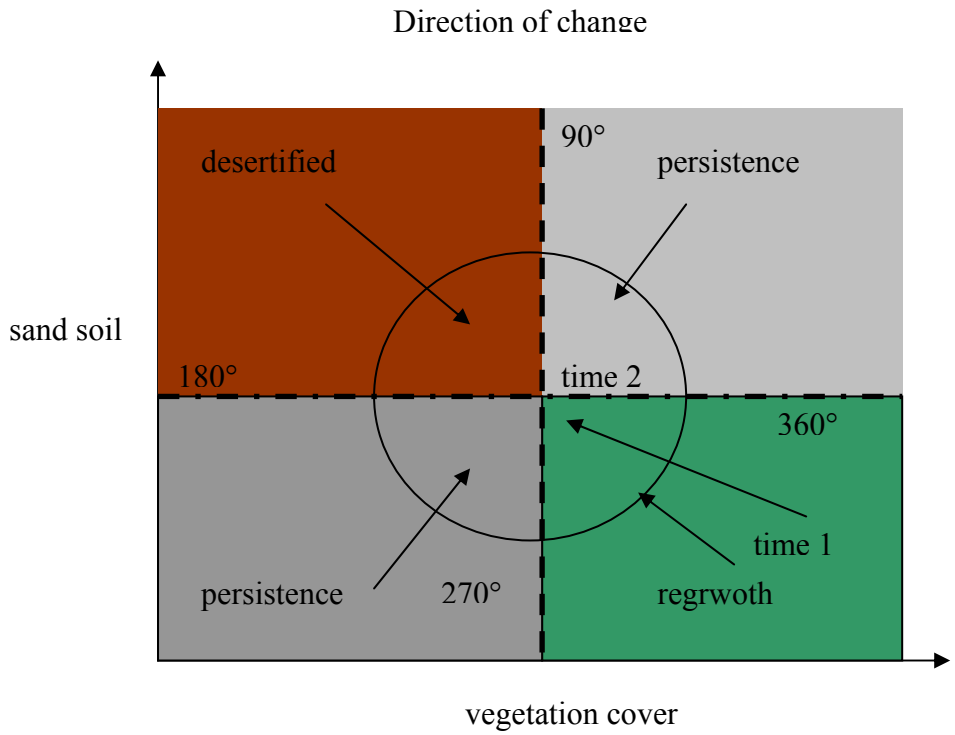

Fig 5.9: The process for detecting the direction of change with change vector analysis

Angels measured between 90° and 180° indicated an increase in soil and decrease in vegetation cover, this representing an increase of desertified areas. Angels measured between 270° and 360° indicate a decrease of sand soil and increase of vegetation cover, this representing re-growth of vegetation cover (Lorena *et al.*, 2002). Angels measured between 0°

to 90° and 180° to 270° indicate either increase or decrease in both of sand soil and vegetation cover. This change is represented as persistence, which is representative of either an increase or decrease in sand soil and vegetation in the study area.

5.9 Statistical analysis

The study used different ways of statistical analysis such as dynamics of change, correlation coefficients and analysis of variance (ANOVA). One way analysis of variance is a parametric test assumes that all the samples are drawn from normally distributed populations with the same standard deviations (variances). This analysis uses to measure significant differences between endmembers among the different years of 1976, 1988 and 2003. Sigma Stat[5] software was used to conduct a one way ANOVA table for measuring the level of significance between different endmembers. Four endmember (shade, green vegetation, sand and salt soil) were compared in 1976, 1988, and 2003 respectively. RMS error for the three years was also compared. The study conducted multiple comparison procedures to isolate the difference between the years of 1976, 1988 and 2003 when running an ANOVA. There are two classes of multiple comparison procedures: firstly, all pair-wise comparisons, where every pair of years is compared and secondly multiple comparisons versus a control. In this procedure all years are compared with a single control year. The study applied pair-wise comparison procedure.

5.10 Field observations

Field work was carried out during the dry season in January.2004 and in the rainy season of July 2005. These two field work periods were established to increase the understanding of the patterns of land cover in the study area during the different seasons. Preliminary image classification and RGB composite images of the study area was printed to indicate target areas to be surveyed depending on the accessibility of each site. The data were collected from different sites depending on the different soil types in the study area. Random sampling techniques were applied and information was collected from 25 sample plots with a 50*50m size. Each plot was registered by using GPS technology to allow for further integration with the spatial data in a geographic information system (GIS) and image classification system.

[5] SigmaStat 2.0 is the statistical analysis software used for ANOVA, produced by Jandel Corporation

Meanwhile, visiting of 60 villages (Appendix 1) in the study area was carried out during the field work (Figure 5.10). Information was collected following the specific procedures such as:

- Identification of the dominant species of trees, shrubs and herbs.
- Detection of physical aspects of soil and vegetation cover in the area.
- Conducting interviews and group discussions with the local people to extract technical information concerning the history of different land cover and land use which can be used for classification system.
- Collection of information about previous covers concerning types, densities, distributions and species, which already disappeared by questioning key informants of local people in the study area.
- Collection of information about the *Wadis* (local names, period and extent of floods, ect.) and the general landscape such as names of rocks, sand dunes and other features of these areas.

In order to verify the selection of the pure land cover materials in the study area field verification was carried out in April 2006 based on the results of endmembers fractions. Systematic selection of the sample plots was adopted for selected sample plots, which represented a pure land cover in fraction images. The information collected about the presented pure land cover was used successfully in the classification process. From field observations and Landsat imagery (Figure 5.11) well identified that most of human activities concentrate around the villages and watering points and this situation led to an increase of degradation of vegetation cover and tree status around the villages. The field work was assistance by four key persons from the study area, who have very good experiences and knowledge.

5.11 Ancillary data

Ancillary data were collected from different reports and departments in the study area. Records in agricultural statistical regarding to crops types, total cultivated areas, productivity and livestock population were collected and used in the analysis and interpretation of the results. Climatic data such as annual rainfall from (1960-2004), wind speed and wind direction from (1970-2000) also were well adopted for the analysis. The study tried to use the optimum availability of ancillary data to achieve the objectives of the study.

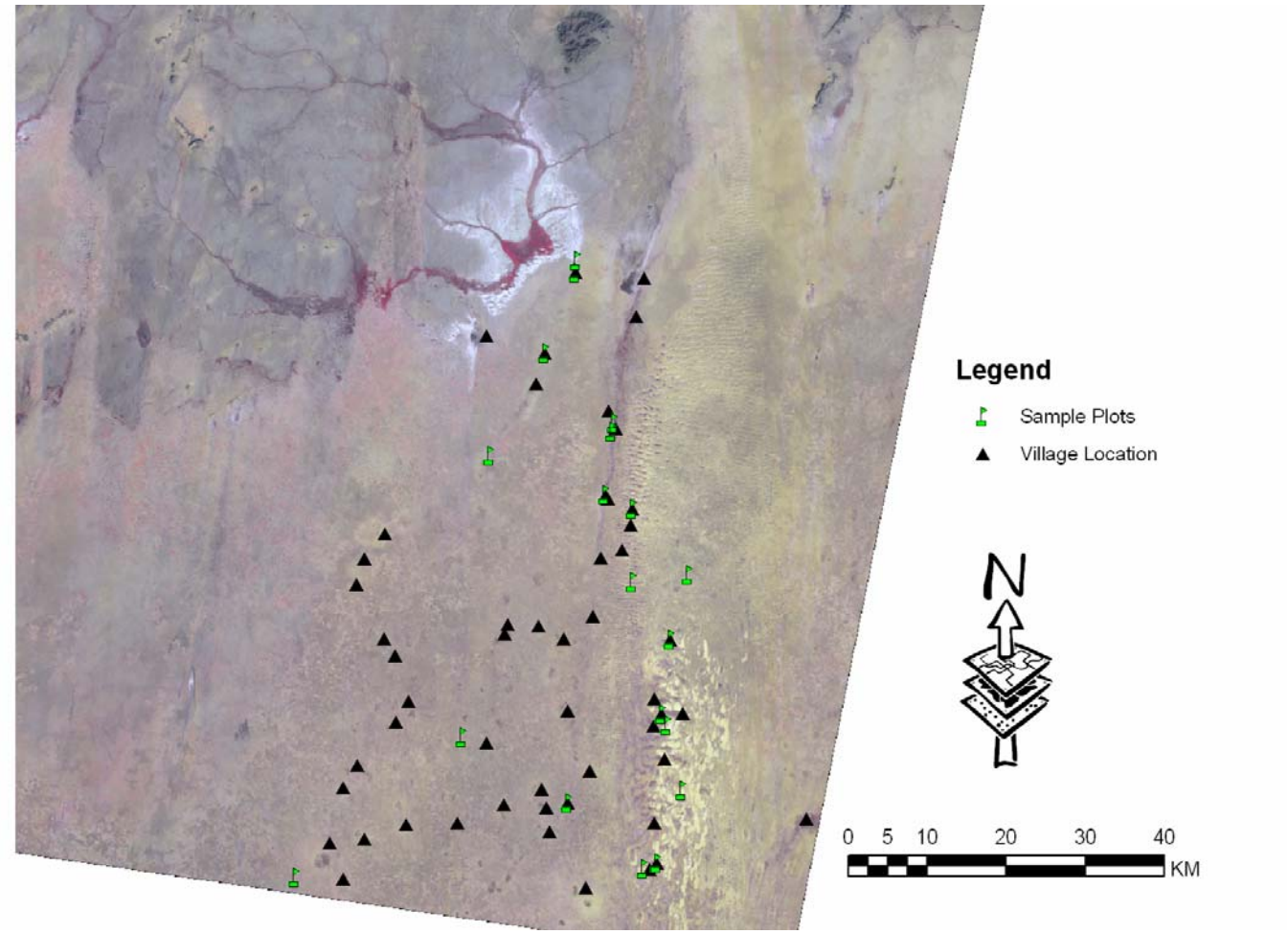

Fig 5.10: Villages and sample plots location during the ground truth in the study area

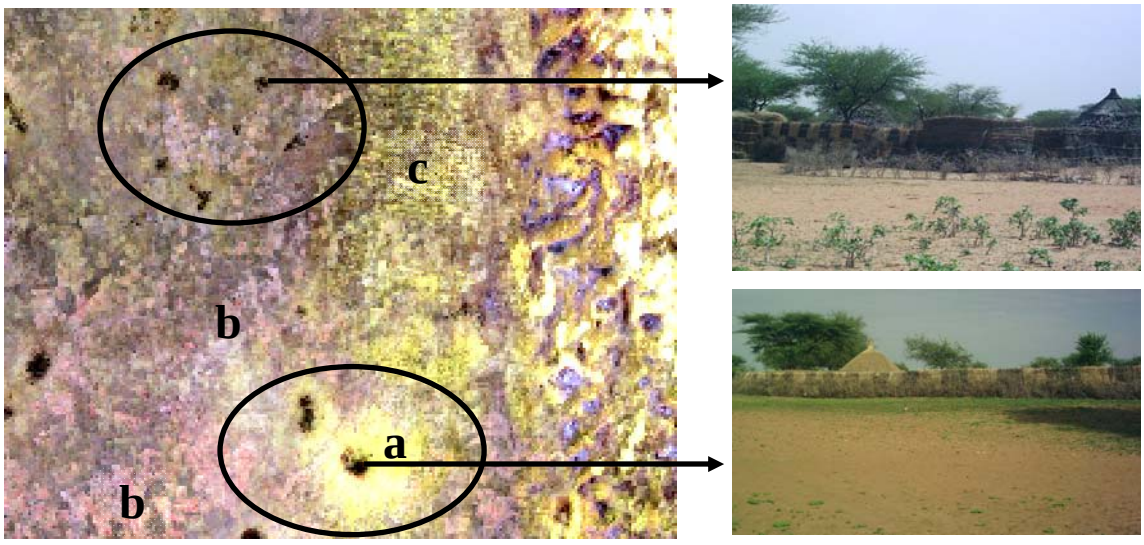

Fig 5.11: Location of villages as they appear in the Landsat 7 ETM+2003 image of the study area (a) desertification ring, (b) rainfed agriculture areas, (c) transversal sand dunes (Photograph by the author, Jan 2004)

PART IV

PRESENTATION AND DISCUSSION OF THE RESULTS

CHAPTER 6: INTERPRETATION AND ANALYSIS OF FRACTIONS IMAGES

6.1 General overview

This part presents and discusses the results of study. This includes presentation of results of spectral mixture analysis (SMA) for the Landsat imagery of MSS, TM and ETM+ for the years 1976, 1988 and 2003, respectively. A linear mixture model (LMM) was adopted using endmembers derived from the image. Four endmembers, shade, green vegetation, salt and sand soils, were selected. The maximum number of endmembers is limited by the number of spectral bands of the Landsat image used in the study. To identify the intrinsic dimensionality of the data the principle component analysis (PCA) was applied. Fractions of endmembers and RMS error were computed. The study used the endmember fractions to conducted two methods for changes identification. Firstly, direct detection of change in fraction images between different years was analysed by use of visual interpretation in addition to statistical analysis. Secondly, change vector analysis (CVA) was applied to determine and analyse land cover change. To map and evaluate the soil erosion in the study area, eolain mapping index (EMI) index was used to identify the areas that are subjected to wind erosion hazard. Statistical measurements such as correlation coefficients, dynamic of change and analysis of variance (ANOVA) were also used. The finial results were qualitatively and quantitatively presented, interpreted and discussed.

6.2 Visualization of fractions images

The most critical step in SMA and production of fractions image is the selection of endmembers. Endmembers must be representative of the main materials in the scenes. Through the mixture model, they include nearly all of the spectral variance of the scenes, thus reducing the total RMS error. The number of endmembers is restricted to the number of Landsat bands used in this analysis. For Landsat MSS 1976 the four bands (band 1, 2, 3 and 4) while for TM 1988 and ETM+ 2003 six bands (band I, 2, 3, 4, 5, 7) excluding the thermal band were used. Based on field observation and relevant literature four endmembers were selected, two soil endmembers explicitly salt and sand soil, in addition to green vegetation and shade. The fraction images and RMS error of each reference endmember were computed for each pixel of the different Landsat imagery. When displayed on an image monitor, areas of high fraction will be brighter than areas of low fraction. RMS residuals error is an indication of goodness of the used mathematical model. A smaller RMS indicates that the model has been constructed correctly and endmembers have been accurately selected (Table

6.1) The shade endmember account for shadows at hilly areas in the northern part of the study area where dominated by isolated hills or clusters of hills in form of inselbergs e.g. *Jbel Abu Sinun* (820m) and *Jbel Umm Shgerira* (846m). Hills in the study area reflect a mixture of dark black and dark red tones because of bare rocks and vegetation. With visual interpretation of fractions images and information from the field observations the results were discussed in a consistent and realistic way.

Table 6.1: RMS residuals for the endmember fractions

Years	RMS residual value
1976	0.002
1988	0.006
2003	0.007

6.2.1 Soil fractions

6.2.1.1 Sand fraction

The fractions and spectral reflectance of sand endmember for MSS, TM and ETM+ are presented in Figure (6.1). The visual interpretation of the resulting fraction images indicates that sand fraction increased from 1976 to 1988 and from 1988 to 2003. This is mainly attributed to the fact that sand encroachment increases following the wind direction from north to south in the study area as shown in Figure (6.1). Climatic data shows that wind speed in the study area increases during the dry season in the north direction, this supporting the finding (Table 6.2). In addition, wind blowing is serious problem in the more arid parts in study area due to low precipitation and high wind velocities during dry season. Accordingly, sand encroachment from north to south was evidently observed by the author during field survey in 2004. It is obvious from the fraction images that the sand increased rapidly from years 1976 to 1988 and from years 1988 to 2003. Percentage of sand fraction was 4.1%, 50.5%, and 59.4% in years 1976, 1988 and 2003, respectively. The undertaken statistical analysis of the dynamic of changes for the addressed period explains that the dynamic change was 8.04 in 1976; while in 1988 and 2003 only 2.0. These results indicate that sand encroachment was rapidly increasing at an increasing rate during years of 1976, 1988 and 2003. The correlation coefficient analysis (Table 6.3) reveals that ETM+ 2003 sand fraction has a negative low correlation ($r = -0.1$) with MSS 1976 sand fraction and a positive low correlation ($r = 0.09$) with TM 1988 sand fraction. This authenticates that the sand increased rapidly during the period from 1976 to 1988 and increased slightly low during the period from

1988 to 2003 as it is clearly visualized in the fraction images (Figure 6.1). This result is highly supported by the valuable scientific efforts provided by Doka *et al.,* (1980). Intensive consideration for mapping and locating eolain features (sand dune) and areas of high wind blowing using Landsat data, it was a core for their study. Perhaps the most telling arguments on the interpretation of the MSS 1976 in the study area are that most of sand dunes were largely created due to wind blowing across the natural barriers a long time ago. Accordingly, desert increases following the windows corridors (Figure 6.2). These findings also offer a logical framework that remote sensing has been applied since long time for monitoring desertification processes in the study area. Figure (6.1) shows the capabilities of SMA for detecting the change and calculating the abundance proportion of sand soil in the study area. From the fraction images it is very easy to detect the dynamic change of sand encroachment from the north to the south part of the study area. This result supports the finding of Baumer (1979) and Lampery (1975) who concluded that the desert moved toward south direction. Their work also indicates that desertification in this region as a phenomenon has been deeply investigated and studied since a long time ago.

Table 6.2: Wind direction and speed in the study area (1971-2000)

Month	**Wind direction**	**Wind speed(MPH)**[1]
Jan	North	9
Feb	North	9
March	North East	9
Apr	North	8
May	South west	7
Jun	South west	9
Jul	South west	9
Aug	South west	8
Sept	South west	6
Oct	North	7
Nov	North	8
Dec	North	8

Source: (Metrological Satiation, *Elobeid,* 2005)

[1] MPH refers to measurement of wind speed by mile (or km) per hour

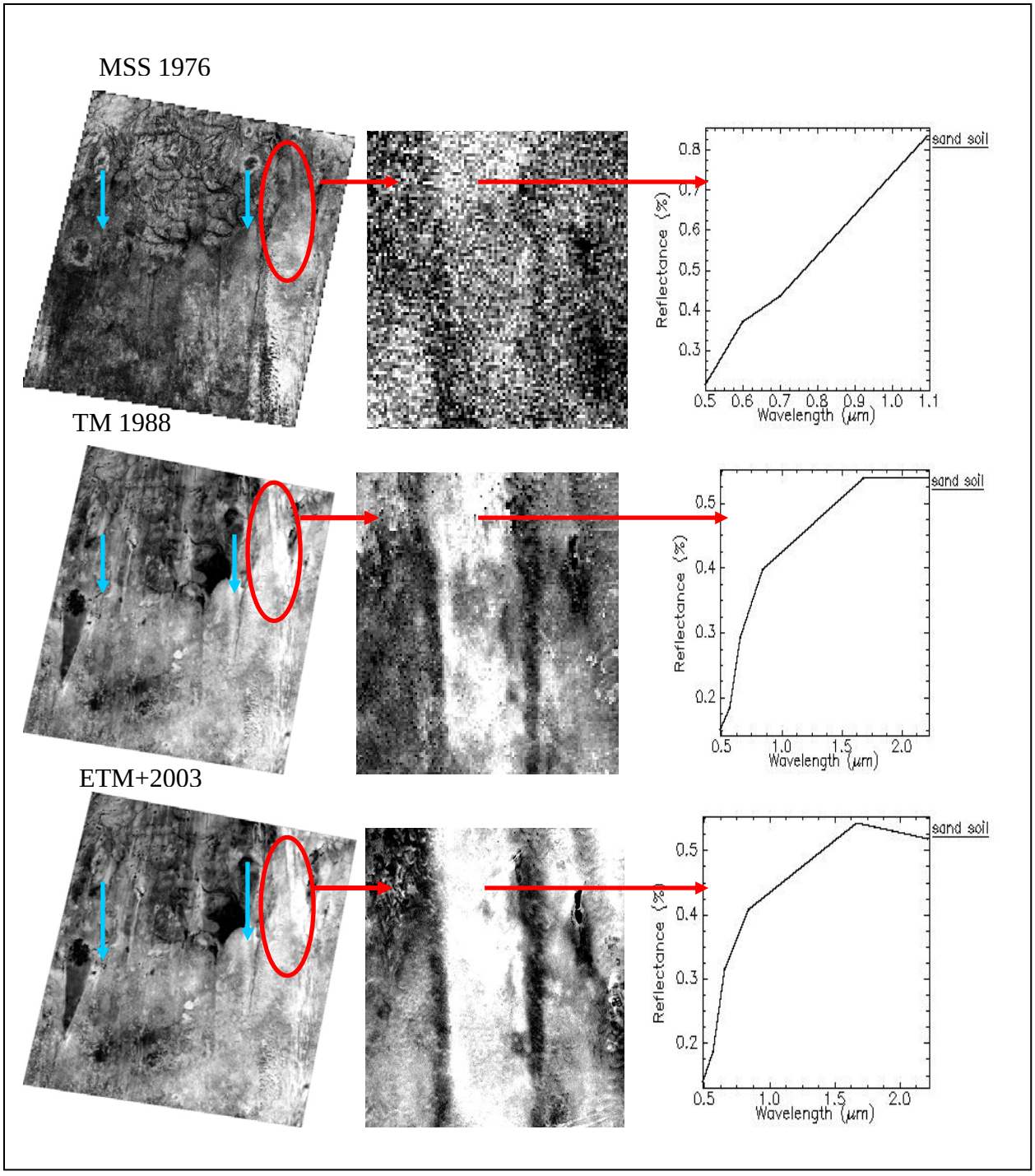

Fig 6.1: Fraction images and spectral reflectance of sand for the Landsat data used in analysis (*Arrows indicate the wind direction and brightness illustrates the very high fraction of sand)*

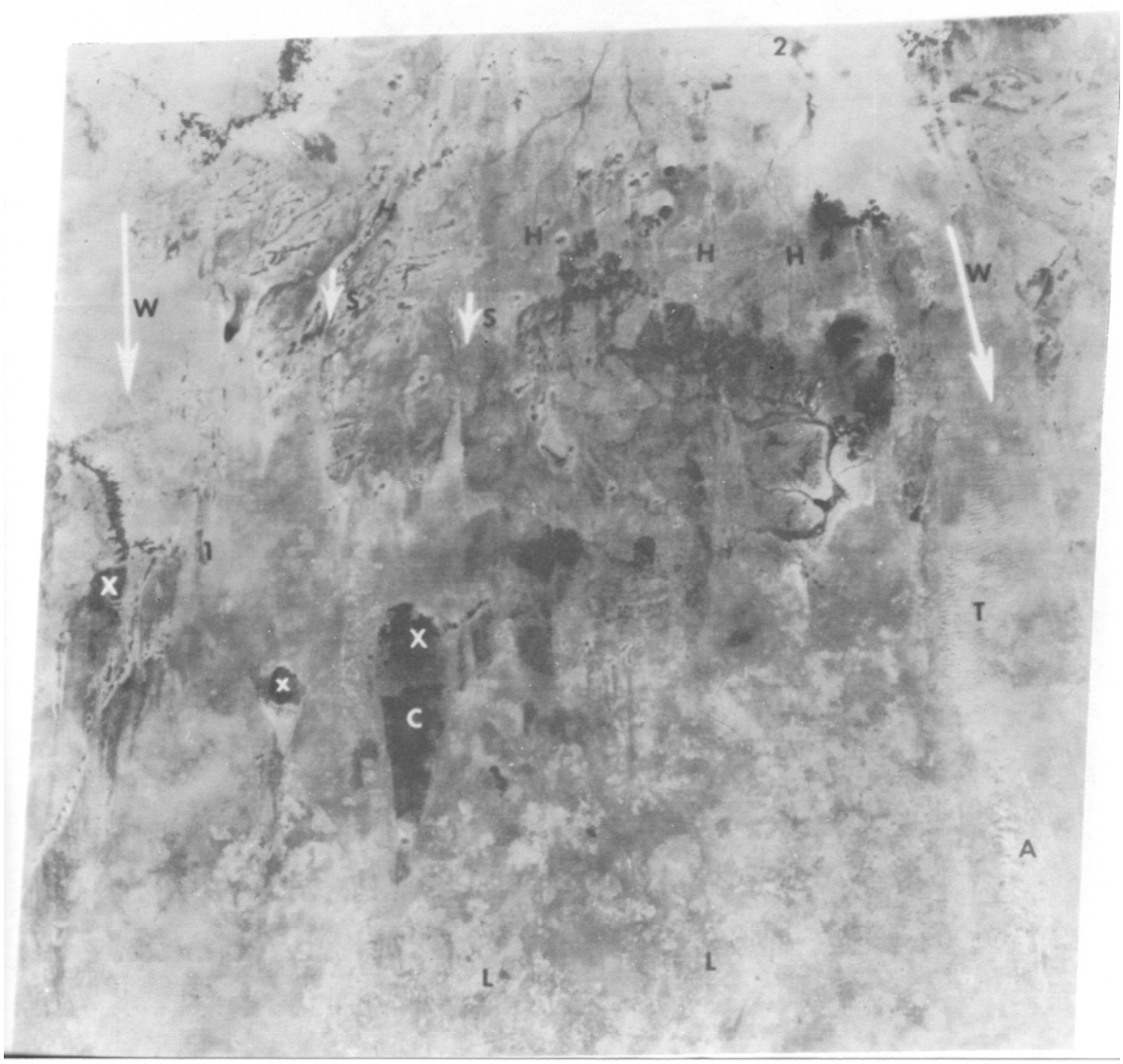

(1) Sodari	*(H) Rocky area of the natural barriers*
(2) Hamrat El Wazz	*(S) Small wind channels*
(W) Wind corridor and the arrows indicate the direction	*(X) Isolated barriers (hills)*
(T) Transversal sand dune	*(C) Clay soil protected by the barriers*
(A) Active sand dune	*(L) Agricultural lands*

Fig 6.2: Landsat MSS 1976 demonstrates the northern natural barriers and two wind corridors in North Kordofan (Doka *et al*., 1980)

Table 6.3: Correlation coefficients of vegetation, sand, salt soil and shade fractions

Green vegetation			
	1976	1988	2003
1976	1	-0.03	0.01
1988	-0.03	1	0.1
2003	0.02	0.04	1
Sand soil			
	1976	1988	2003
1976	1	-0.03	-0.1
1988	-0.03	1	0.09
2003	-0.1	0.09	1
Salt soil			
	1976	1988	2003
1976	1	0.4	-0.3
1988	0.4	1	0.2
2003	-0.3	0.2	1
Shade			
	1976	1988	2003
1976	1	0.30	-0.13
1988	0.30	1	0.31
2003	-0.13	0.31	1

Nevertheless, visualisation of fraction imagery shows that a considerable increment of sand soil in the southern part of the study area can also be detected from 1976 to 1988 and from 1988 to 2003. Under these circumstances, the *qoz* soils and sand dunes as in *Elbashiri* and *Eltawil* areas represented dominate features (Figure 6.3). These dunes are stabilised with trees and shrubs such as *Leptadenia pyrotechnica, Acacia tortilis, Panicum turgidum,* and *Aristida mutabilis*. Despite their poor actual and potential fertility, these areas support rainfed arable agriculture activities during dry and rainy season. It is worth mentioning that local people cultivate some crops like millet (*Dukhn*), sesame (*Simsim*), hibiscus (*karakdeh*), watermelon and some vegetables. These activities diminish the tree cover in this area and thus increase the degradation processes. This means that additional to the encroachment of sand from northern part of the study area due to wind blowing and other climatic factors, most of the desert stricken areas in the southern part affected by human activities related to rainfed crop cultivation, intensive grazing and fuel wood collection.

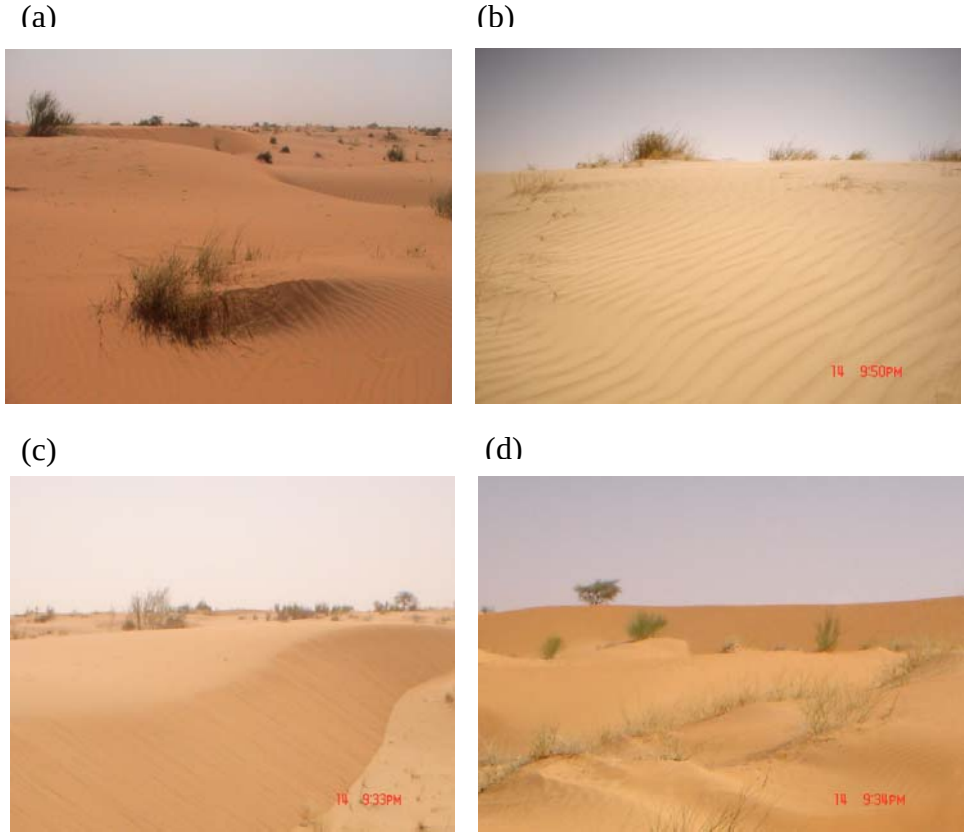

Fig 6.3: Sand dunes in *Elbashiri* and *Eltawil* areas (a & b) sand dunes in *Elbashiri* qoz and (c & d) sand dunes in *Eltawil* qoz (Photograph by the author, Jan 2004)

6.2.1.2 Salt soil fraction

Analyse averages of salt soil fraction are 3.2%, -2.4%, and -18.2% in years 1976, 1988 and 2003, respectively. The negative fraction value of salt soil could be expected theoretically due to the mathematics calculation of the model. It is possible to get negative fraction of endmember since an unconstrained method is used. This indicates that this endmember is unnecessary for modelling the reflectance of particular pixels[2]. This is more accepted for salt soil endmember which is concentrated in specific pixels in the image and do not cover all pixels in the scene i.e batches spatial distribution. Thus the fraction of this endmember is a very low negative value compared to others. Figure (6.4) illustrates the characteristic spectral reflectance of salt soil which is very high compared to sand soil (Figure 6.1). This is due to high albedo of salt soil thus showing a very bright tone (Figures 6.5 and 6.6). Salt soil is concentrated mainly in the northern part of the study area and is used for salt production (Figure 6.6). Visual interpretation of fraction imagery explains that salt soil is increased from 1976 to 1988 and 1988 to 2003. ETM+ 2003 salt fraction shows very low negative correlation

[2] Interpretation of this phrase is given in part III

(r = -0.3) with salt soil MSS 1976 indicating that salt soil changed rapidly from 1976 to 2003. On the other hand, the correlation coefficient between 1976 and 1988 is 0.4 (Table 6.3). These results are confirmed also by the dynamic of change. The dynamic change in 1976 is very high (6.1) compared to that of 1988 and 2003 with values of 2.0 and 1.9 respectively.

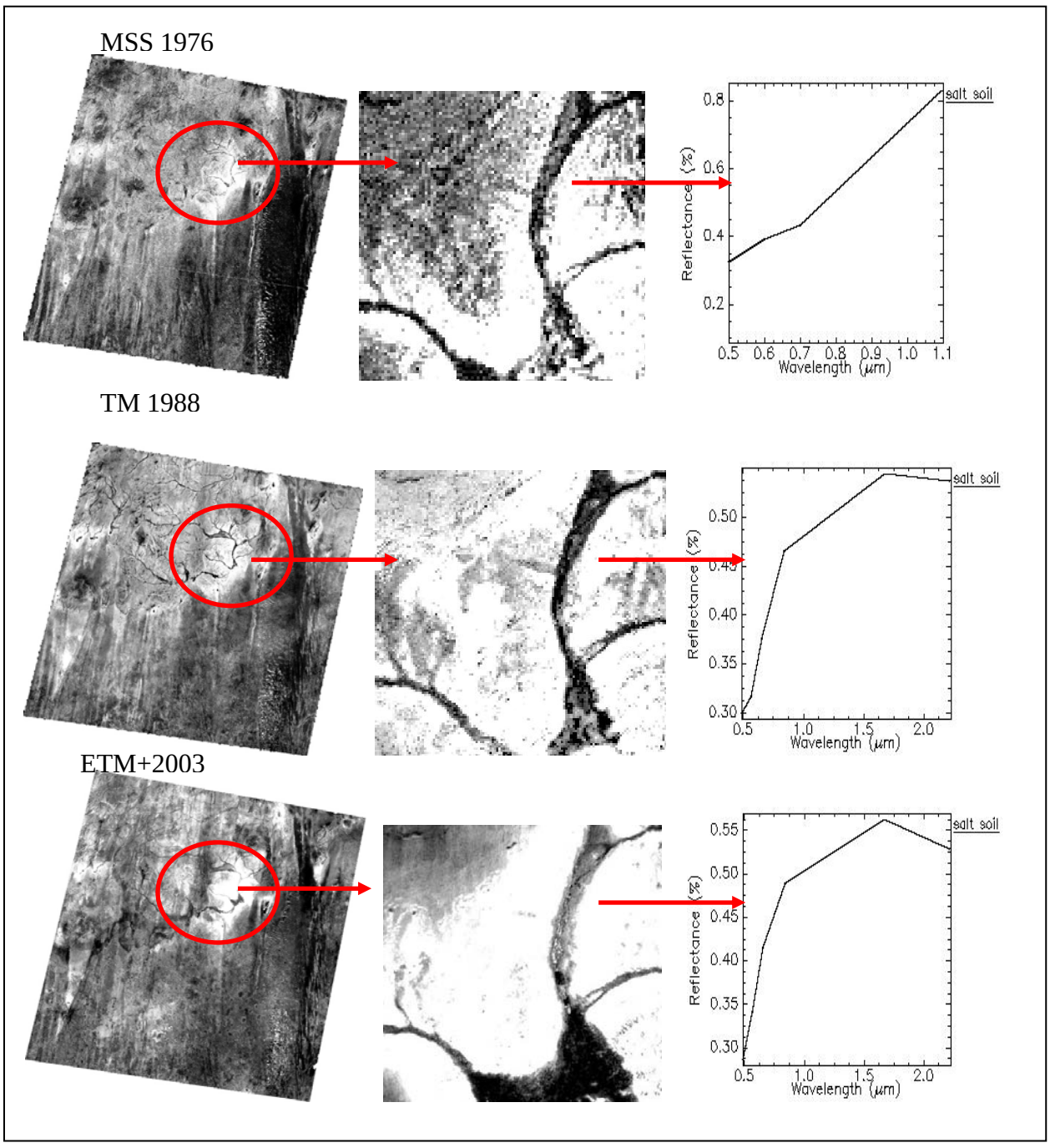

Fig 6.4: Fraction images and spectral reflectance of salt soil for the Landsat data used in analysis (*Brightness indicates high fraction of salt soil and black colour indicates the vegetation in Wadis)*

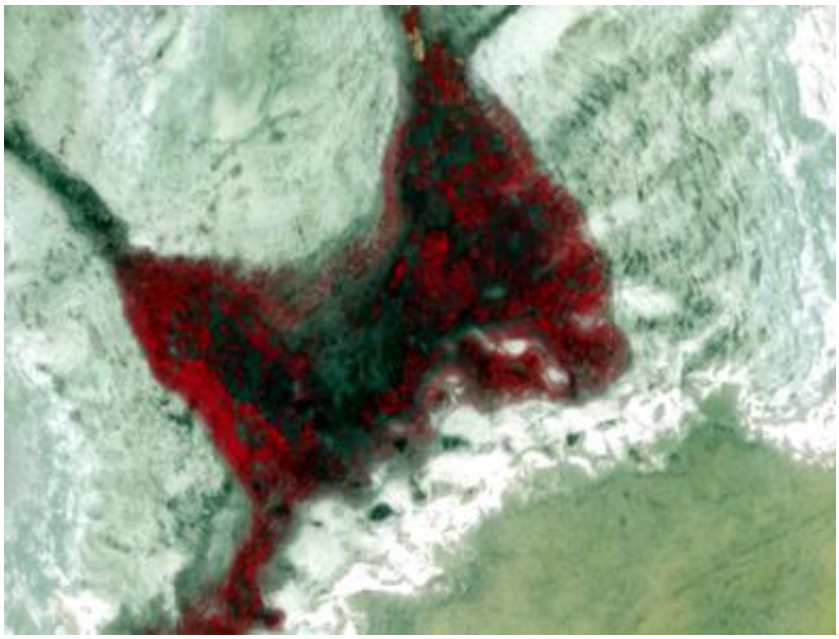

Fig 6.5: Salt areas in ETM+ 2003 image in northern part of the study area (*White colour indicates salt soil and red colour indicates the vegetation in Wadis)*

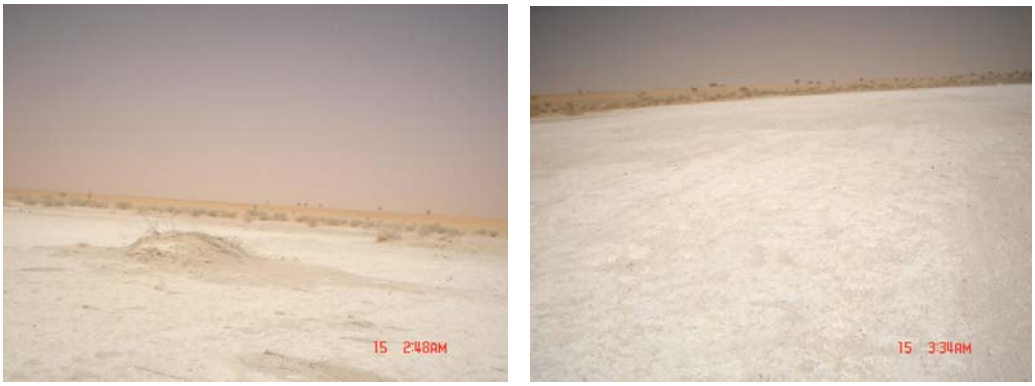

Fig 6.6: Salt soil in *Elgaa* village northern part of the study area (Photograph by the author, Jan 2004)

During the field survey in January 2004, it is well observed that people in these areas such as *Elgaa*, which depends heavily on producing and marketing salt in *Elobeid* city and other markets as a vital source of income. They produce salt from underground salty water. They take up the water from the dug well (Figure 6.7) and then they evaporate water by using fuel wood and they harvesting the reaming salt. This traditional practice has negative effects on tree cover as experienced in most part. It is worth to mention that Forest National Corporations (FNC) and German Aid Organisations started to confess the salt producers in this area to use solar energy in the process of evaporation of water and harvesting salt by providing them with sun resistant plastic ponds (Figure 6.8).

Fig 6.7: Dug well for salt production from ground water in *Elgaa* village (Photograph by the author, Jan 2004)

Fig 6.8: Solar energy ponds for salt drying in *Elgaa* village (Photograph by the author, Jan 2004)

6.2.2 Vegetation fraction

The visual interpretation of vegetation fraction shows very significant decrease of vegetation from 1976 to 1988 and from 1988 to 2003 (Figure 6.9). The total vegetation fraction in 1976 is 42.1% compared to 5.8 %, and 2.3% in 1988 and 2003, respectively.

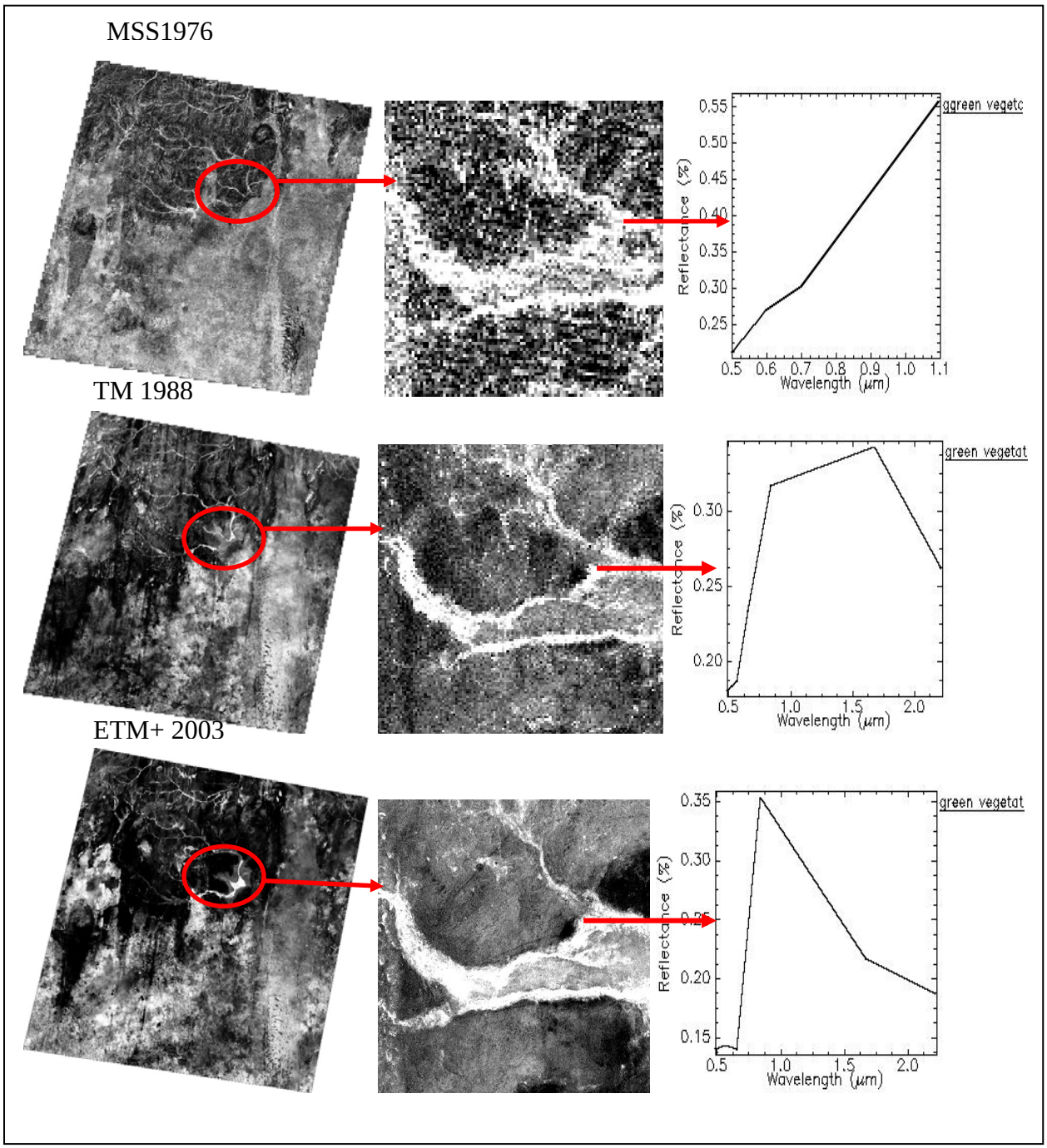

Fig 6.9: Fraction images and spectral reflectance of vegetation for Landsat used in analysis (*Brightness indicates a high fraction of vegetation)*

The correlation of vegetation fraction in 1976 proves very low negative correlation with 1988 (r = -0.03), while the correlation between 1988 and 2003 shows positive correlation (r = 0.4). This result demonstrates that the decreasing pattern of vegetation from 1976 to 1988 is very high meanwhile this pattern remained slightly low for the period 1988 to 2003. The comparison between the change in vegetation and sand fractions in the study area shows very high increase in sand soil and decrease in vegetation cover during the addressed periods (Figure 6.10). This indicates that the area had been subjected to desertification processes with special regard to wind erosion and denudation of vegetation cover as desertification indicators.

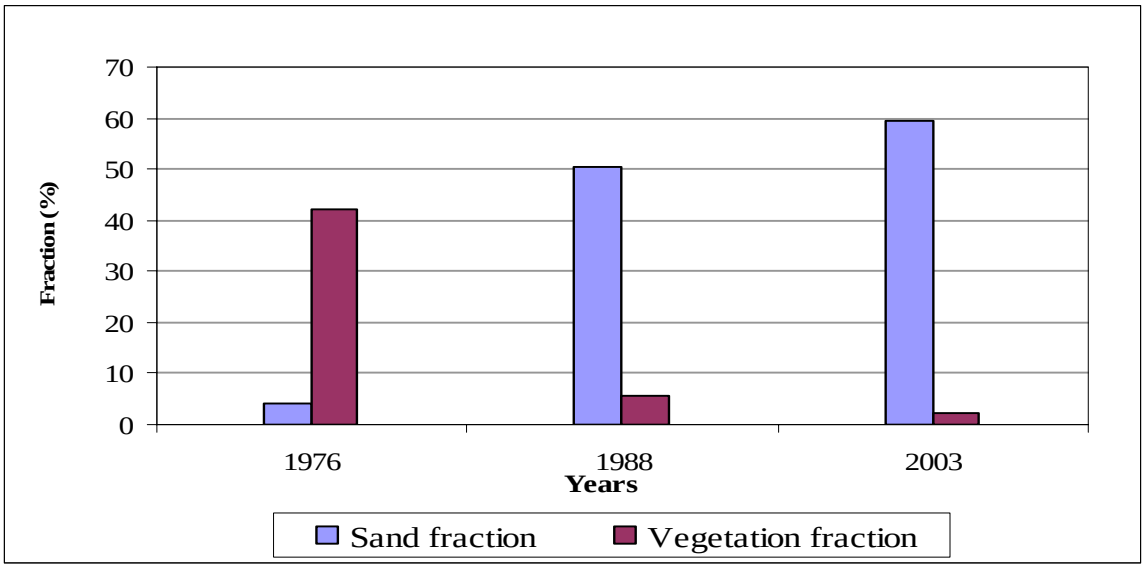

Fig 6.10: Comparison between sand and vegetation fractions during addressed period 1976-2003

The visual interpretation of the vegetation fraction image of 1976 (Figure 6.9) demonstrates that vegetation cover in the southern part is decreasing in 1988, while in 2003 the southern part of the study recovered compared to 1988. Referring to the spectral reflectance of vegetation cover in ETM+ 2003 (Figure 6.9), vegetation shows a curve very similar to the standard signature printing for good coverage of healthy vegetation. On the other hand the signature of vegetation of TM 1988 was comparatively different from the standard one. This can be attributed to better growing conditions for vegetation during 2003 due to high rainfall (400mm in 2003). However, good status of vegetation cover during 2003 on compact non-cracking clay soil (*gardud*)[3] could be attributed to the hardness of these soils which are not suitable for traditional rainfed agriculture.

[3] *gardud* soil is non-cracking compact clay soil with dark colour

6.2.3 Shade fraction

The shade fraction in the study area accounts for the shading due to variation in lightness related to local incidence angle, and shadows in hilly areas in the northern part of the study area. The visual interpretation and statistical calculation of shade fraction illustrates very high average fraction in 1976 (50.3%), in 1988 (45.4%) and in 2003 (55.8%).

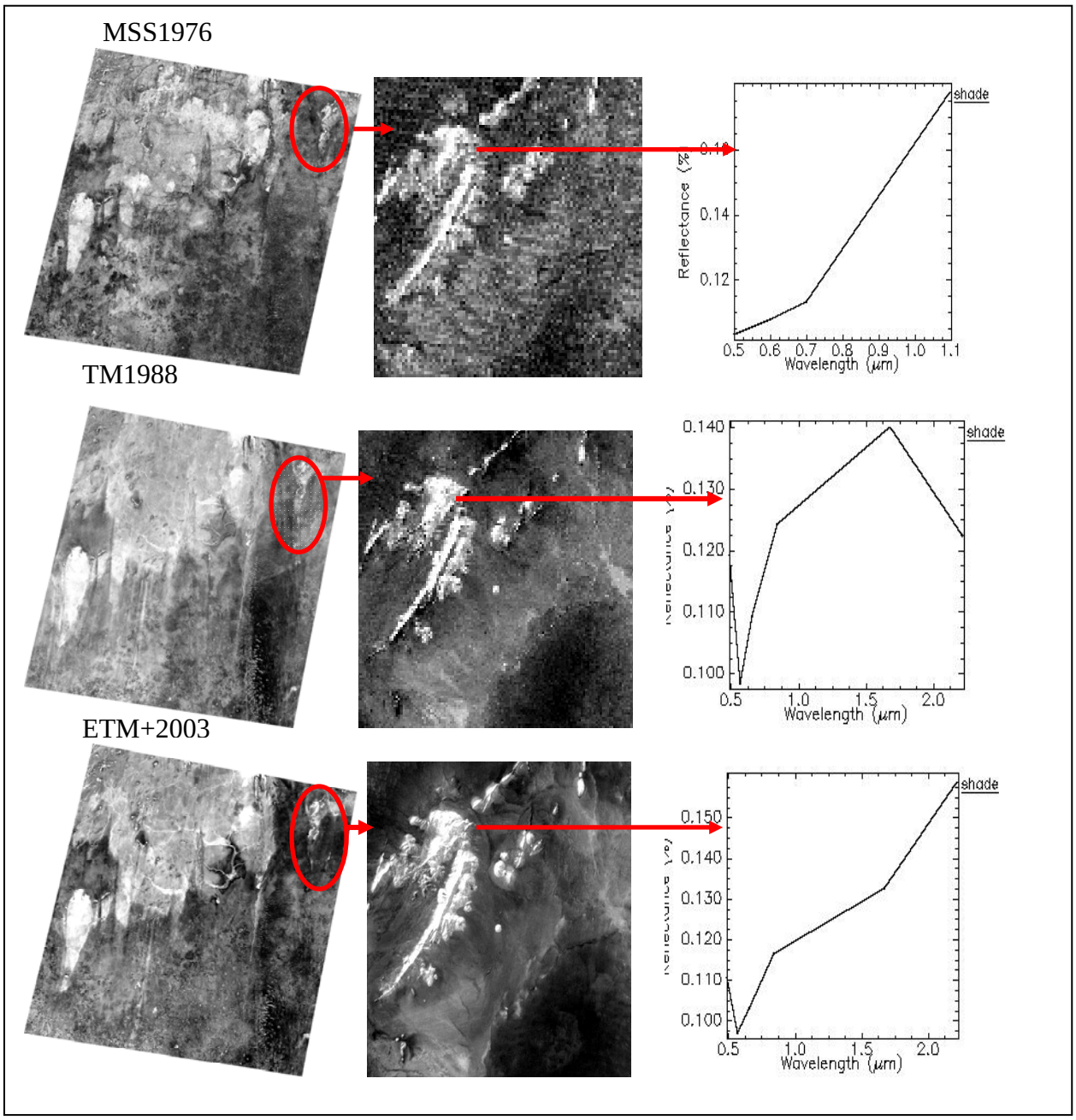

Fig 6.11: Shade fraction images and spectral reflectance of shade for Landsat data used in analysis *(Brightness indicates the high fraction of shade)*

As it is shown in the fraction image (Figure 6.11) shade concentrates in the hilly areas in the northern part of the study area and includes also the protected areas under these hills which are dark clay soil (*gardud)*. Shade fraction in 1976 shows negative low correlation with 2003 (r = -0.1) compared to positive low correlation with 1988 (r = 0.3) (Table 6.3). This result indicates that the shade is increased in 2003. Negative correlation between shade fraction and vegetation fraction in the addressed period indicates that normalization of shade to account of vegetation fraction in this study was not useful, because the area was not covered with dense vegetation canopy. However, the approaches of normalisation of shade are very useful in environment where the shade is strongly correlated with vegetation cover (Smith *et al.*, 1990).The study area, as mentioned before, is open canopy and mostly hilly in the northern part with some vegetated between the *Wadis*. Figure (6.12) illustrates the digital elevation image which was produced from a Shuttle Radar Topography Mission (SRTM) image of the study area. It demonstrates obviously the hilly areas and clay soil *gardud* protected by barriers in the northern part of the study area. Also it detected the window corridors and the sand encroachment from north to south direction.

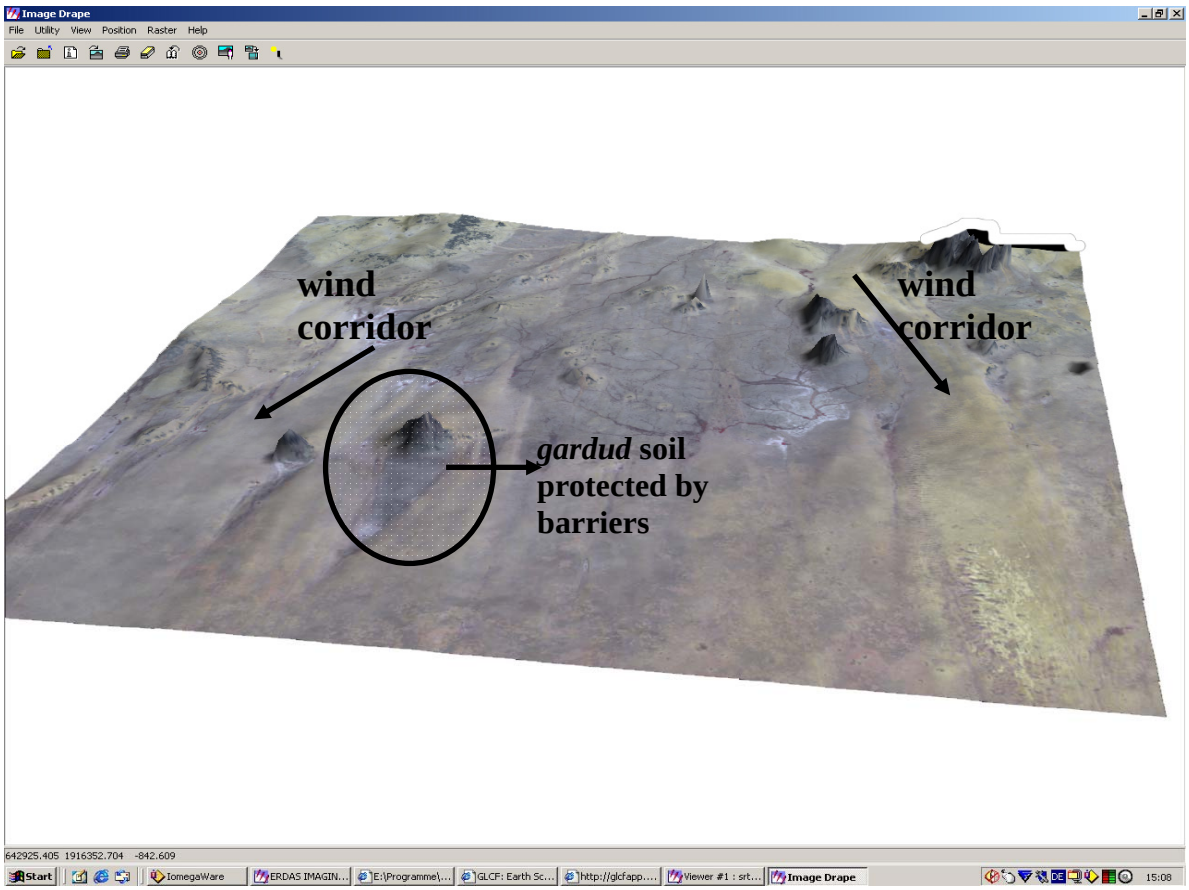

Fig 6.12: Digital elevation image of the study area based of SRTM data of 2003

(Developed by the author 2006)

Comparison between shade, green vegetation salt soil and sand fractions is shown in Figure 6.13. These four endmembers (shade, green vegetation, salt and sand) are compared for each of years 1976, 1988, and 2003 by using analysis of variance (ANOVA) for testing statistically to what extend these fractions are different and/or similar during the addressed period. The RMS error for the three years is also compared. The analysis of variance indicates significant differences (P =< 0.001) between the four endmembers during the addressed period. RMS error for 1976, 1988 and 2003 shows that there is no significant difference (P = 0.997) between different years (Appendices, 2, 3, 4, 5 and 6).

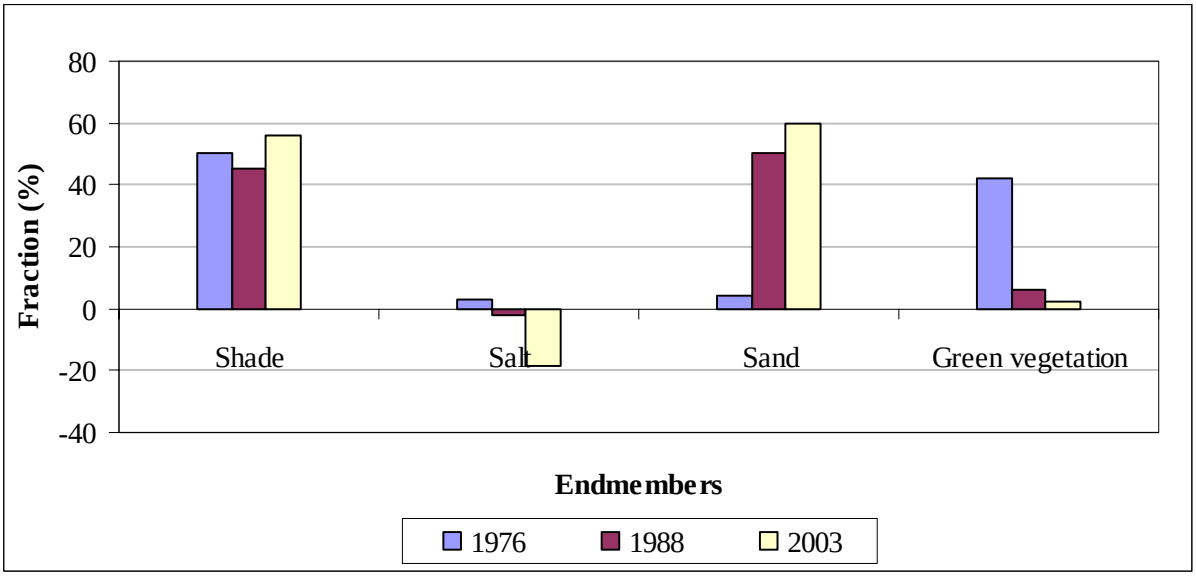

Fig 6.13: Comparison between the four endmembers fractions in the addressed periods

Using the nonlinear regression models and Curve Expert[4] by aid of Sigma Stat software the study measured the trend for shade, green vegetation, salt soil and sand soil during the addressed period. Figures 6.14a, 6.14b, 6.14c and 6.14d show this trend by using exponential transformation for each endmember during the different time. It is clear from the sand soil curve that the sand soil trend line increase with time. This pattern is similar for shade fraction while salt soils and vegetation show a decreasing trend. This finding agrees with the above mentioned facts derived from visual interpretation.

[4]CurveExpert 1.3 is a comprehensive curve fitting system for Windows. It employs a large number of regression models (both linear and nonlinear) as well as various interpolation schemes to represent data in the most precise and convenient way

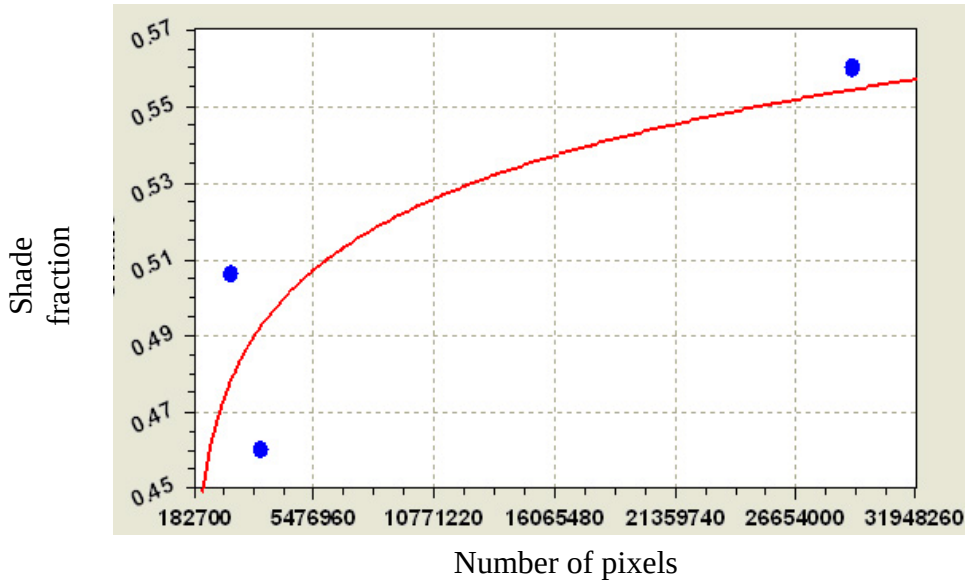

Fig 6.14a: Trend line of increasing shade fraction

$Y = ax^b$
Coefficient Data:
a = 0.21516373
b = 0.055172247
Standard Error: 0.0446898
Correlation Coefficient: 0.7962009

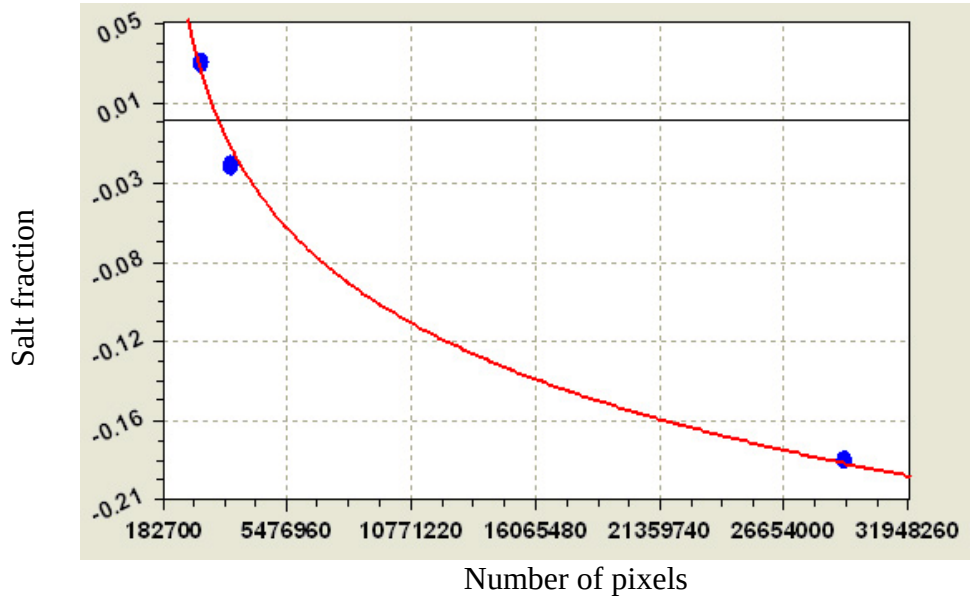

Fig 6.14b: Trend line of decreasing salt fraction

Y = a+b*ln(x)
Coefficient Data:
a = 1.1214523
b = -0.076029774
Standard Error: 0.0107306
Correlation Coefficient: 0.9977

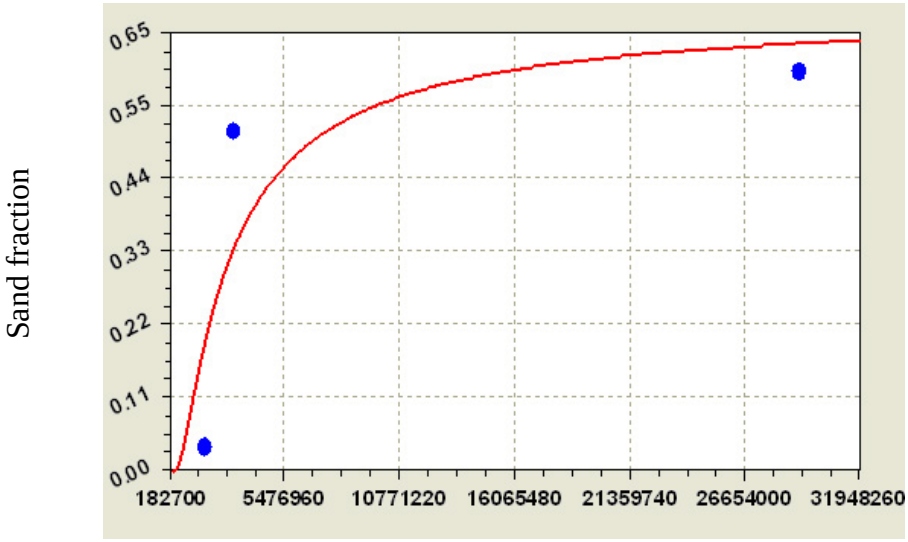

Fig 6.14c: Trend line of increasing sand fraction

Y = a*exp (b/x)
Coefficient Data:
a = 0.69014622
b = -2254605.1
Standard Error: 0.2388152
Correlation Coefficient: 0.8257815

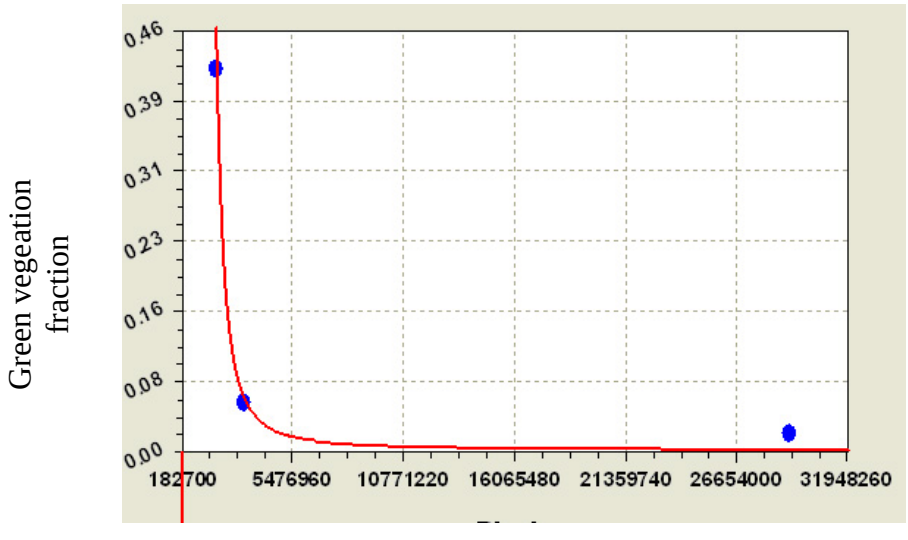

Fig 6.14d: Trend line of decreasing green vegetation fraction

Y = a*exp (b/x)
Coefficient Data:
a = 0.0042341075
b = 8407447.7
Standard Error: 0.0183441
Correlation Coefficient: 0.9982738

6.4 Visualization of the EMI images

The results of Eolian Mapping Index (EMI) analysis for MSS 1976, TM 1988 and ETM+ 2003 are revealed in Figures (6.15a, 6.15b and 6.15c), respectively. EMI allows for mapping the level of vulnerability of surfaces to wind erosion in the study area (Chavez, 1992). EMI generate an image which maps the areas related to the amount of vegetation density and bare high reflectance soils. Using the combination of (NIR, R and R/NIR) as RGB composite the resulting image highlights areas with low vegetation density and high surface soil reflectance in various shades of yellow colour. The pixels having duller shade of yellow are generally areas that have medium to high vulnerability of wind than the brighter ones, while the non-yellow areas having little or no wind erosion potential. From visual interpretation of EMI imagery for 1976, 1988 and 2003 it is clear that in 1976 the potential of wind erosion is very low (c) in the northern part of the study area (Figure 6.15a). The dull tone of yellow colour (c) indicates the high density of vegetation cover and low reflectance of soil. This result is corresponding to the finding by SMA analysis which indicates also the high fraction of vegetation and low fraction of sand in 1976. It also highlights that areas of sand dunes and sand sheet have high vulnerability (a) to wind erosion compared to *gardud* soil.

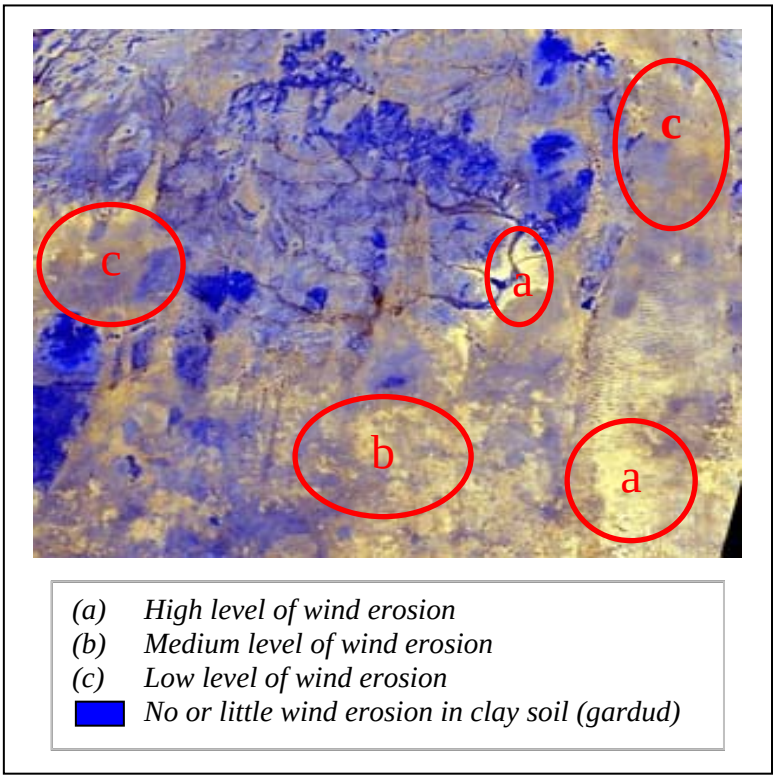

Fig 6.15a: EMI image of MSS 1976 of the study area

The brighter tone of yellow colour (a) indicates the low density of vegetation cover and high reflectance of soil. Nevertheless the EMI image shows some southern part with medium level (b) of wind erosion and low level (c) of wind erosion in northern part due the good status of vegetation coverage in these areas.

Figure (6.15b) shows the EMI image of 1988. The very brighter tone (a) of yellow occurs in northern part and southern part especially in sand dunes and sand sheet areas. These areas in 1976 appeared to have low wind erosion potential (Figure 6.15a). Thus a very high level of vulnerability to wind erosion in 1988 compared to MSS 1976. Related to spectral mixture analysis of MSS 1976 the decrease of vegetation cover from 1976 to 1988 led to increase the susceptible topsoil to wind erosion and encroached sand creeping southwards in the study area.

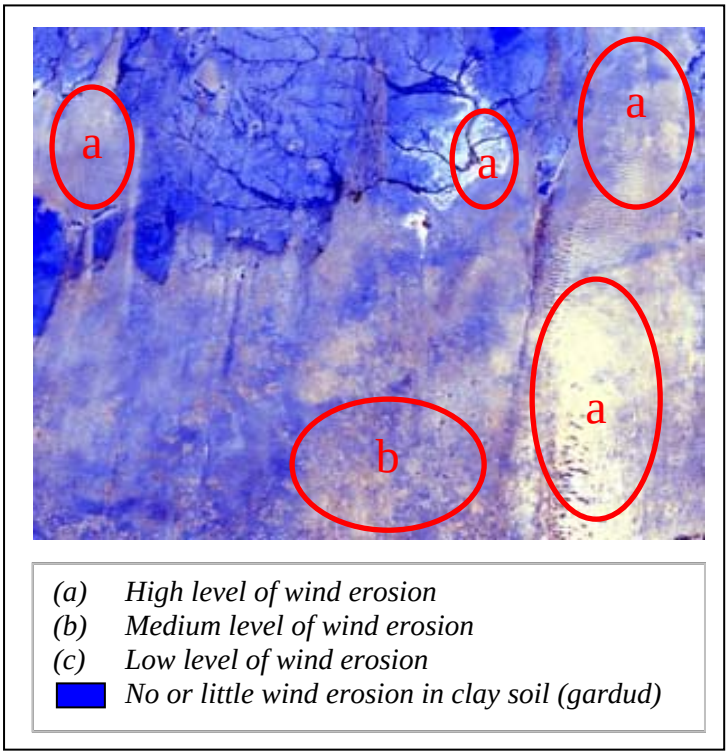

Fig 6.15b: EMI image of TM 1988 of the study area

EMI of ETM+ 2003 explains that very brighter tone (a) of yellow occurs in northern part and southern part especially in sand dunes and sand sheet areas. Meanwhile there is good status of vegetation cover in some parts of the study area which is indicated by very dull yellow tones (c) (Figure 6.15c). This recovery reduces the wind erosion in these areas despite their over-exploitation in different land uses. In 2003, upper left portion of the study area shows low vulnerability as indicated by the very dull tone (c) while in 1988 demonstrates higher

vulnerability level to wind erosion (a). This finding supports the visual interpretation result of SMA image 2003 which indicates recovery of vegetation cover in this area (Figure 6.9).

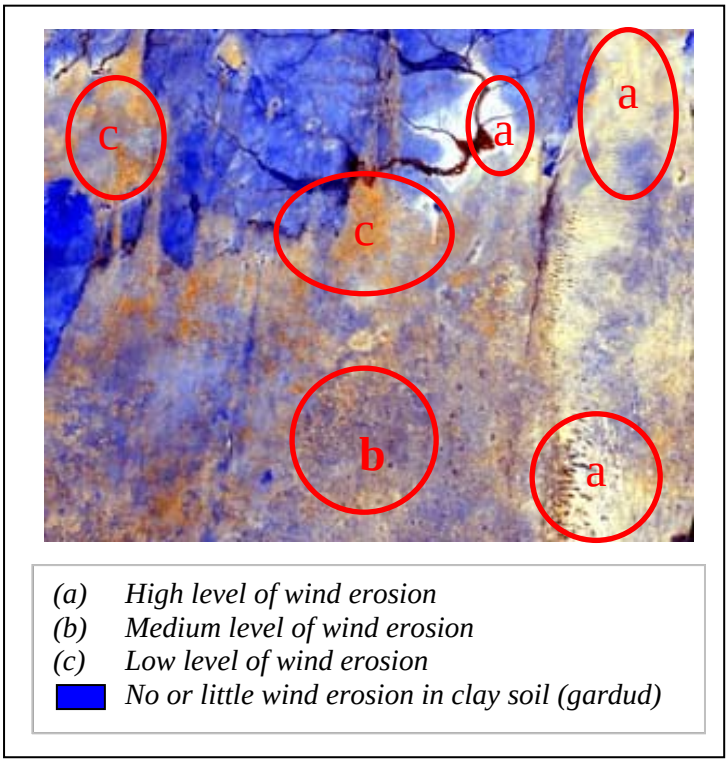

Fig 6.15c: EMI image of ETM+ 2003 of the study area

The visualisation and interpretation of EMI imagery of MSS1976, TM1988 and ETM+2003 gives a guide to the relative level of erosion potential and vulnerability to wind. The salt soil areas in northern part appear in very bright colour which indicates their high vulnerability to wind erosion. This could be attributed to human activities related to tree cutting for salt production. The comparison of the three EMI imagery of the study area shows that the vulnerability to wind erosion is increase in sand dunes and sand sheet soils and less or even nil in clay (*gardud)* soil. This could be due to the strong compactness of this soil which obstructs its use in traditional rainfed agriculture. The results obtained by SMA analysis are compatible with visual interpretation of EMI results. This relatively supports the finding of increasing degradation processes and thus sand encroachment in the study area during the addressed periods. The visualisation of EMI imagery by using multispectral MSS, TM and ETM+ data explain easy and practical method to generate a wind erosion vulnerability image (WEVI) of the study area. Figure (6.16) shows different situations of wind erosion processes in the study area related to affected trees such as *Balantites aegyptiaca*.

(a) (b)

Fig 6.16: Effect of the wind erosion in the study area (a) *Balantites aegyptiaca (Higlig* tree) in the northern part of the study area during the rainy season, (b) *Balantites aegyptiaca* in the southern part of the study area during dry season (Photograph by the author 2006)

6.5 Change detection analysis

6.5.1 Endmembers fraction change detection

6.5.1.1 Vegetation fraction change

Qualitative changes in the vegetation fractions are visually interpreted by displaying fractions for year 1976 in blue, year1988 in green and year 2003 in red (Figure 6.17). The visual interpretation of colour composite imagery shows that the major changes have the most saturated colours while minor changes have less saturated colours. White and grey tones indicate no temporal change. Figure (6.17) demonstrates the change in vegetation fraction during 1988 in the study area which, characterised by saturated green colour as in area (b). The southern part of the study area illustrates a good status of vegetation cover during 2003 as shown by dominant saturated red colour (a). Sand dunes show stable vegetation cover during the addressed period related to the bright white tone as highlighted in (d). The northern part shows higher fractions of vegetation cover during 1976 in comparison with the other years as it is clear from high saturated blue colour as in area (c).

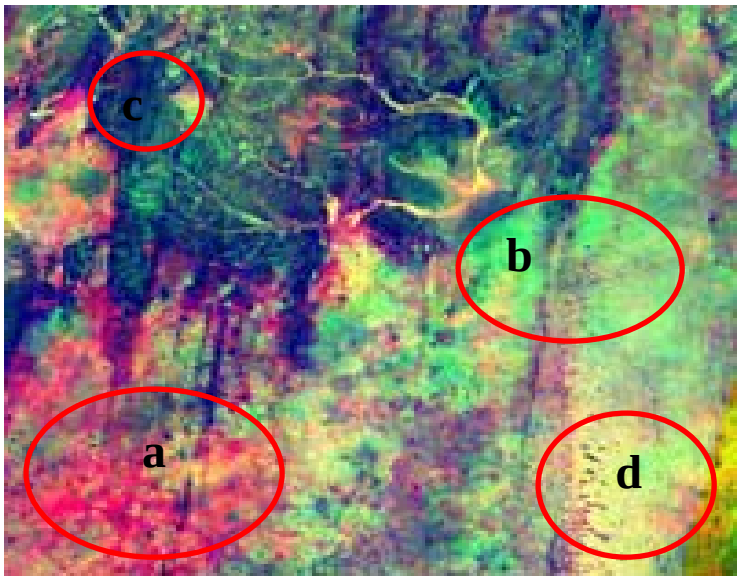

(a) Change in 2003 *(c) Change in 1976*
(b) Change in 1988 *(d) No change*

Fig 6.17: Colour composite image of vegetation fractions *(1976 in blue, 1988 in green and 2003 in red)*

6.5.1.2 Sand fraction change

Figure (6.18) illustrates the colour composite of sand fractions of years 1976, 1988 and 2003 displayed in blue, green and red, respectively. The northern part of the study area shows drastic change in sand fraction. However, the area around *Wadis* highlights a stable sand fraction as in area (c) which is still dominated by a saturated colour related to 1976. Increase in sand fraction during 1988 constitutes the major dominant change in the study area as shown in area (b). During 2003 sand fraction is increasing in the upper right portion of the study area as shown in area (a). The southern part is undergone a rapid increase in sand fraction as revealed in area (b) which shows saturated green colour. The sand dunes demonstrates a stable status of sand fraction during the addressed period as exposed in area (d) with dominant white colour. The visual interpretation of colour composites proves an increase of sand in the study area, and hence distinguishes the temporal changes. The visual interpretation of the colour composite image explains in a very practical and simple way the changes in vegetation and sand soil fractions. The results prove the usefulness of spectral mixture analysis in producing abundance fractions for categorising land covers classes in the study area.

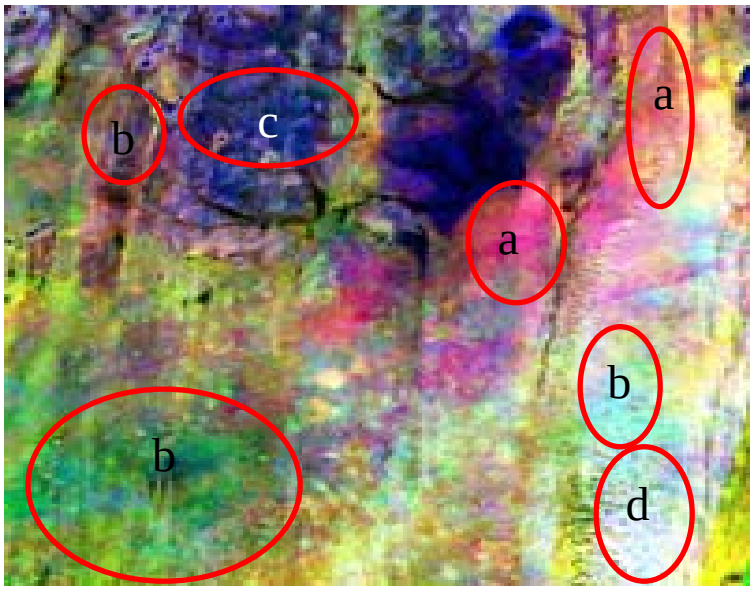

(a) Change in 2003 *(c) Change in 1976*
(b) Change in 1988 *(d) No change*

Fig 6.18: Colour composite image of sand fractions *(1976 in blue, 1988 in green and 2003 in red)*

6.5.2 Change Vector Analysis (CVA)

The sand and vegetation fractions from SMA were used as an input for Change Vector Analysis (CVA) to stratify and analyse desertification processes in the period of 1976 to1988 and of 1988 to 2003. The resulting images of CVA display magnitudes and directions of the changes[5]. The change detection image was generated from the colour composite of the magnitudes and angle of change direction in vegetation fraction. Since only sand and vegetation fractions were applied in this analysis, only three possible classes of change were being recognised (Table 6.4).

Table 6.4: Possible change classes from both input and related types of change

Class name	Sand fraction	Vegetation fraction
Desertified	+	-
Re-growth	-	+
Persistence	+ -	+ -

[5] Detail interpretation of this phrase in Part III

The desertified areas in CVA are characterised by an increase of sand fraction and decrease in vegetation fraction. This is measured by a positive angle of sand fraction and a negative angle of vegetation fraction. The re-growth class was characterised by an increase of vegetation cover and a decrease of sand soil. The persistence class was indicated by simultaneous increase or decrease in both sand and vegetation fractions. The examples of the change classes are presented in Figure (6.19) between 1976 to 1988 and 1988 to 2003 respectively. The threshold of final magnitude was defined for each change class by interactive adjustments (Table 6.5). Hybrid unsupervised/supervised classification approach was used to classify the image of change vector and angles.

Table 6.5: Magnitude threshold of change for each class during 1976-1988 and 1988-2003

Class name	**Threshold 1976/1988**		**Threshold1988/2003**	
	Magnitude	**Angle of vegetation (degrees)**	**Magnitude**	**Angle of vegetation (degrees)**
Desertified	39	129	25	123
Re-growth	100	15	24	21
Persistence	7	30	17	79

6.5.2.1 CVA of period 1976 to 1988

The classified image of magnitude and direction with reference to the years 1976 and 1988 (Figure 6.19) highlights an intensive dynamics related to the different classes during this periods characterised by the increase of sand soil and decrease in vegetation cover in the study area. The change image as presented in Table 6.6 shows that the desertification class covers about 83.35% of the total area. Meanwhile the re-growth and persistence classes cover only 12.2% and 4.4% respectively. This indicates the trend of increasing sand encroachment in the study area during this period. Persistence class in 1976 to 1988 covers 4.4% of the total area and it is dominating in hilly and *Wadis* areas in the northern part of the study area.

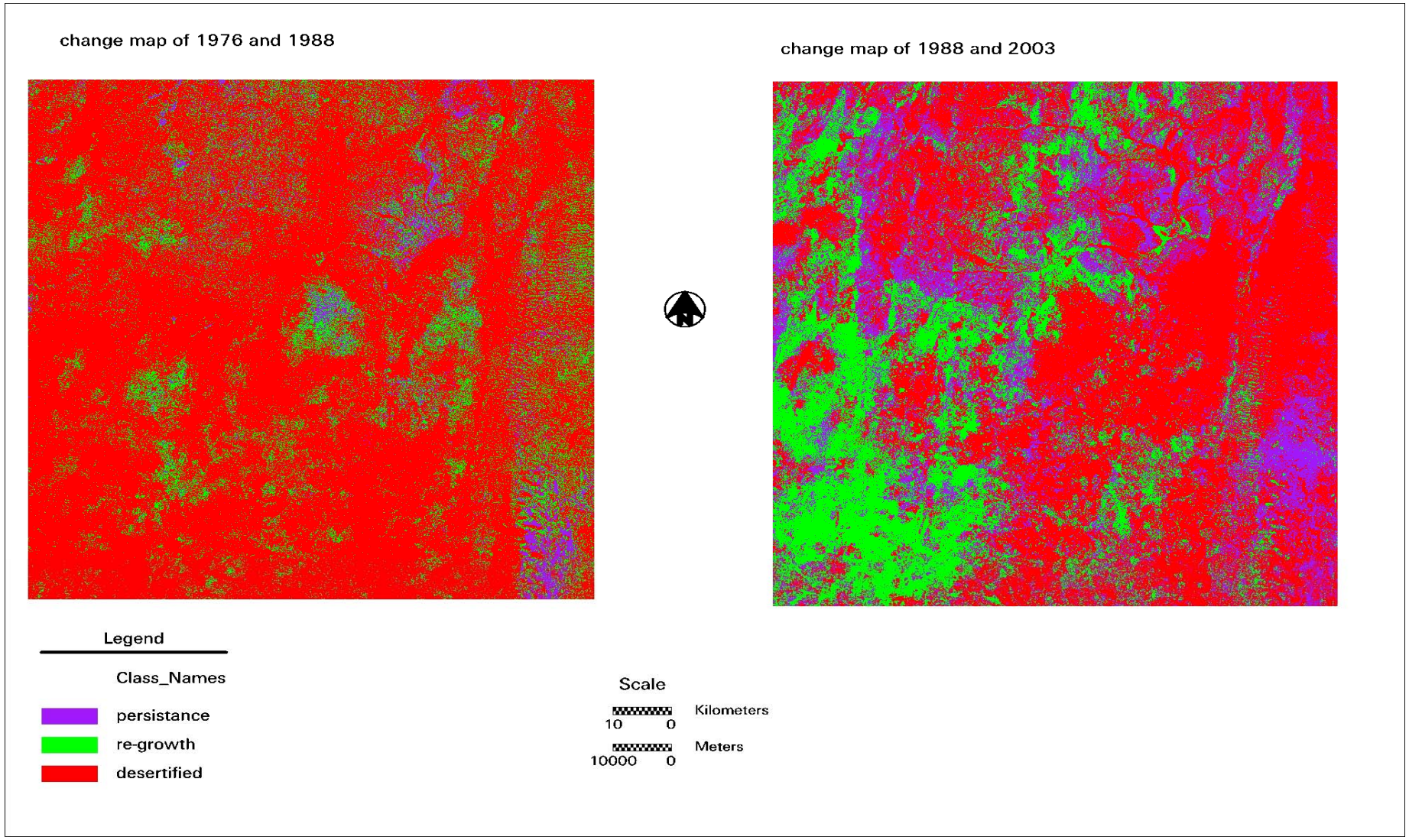

Fig 6.19: Classified image of CVA for periods 1976-1988 and 1988-2003

Table 6.6: Distributions of classes of change image 1976 and 1988

Class name	Area (ha)	Area (%)
Desertified	1979149	83.3
Re-growth	289935.5	12.2
Persistence	105944.6	4.4
Total	**2375029.1**	**100**

6.5.2.1 CVA of period 1988 to 2003

The change image referring to years 1988 and 2003 (Figure 6.19) reflects different patterns of change in desertified and re-growth classes. The desertified class appears to have very high intensity in the northern part of the study area. Meanwhile the re-growth class dominated in the southern west part of the study area. Contrasting with the change map of 1976 and 1988 indicates increase in the re-growth class in the study area in the addressed period. Table 6.7 shows that the re-growth class covers 17.9 % in the period of 1988 and 2003 compared to only 12.2% in period 1976 and 1988. Nevertheless, the desertified class is decreased to 60.9% during the periods 1988-2003 from 83.3% during the period 1976-1988. Period 1988 to 2003 in comparison with period 1976-1988 witnessed decrease in desertified areas and increase in re-growth areas (Figure 6.20). In addition, persistence areas relatively increased from 4.4% during period of 1976-1988 to 21.1% during the next period 1988-2003.

Table 6.7: Distributions of classes of change image for addressed period 1988 to 2003

Classes name	Area (ha)	Area (%)
Desertified	1446212	60.9
Re-growth	426821	17.9
Persistence	499783.2	21.1
Total	**2372817**	**100**

This result is contradict with the findings of SMA fractions which indicates that sand fraction is highly increased during period 1976-1988 compared to slightly increase during period 1988-2003(Figure 6.10).This could refer to the reliability of SMA in classifying sand and vegetation cover compared to CVA. SMA provides the spectral data in terms of multiple endmember fraction coverage and not as a single pixel classification, hence allowing a more detailed analysis of pixel contents (Adams *et al*., 1993). As shown in Figure (6.19), desertified class dominates on sand dunes and sand sheets. On the other hand, green vegetation is recovered during 2003 in the southern west part which is mostly covered by compact non-cracking clay soil (*gardud*). Additionally, field survey in January 2004 proves that these areas suffer from lack of ground water and intensive use for Gum Arabic production. Therefore the

pattern of heavy grazing and shifting cultivation is less in comparison with *qoz* and sand dunes. With reference to the acquired meteorological data, the annual precipitation in study area during 2003 was comparatively high (400 mm/annum). The vegetation cover in 2003 revealed relatively good coverage compared to 1988. Thus, the amount of rainfall is suggested to be one of the most factors responsible for variability in re-growth of vegetation cover during the addressed periods.

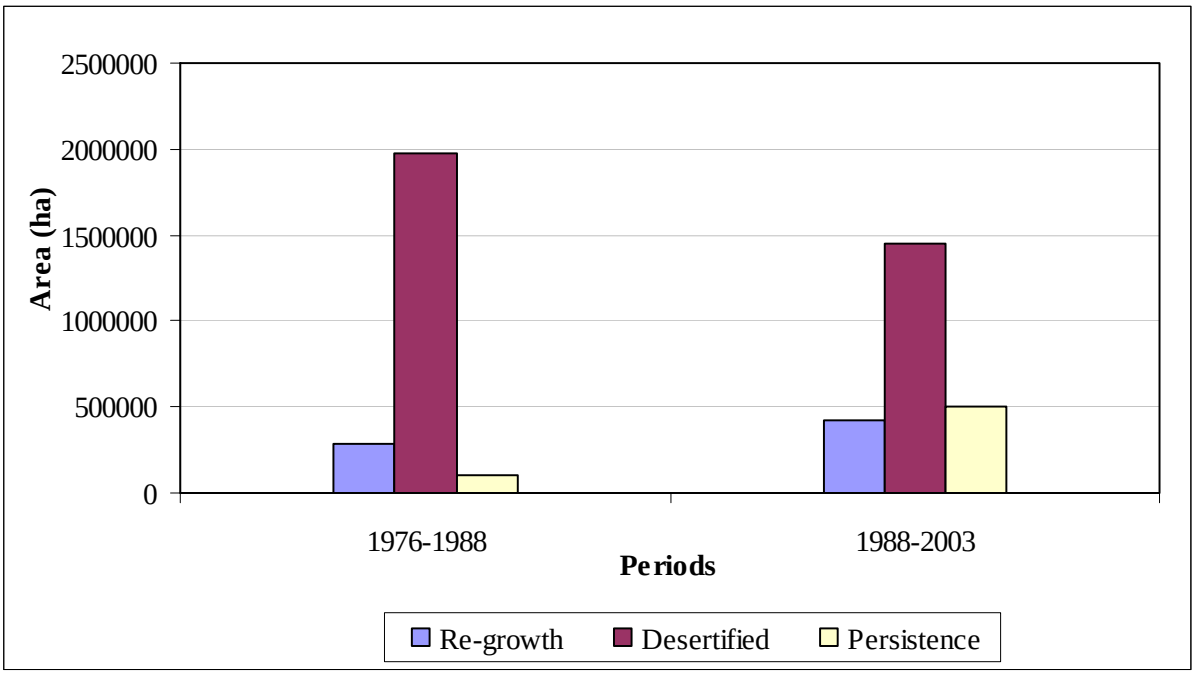

Fig 6.20: Comparison between classes from change vector maps of 1976-1988 and 1988-2003

6.6 Discussion of dynamics of change

6.6.1 Dynamics of change during the period 1976-1988

Based on the visual interpretation of the change map for the period 1976-1988, in addition to information obtained during field surveys, secondary data and relevant literature, it can be indicate that a rapid encroachment of sand and high decrease of vegetation cover in the study area is evident. Figure (6.21), includes a subset of the change map of 1976-1988, showing the most affected areas with desertification in the northern part of the study area. In this regards, findings of both SMA and CVA illustrate that the sand soil has been rapidly increased during the period 1976-1988.

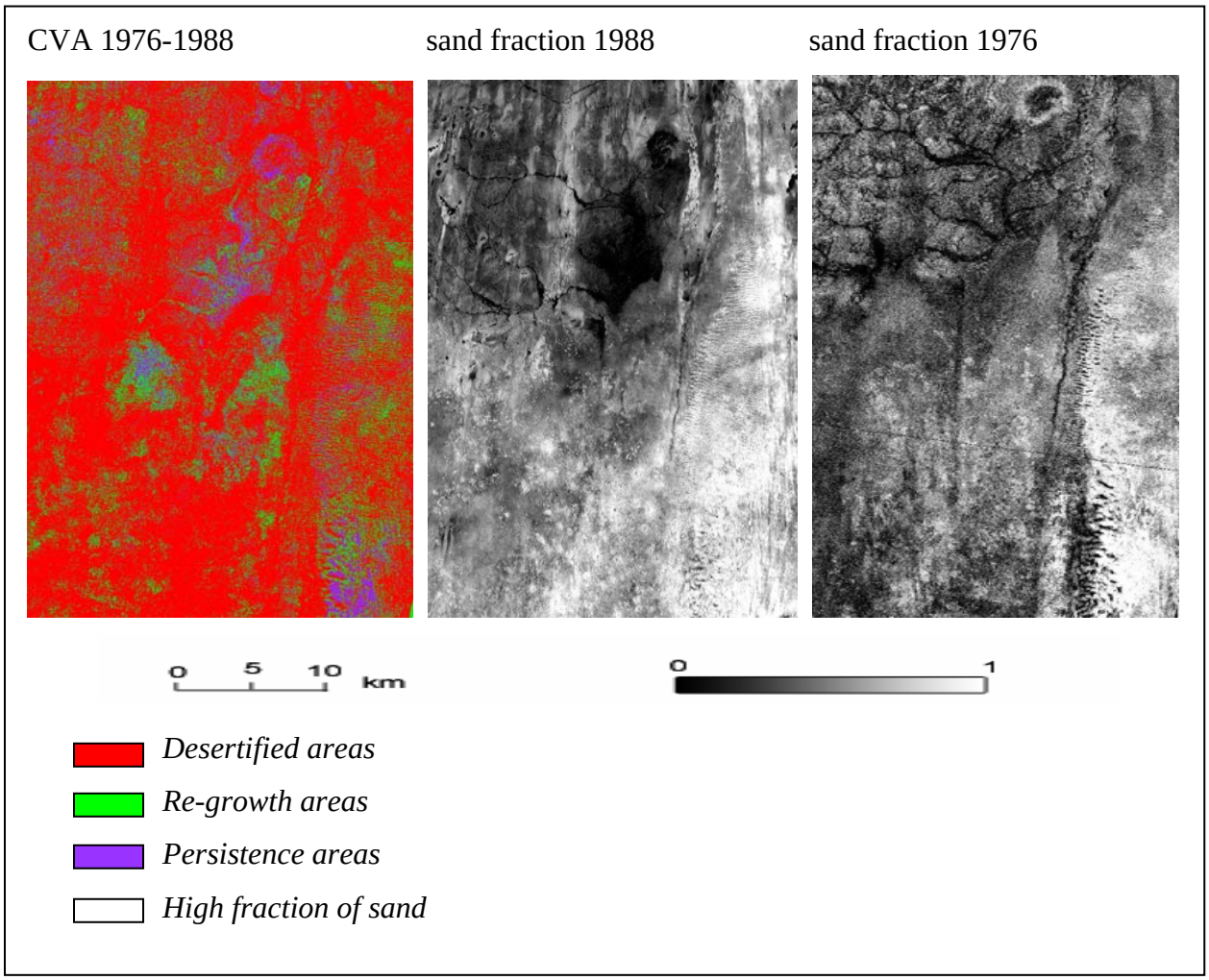

Fig 6.21: Subsets of change map of 1976-1988 and fraction image of sand 1988 and 1976 of northern part

In the northern part of the study area the pattern of change evidently highlights the pressure of human interferences and its negative effects on fragile natural resources. These pressures are related to overgrazing by livestock and rainfed agriculture. Continuous use of rangelands in northern part, particularly the heavy grazing during the wet seasons, when vegetation cover is actively growing, by sedentary as well as nomadic and semi-nomadic tribes, results in degradation of vegetation cover and exposition of soil to wind erosion. Rangelands degradation is further aggravated by expansion of the areas under shifting cultivation and thus leading to destruction of vegetation cover in these areas. It is extensively recognised that most of the pastoral nomadic tribes are concentrated in the northern part of the study area. Many of these tribes such as *Kababish, Hawaweer and Kawahla* raise animals, especially camels and sheep which are eventually enhancing severe uprooting of trees and shrubs (Analysis of field survey, 2004). During the drought periods of 1980s and early 1990s and due to increasing total population as shown in Figure (6.22), the study area was subjected to severe grazing

pressure from nomadic tribes. It is suggested that increasing population is one of most important driving factor for desertification in the study area .The field observations showed evidently the overgrazing around *Bara, Elbashiri* and *Elmazrub*, particularly by the herds of camels, sheep, and domestic goats which had significant contributed to the expansion of desert encroachment in the area. Moreover, the growth of livestock during over the selected years in study area (Table 6.8) shows that total population of livestock especially cattle and camels, has been declined following the 1984 drought. Those tribes which had lost their animal changed to rainfed shifting cultivation. This could be an important factor for land use changes which led eventually to an increase of cultivated areas which is normally combined with trees clearing and hence land degradation. Nevertheless, the increased livestock population in the 1990s also subjected the study area to over-grazing pressure.

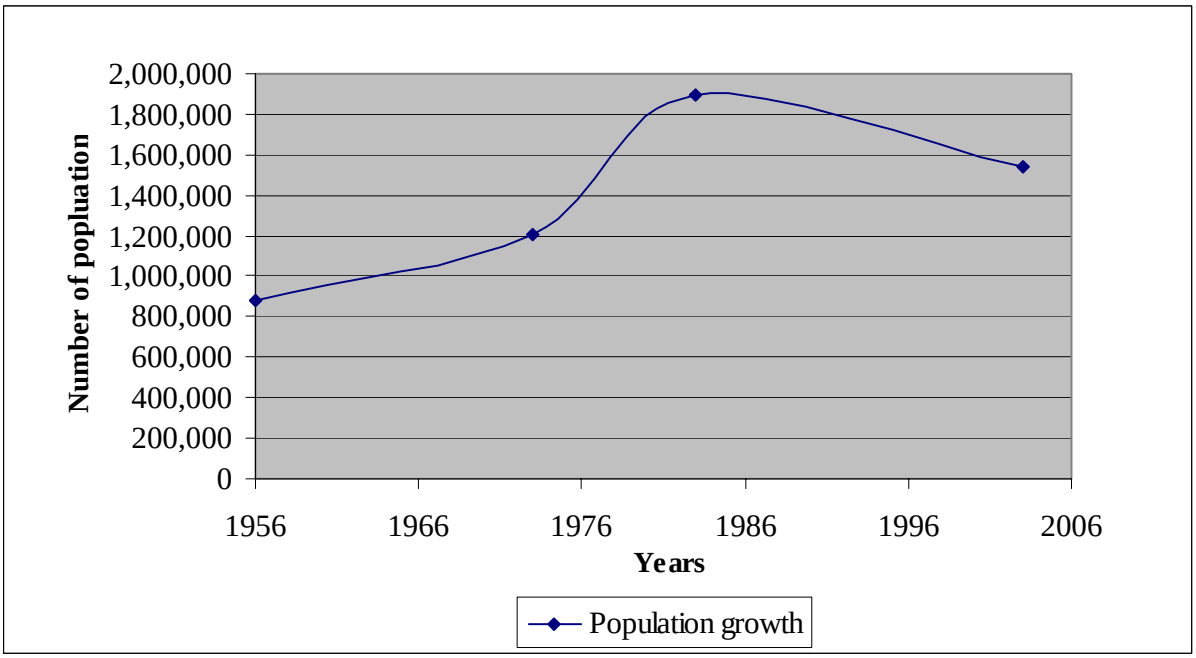

Fig 6.22: Population breakdown in North Kordofan (UN, 2003)

Table 6.8: Livestock population (in head) in Northern Kordofan State

Livestock type	1983	1998	1999	2000	2003
Cattle	1,187,573	489,943	507,524	525,487	562,785
Sheep	2,759,124	3,405,985	3,602,081	3,706,038	3,831,000
Goats	2,380,000	1,971,790	2,017,723	2,082,664	1,910,720
Camels	853,000	561,790	572,557	587,103	1,303,896
Total	**7,179,697**	**6,429,625**	**6,699,884**	**6,901,292**	**7,608,400**

Sources: (Ministry of Agriculture and Animal Wealth & UN, 2003)

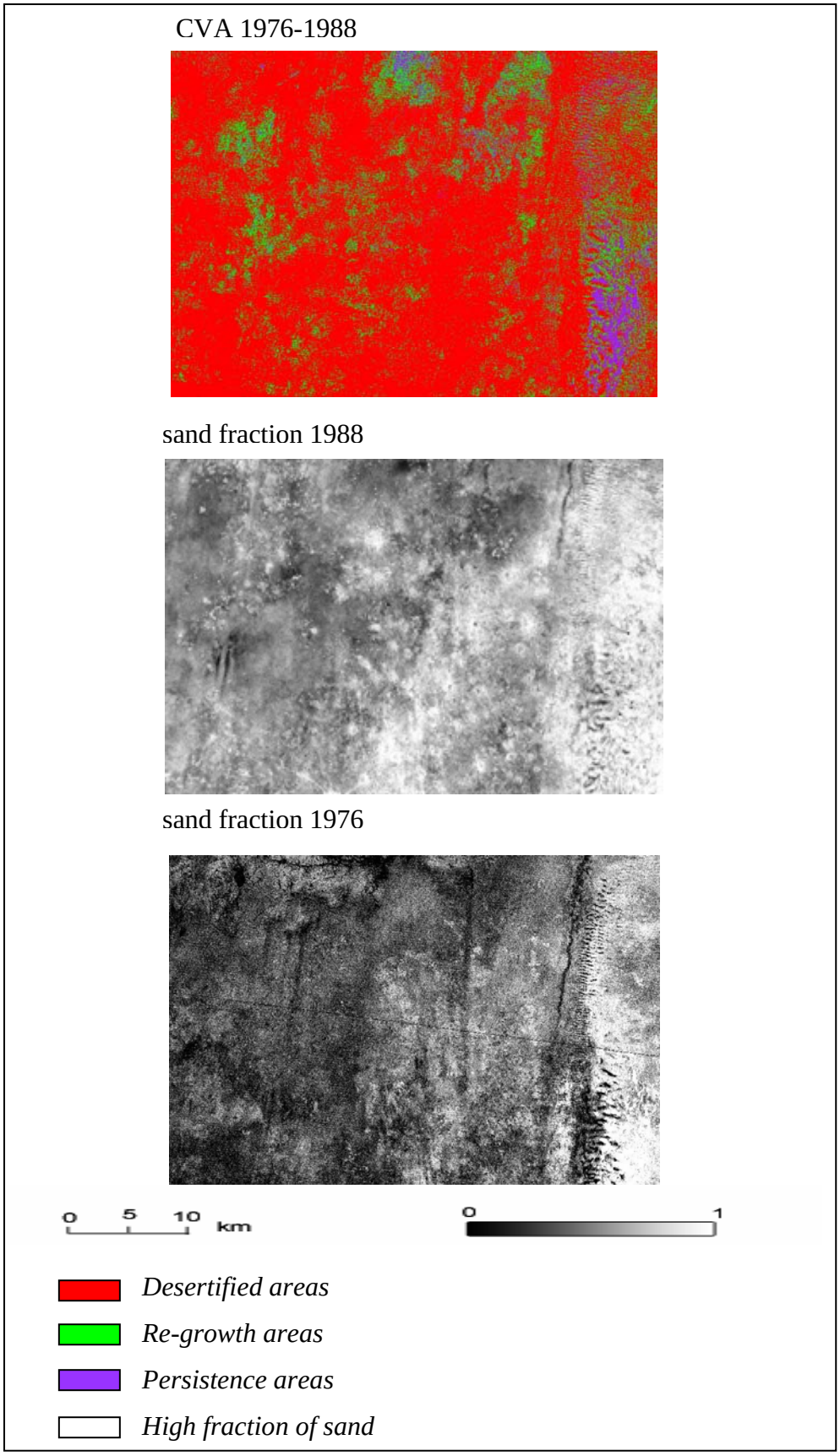

Fig 6.23: Subsets of change vector map of 1976-1988 and sand fraction image of 1988 and 1976 of the southern part

Figure (6.23), which based on subset of the change map of 1976-1988, shows the most affected areas with desertification in the southern part of the study area. Southern part has been severely affected by desertification especially in *gardud* and sand sheets areas around *Elmazrub, Elbashiri* and *Bara.* Increasing of desertified areas in both *gardud* and *qoz* soil is traced back to the impact of over-grazing and cultivation pressure in these areas. Local people stated that intensive grazing pressure has led to a decrease of palatable weed species such as *Dactyloctenium aegyptium (Aboasabeia), Eragrostis tremula (Bano) and Gisekia pharnacoides (Rabaa)* and removal of some tree species such as *Salvadora persica* (Analysis of field survey, 2004). These results agree with finding of Hellden (1988), stating that desertification in North Kordofan takes place through systematic expansions of desertified village and water hole perimeters. Figures 6.24 and 6.25 show the grazing practice around the villages and traditional methods for water taking from wells by traditional containers used for water transport and storage.

(a) (b)

Fig 6.24: Grazing lands and in the study area (a) accumulation of livestock around watering points in vicinity of *Damurat Eltom* village, (b) traditional methods for water taking from wells and containers used for water transport and storage (Photograph by the author Jan 2004)

(a) (b)

Fig 6.25: Different rangelands types in the study area (a) during rainy season, (b) during dry season (Photograph by the author 2004)

Another enforcing factor which contributes to an increasing of desertified areas in the southern part is pressure of traditional shifting cultivation performed by both the settlers and nomadic tribes who emigrated from the northern parts. During rainy season they cultivate some annual crops such as millet, sorghum and groundnuts for home consumption and fodder. In high precipitation season, farmers practice large scale cultivation of cereal crops. Accordingly, this severely reduces vegetation cover and leads to soil erosion in the southern part of the study area. This situation was extremely worsened in years of low precipitation, when farmers started to cultivate add land and uprooting the trees rather than conserving the vegetation cover and soil. Thus erosion of soil is highly profound under such conditions. Figure (6.26) shows the negative impact of human activities on natural resources during the rainy and dry season related to practices conducted in the traditional shifting cultivation and over-grazing. The problem was aggravated as result of pressure from an increase of human population as well as livestock numbers. This system of cultivation where leaves the land bare for to up nine months per year exposes soil to serious erosion and thus to increasing desertification in the study area. This finding is supported by conclusions of Yagoub *et al.* (1994) summarising that the land degradation and ecological imbalance in northern Kordofan was largely associated with the combined adverse effects of rainfall and mismanagement of land.

(a) (b)

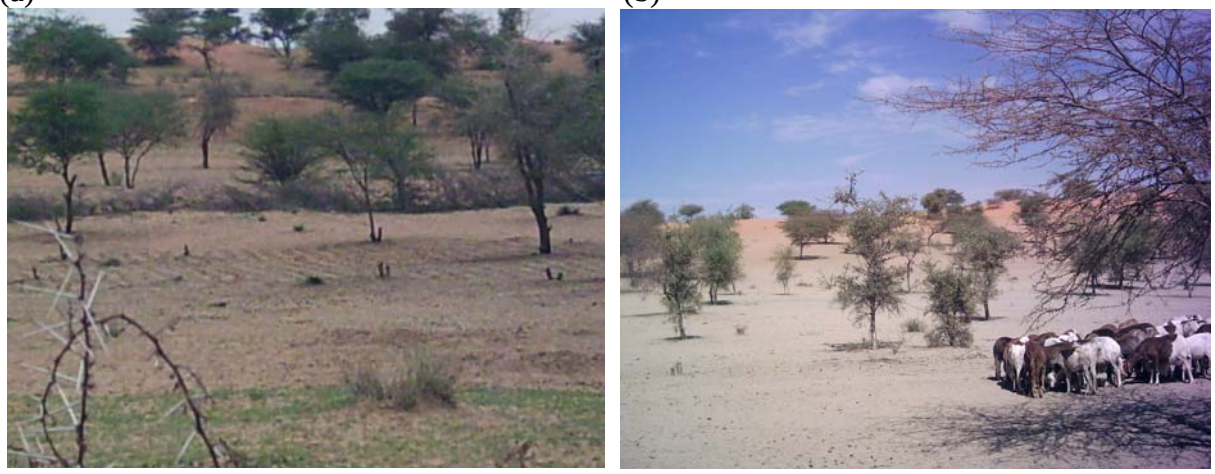

Fig 6.26: Human impacts in study area (a) clearance of trees for cultivation during dry season around *Bara* area (b) grazing in the *Elbashiri* area (Photograph by the author, Jan 2004)

6.6.2 Dynamics of change during period 1988-2003

CVA for the period 1988-2003 shows an increase in the re-growth class and a decrease in the desertified class. In addition persistence areas increased and concentrating mainly on *Wadi* areas in the northern part as shown in Figure 6.27. Noticeably, vegetation cover is well developed in these *Wadis* due to the fertile soil and water availability. From field surveys, it is well observed that *Acacia mellifera* (*Keetr* tree) grew well in these areas. Visual interpretation of Figure (6.27) demonstrates the dominant re-growth in the southern western part of the study area which is dominated by *gardud* soil as mentioned before. Meanwhile the desertified class is still dominant in sand dunes and sand sheet areas. From the geographical point of view, the study area is located in the semi-arid eco-climatic zone with very harsh conditions and diverse human activities. No doubt, under these circumstances man plays a pivotal and persistent role in causing and/or combating desertification processes in the study area. Increase of traditional shifting cultivation is considered to be one of the major factors for land degradation in the study area. Figures 4.28 and 4.29 show an increase of total cultivated areas in *Bara* and *Sodari* localities during 1989 to 2000.

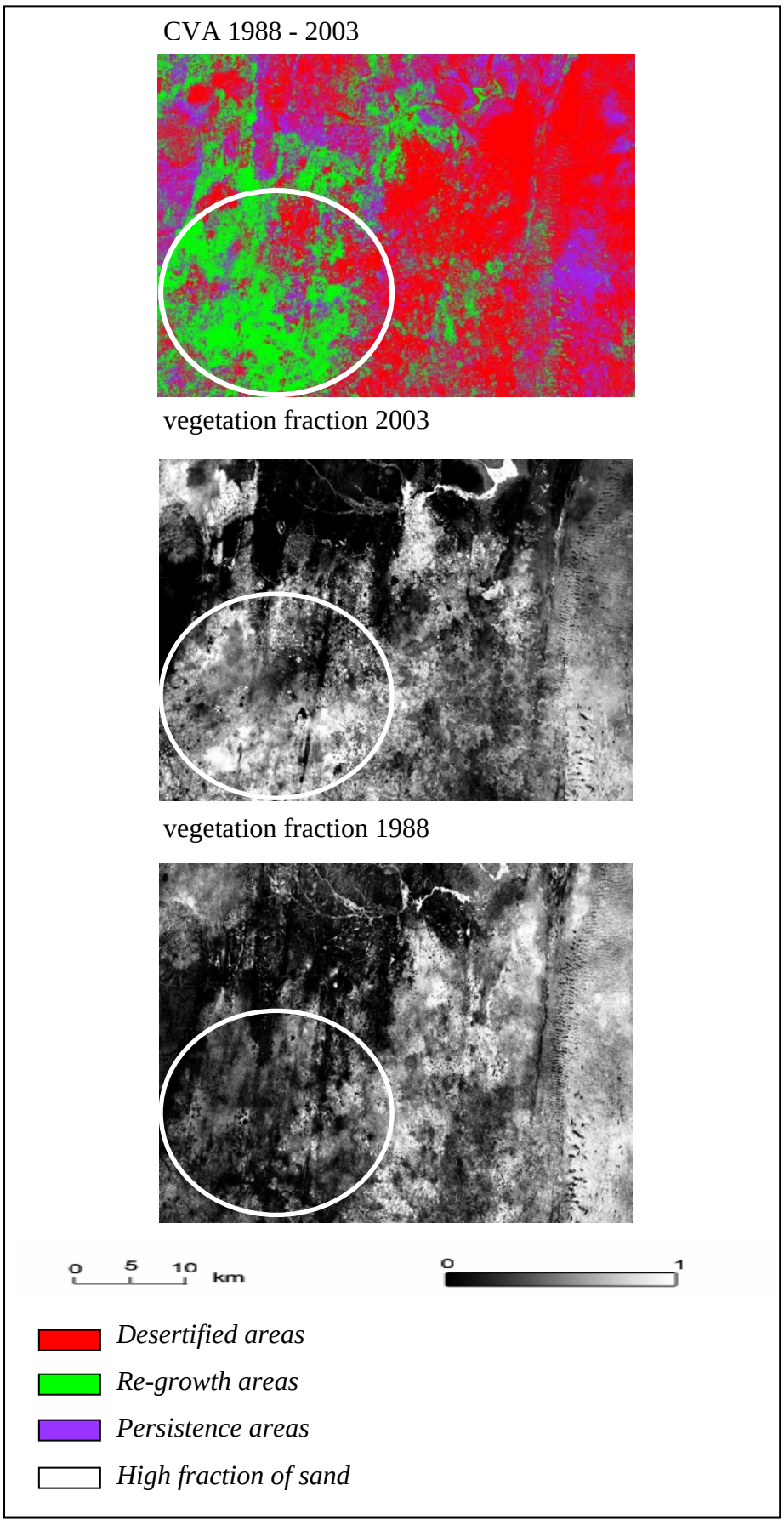

Fig 6.27: Subsets of change vector map of 1988/2003 and fraction image of vegetation 2003 and 1988 of the southern part

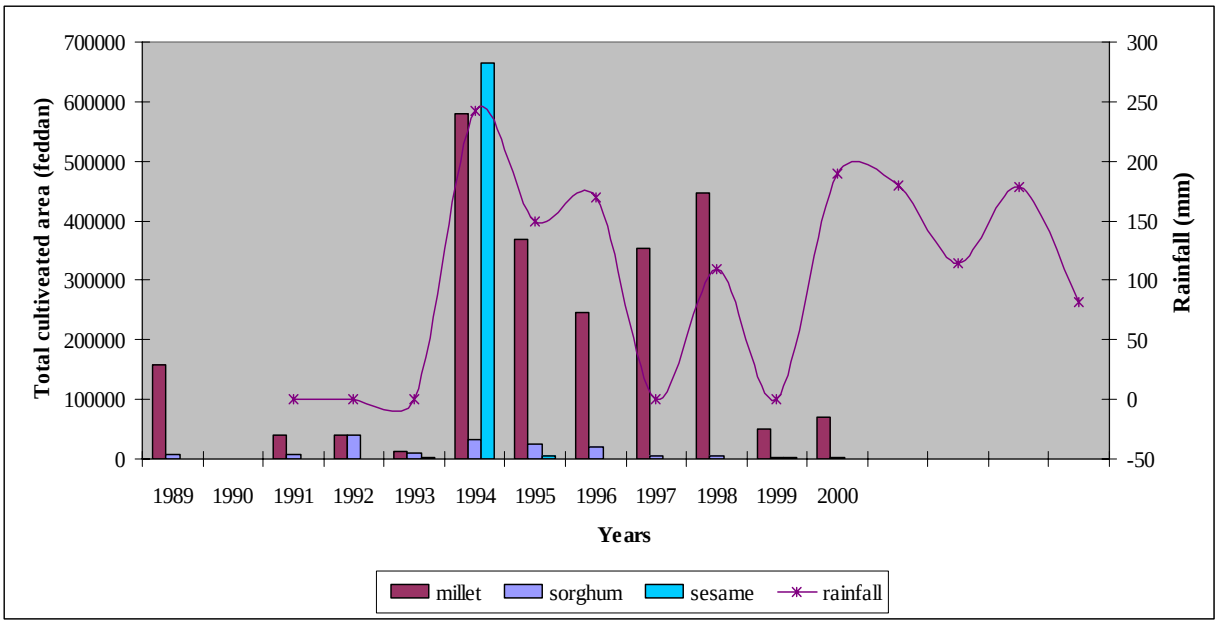

Fig 6.28: Total of cultivated areas and annual rainfall from 1989-2000 in *Sodari*
(Ministry of Agriculture and Animal Wealth, North Kordofan, 2005)

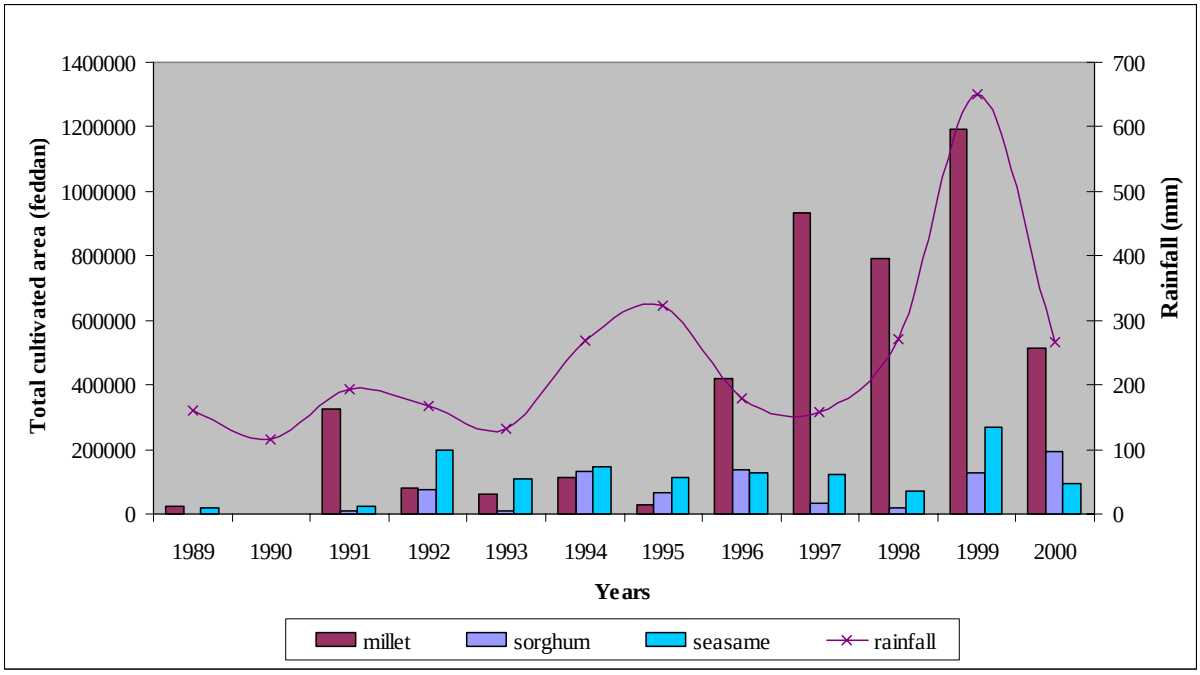

Fig 6.29: Total of cultivated areas and annual rainfall from 1989-2000 in *Bara*
(Ministry of Agriculture and Animal Wealth, North Kordofan, 2005)

Figures 6.28 and 6.29 show an increase in the total of cultivated areas in 1999 with millet and sesame crops in *Bara* and increase of precipitation (651 mm/annum). However, in *Sodari* in 1994 an increase in the total of cultivated areas with millet and sesame and a decrease in precipitation (242 mm/annum) are evident. This however highlights an inconsistence relation between shifting cultivation and precipitation. The farmers in the study area clearly stated that

the intensity of the first rain incident is a sign of successful/failure of the rainy season, thus they increase/decrease the cultivated areas according to that. (Analysis of field survey, 2004) Therefore they have developed what can be called a psychological early warning system. Increasing of cultivated areas promotes a favourable condition for land degradation especially for sand encroachment. The inconsistency and unreliability in rainfall are prominent characteristics of the study area. Figure (6.30) illustrates the fluctuation of rainfall in the study area since 1960.

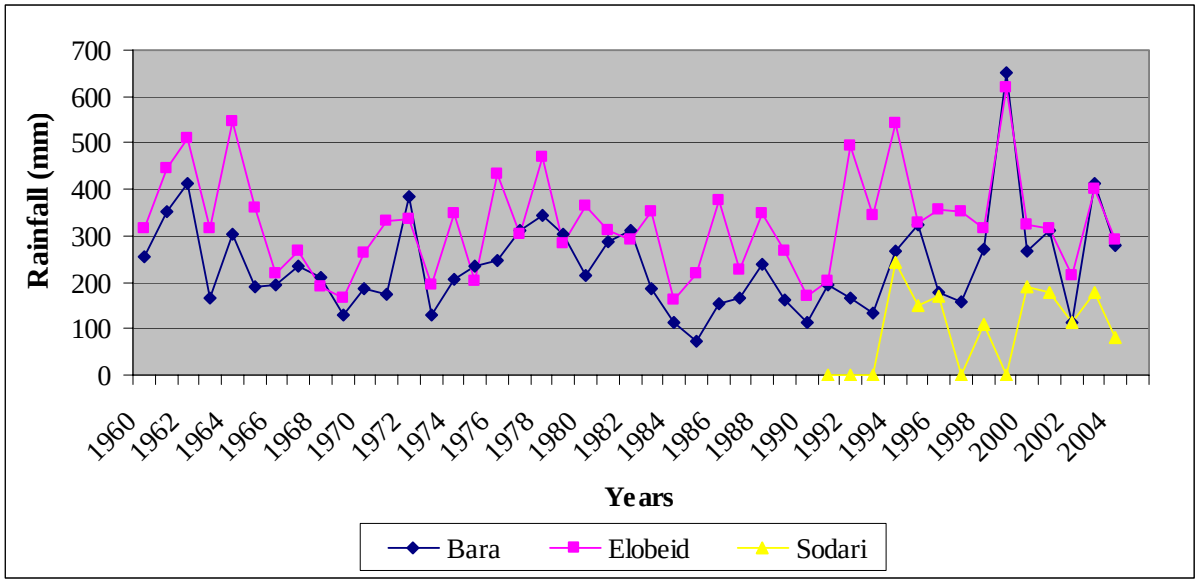

Fig 6.30: Distributions of annual rainfall in the study area from1960-2004 (IFAD, 1999)

Another forcing factor for land degradation and desertification in the study area is the shortage in water resources. As mentioned before the main resources of water in the study area are rainfall, surface and ground water. Conflicts over resources are commonly evolved between residents and nomads in their movements from the northern part to southern part searching for watering points and rangelands. Most of the human (60%) and animal population depend heavily on the ground water for their living (El Smmani and Abdel Nour, 1986). Despite the ongoing efforts to improve the rural water systems in north Kordofan, water shortage remains a chronic problem in the study area, particularly in most drought stricken areas like *Sodari* and *Elmazrub* localities. 75% of the population still has the little or no access to clean affordable water (UN, 2003). The low and scarce rainfall resulted in deficiency in water catchments by the artificial traditional water reservoirs which are locally named *Hafirs* and *Fula*. These *Hafir* and *Fulas* provide 80% of the available water for consumption. The groundwater of deep and shallow wells provides 20%. About 200 hand

pumps and 40 deep boreholes were established in North Kordofan State (UN, 2003). This has negative impact on both human livelihood and their livestock in the study area and leading to accumulation of livestock around watering points. The vegetation cover around these areas is intensively exhausted by grazing and hence produce desertified hotspot areas. From Landsat imagery and field observations, over-grazing is well perceived as phenomena related to villages since water points exist in villages' vicinities. Based on this finding desertification could be caused by a combined impact of man and climate as shown by related increase/decrease patterns of land use for rainfed agriculture and fluctuating patterns of rainfall in addition to high wind speed (Table 6.1). Based on the results obtained it is obvious that, study area has experienced considerable increase in sand encroachment during the addressed period of the study. In spite to the investigation and observation provide by this study with regards to the above mentioned causes of soil degradation and sand encroachment in the study area. These facts disagree with findings of Olsson (1985) and Ahlcrona (1988) that the land degradation has been caused by climatic factors rather than by man.

6.7 Overall evaluation of SMA in mapping desertification processes in the study area

SMA provides better estimations of desertified areas, since clear images of vegetation and soil proportions were calculated. Fractions of sand, salt soil, shade and vegetation have been used effectively in mapping the land cover changes in the study area. These results agree with finding of Elmore *et al.* (2000), Roberts *et al*. (2002) and Rogan *et a*l. (2002). The fractions of sand and vegetation identify the phenomena of desertification in the study area by measurement of decrease in vegetation and increase in sand fraction between different images. From the fraction image of sand and vegetation it is possible to detect and monitor the trend of sand encroachment and human activities by visualising the areas affected by heavy grazing and by over-cultivation pressure of rainfed agriculture. More specific views of the human activities and change in land use patterns as results of short-term changes in farming practise is presented in Figures 6.31, 6.31, 6.32, 6.3 3 and 6.33.

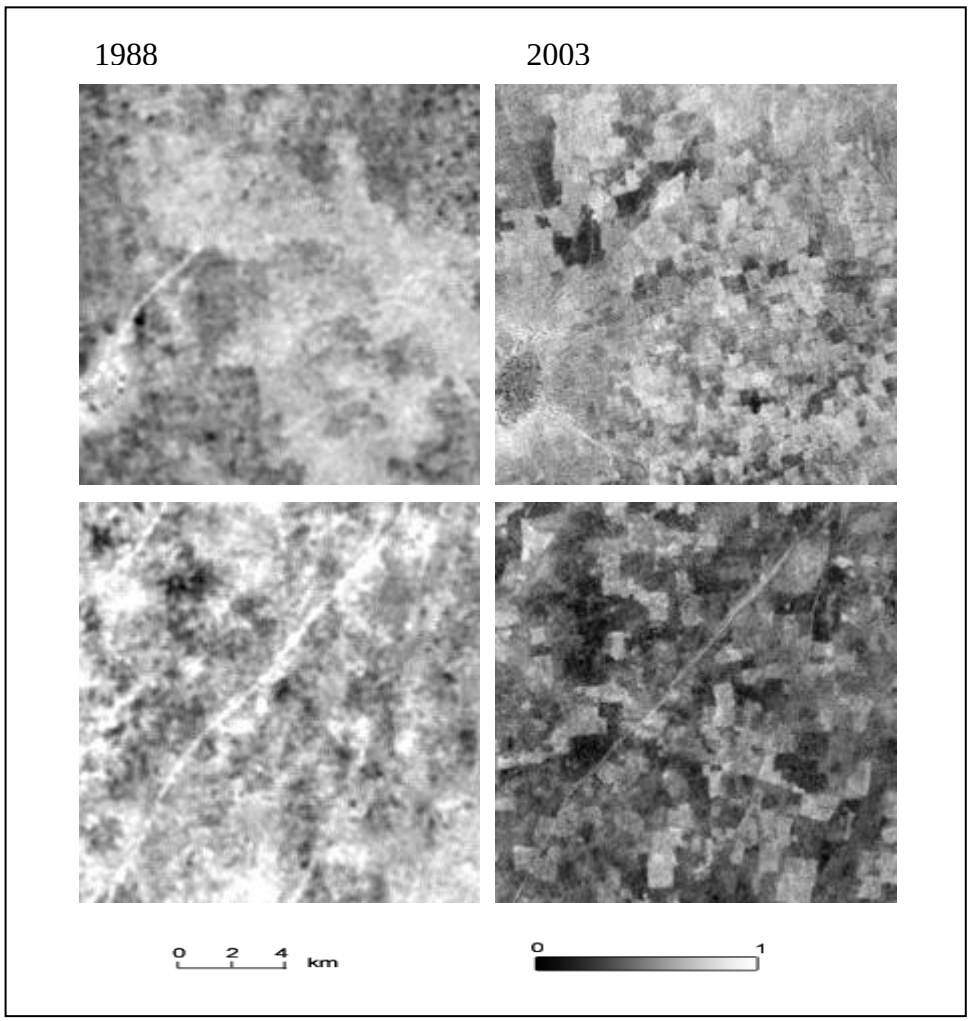

Fig 6.31: Increase of rainfed agricultural areas from 1988 to 2003 around *Elmazrub* village *(Brightness indicates the high fraction of sand)*

Figure (6.31) shows subsets of sand fractions image of SMA in traditional rainfed agriculture in the study area for years 1988 and 2003. Small irregular shapes with high brightness are related to areas with very high of sand fraction, which is increased in 2003, compared to 1988 around the *Elmazrub* village. Over-grazing around the villages in the study area and increase of village size is very clearly shown in Figure (6.32), which allows for detecting and mapping the pressure of grazing around watering points near villages. The visual interpretation of Figure (6.32) indicates the increase of the grazing activities around the villages in 2003 compared to 1988 by increase of areas of high sand fraction.

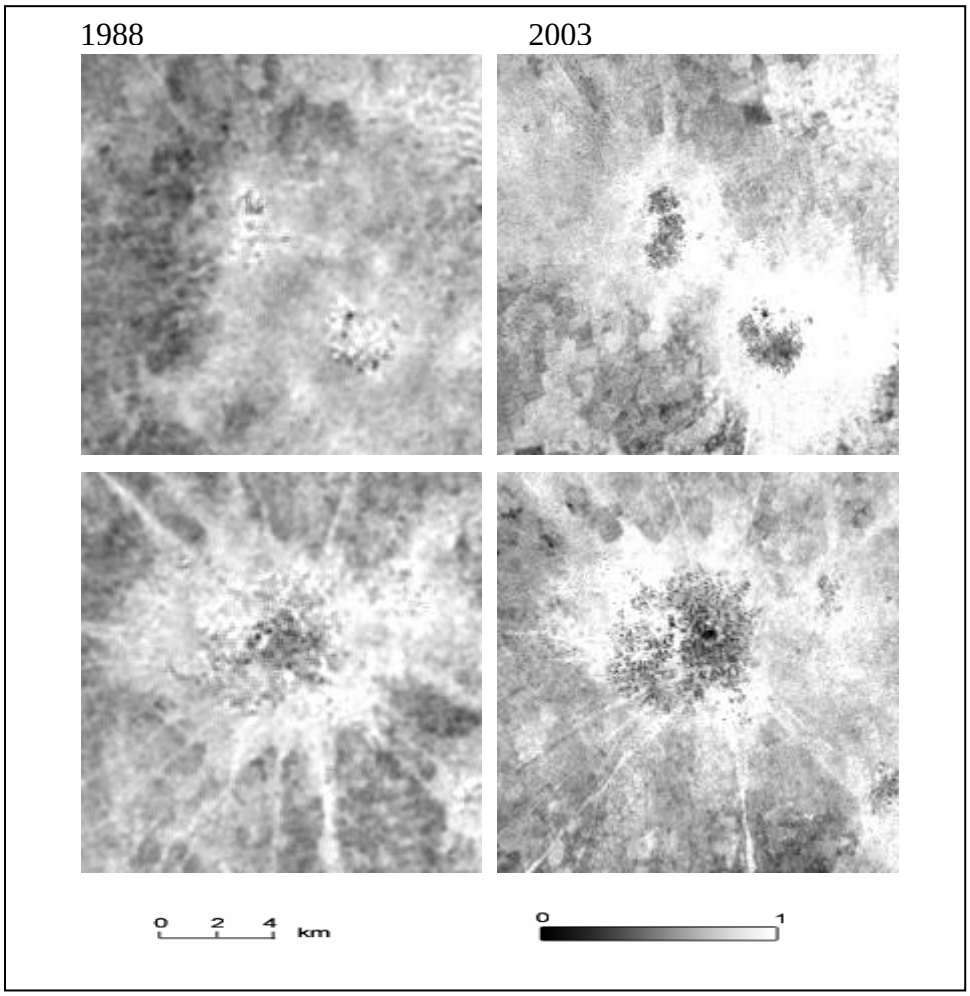

Fig 6.32: Over-grazing pressure around villages in southern part of the study area
(Brightness indicates the high fraction of sand)

Moreover, the fractions of sand identify and characterised sand dunes around *Elbashiri* and their temporal dynamics from 1988 to 2003 as indicated by increase of brightness in fraction image 2003 (Figure 6.33). This result agrees with findings of Chen *et al*. (1998), Smith *et al*. (1990a) and Tucker *et al*. (1991 and 1994), who stated that SMA can easily detect the temporal dynamic change of sand dunes.

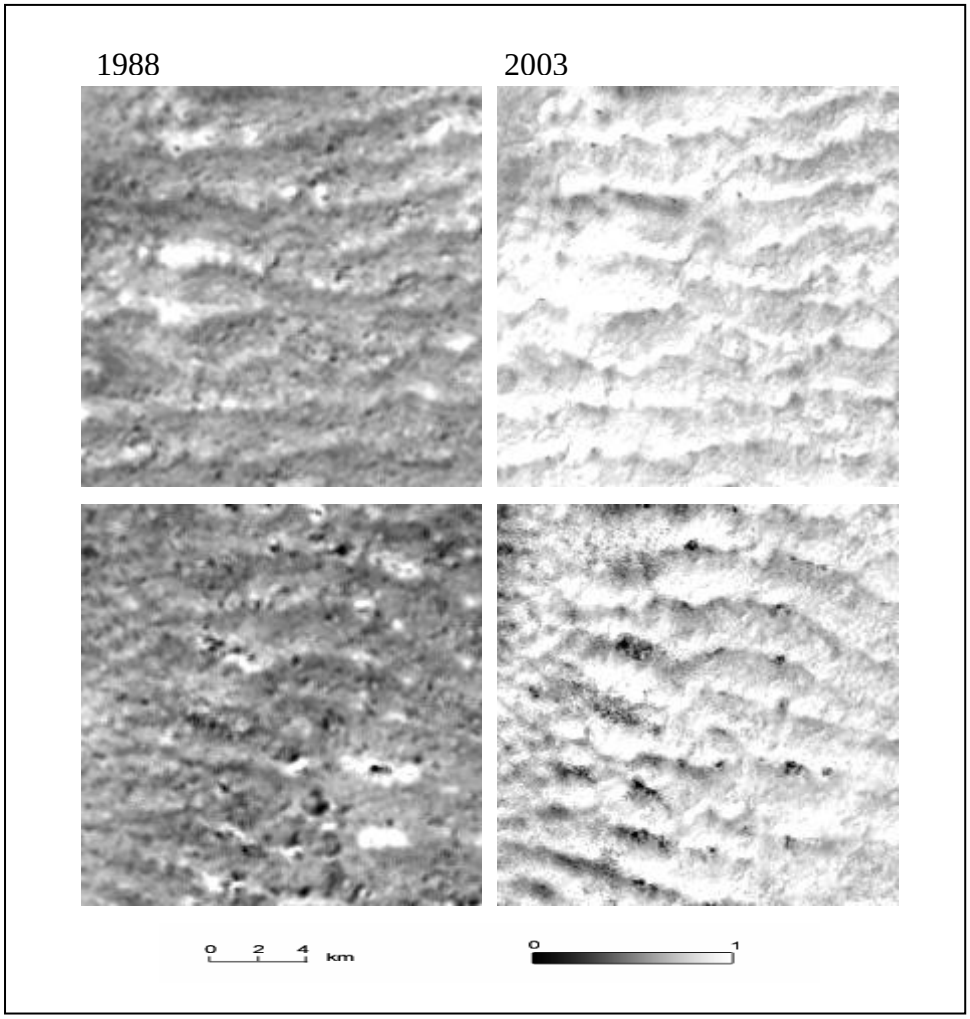

Fig 6.33: Temporal dynamic changes in traversal sand dunes in *Elbashiri* areas
(Brightness indicates high fraction of sand)

Vegetation fraction produced by SMA can easily describe vegetation cover (Cross *et al*., 1991). The temporal dynamics changes of vegetation cover in *Wadis* in the northern part of the study area is well detected and mapped due to its high brightness in fraction image as shown in Figure (6.34).

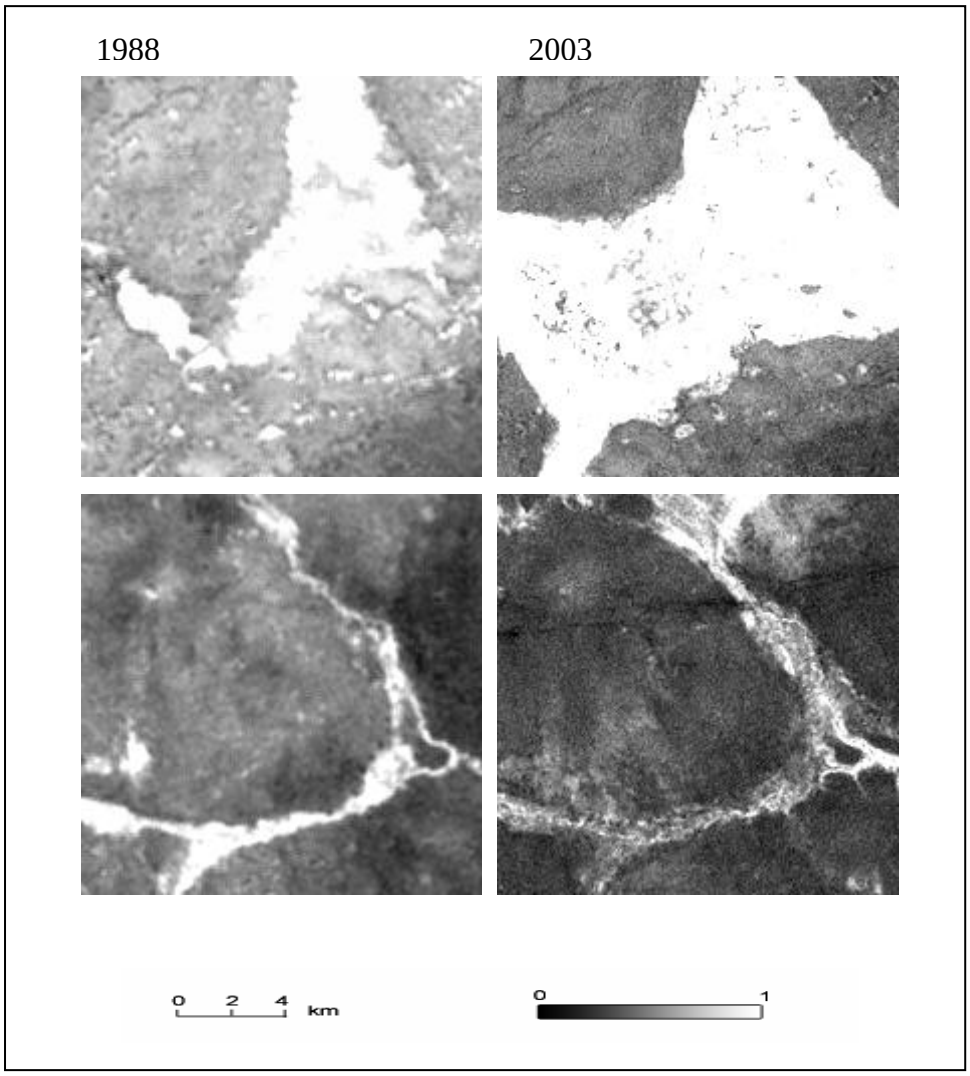

Fig 6.34: Temporal dynamics change in vegetation cover in *Wadis* areas in northern part of the study area *(Brightness indicates high fraction of vegetation)*

6.8 Comparison between CVA and SMA

The analysis of change vectors applied to the fraction images from linear-mixture model allowed for identification and characterisation of desertified and re-growth areas in the study area. The additional analysis in sand and vegetation fractions by CVA allow for more detailed classification of land cover. This may be attributed to an increase of separability between classes as result of increase of purity of each pixel in relation to different endmembers. Figure (6.35) shows that sand dunes in SMA were also clearly classified by use of CVA. From both CVA and SMA the patches of various shapes and size of re-growth and desertified areas were detected. SMA and CVA showed the same pattern related to mapping and detecting the temporal change in rainfed agriculture areas as shown in Figure (6.36). The rainfed areas with high vegetation fraction in SMA were accurately classified using CVA. It evident that CVA with use of fractions showed a consistence pattern of classified land use classes.

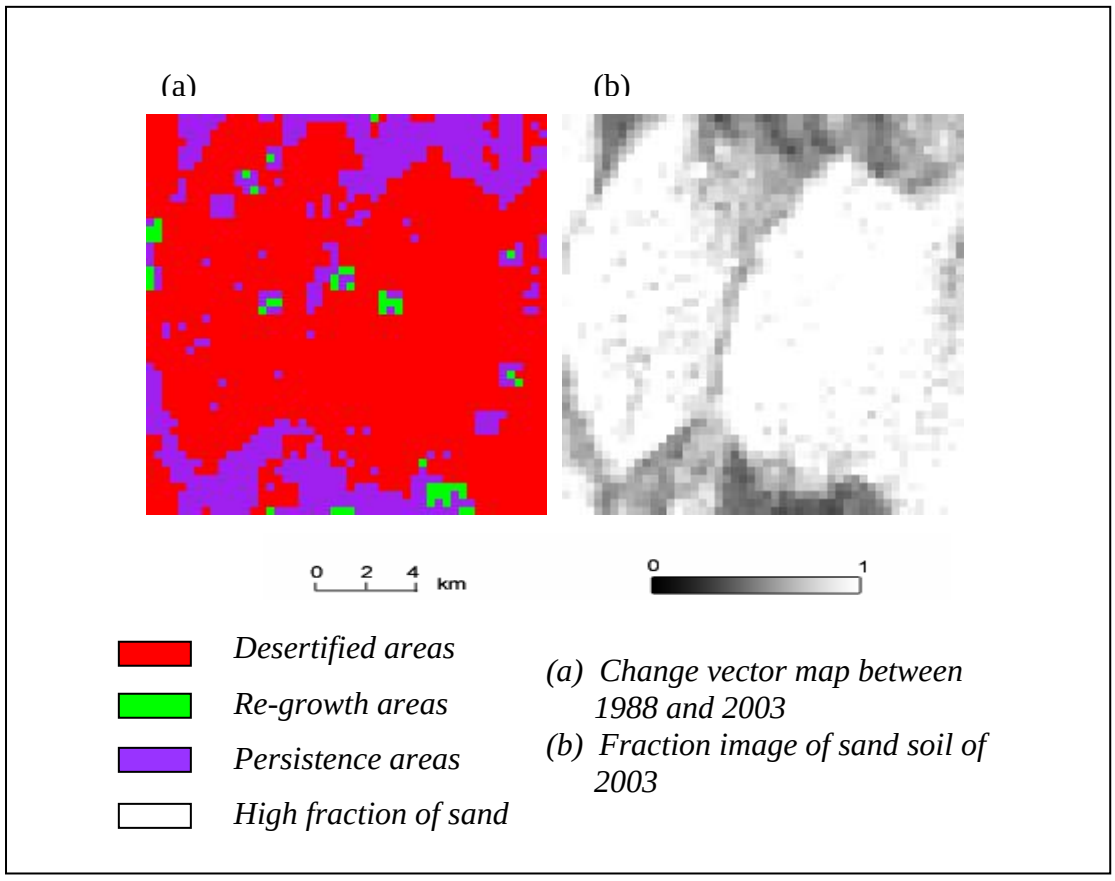

Fig 6.35: Comparison between SMA and CVA to classify and map sand dunes in *Elbashiri* areas

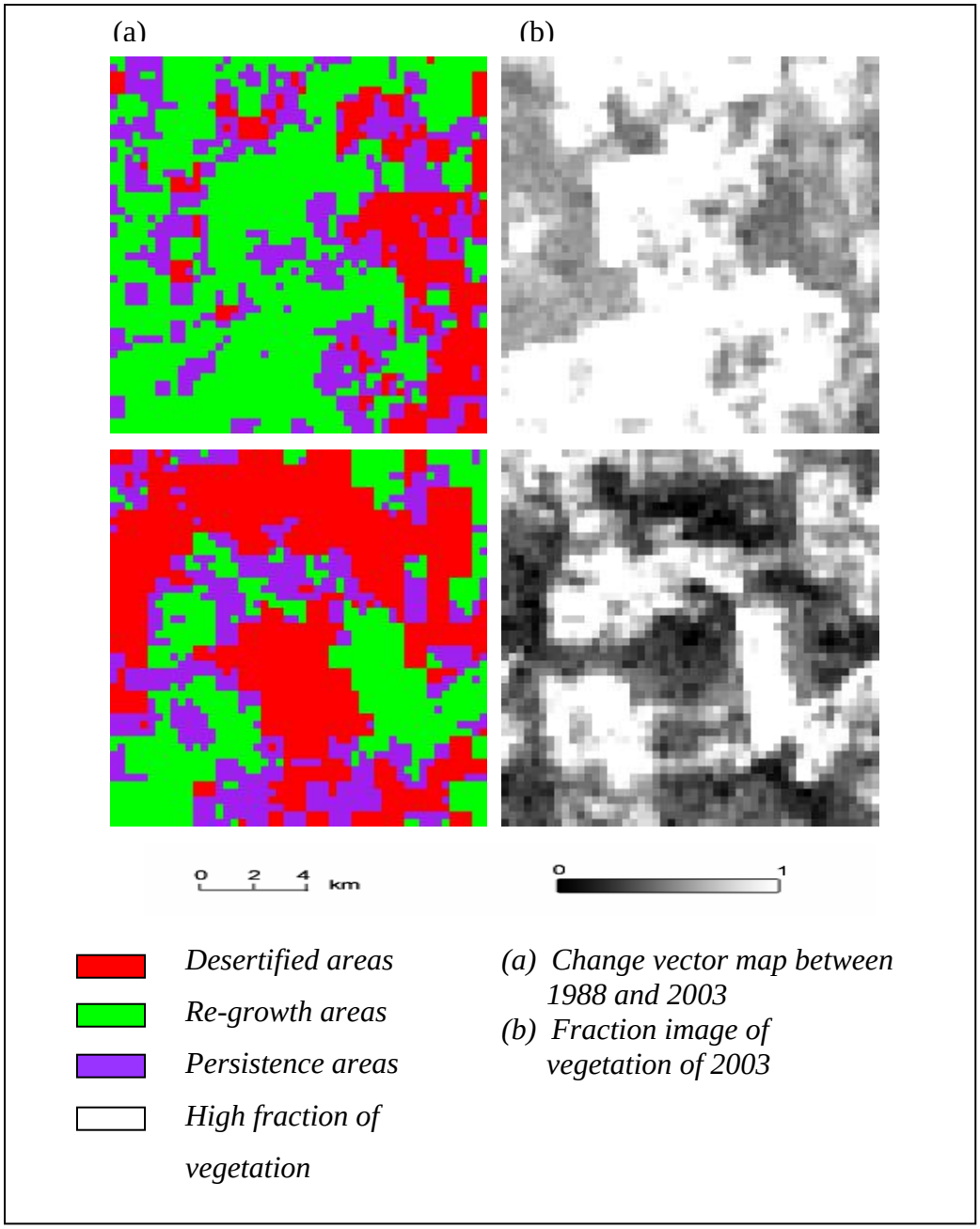

Fig 6.36: Comparison between SMA and CVA analysis to classify and map the farming areas in *Elmazrub* village

6.9 Uncertainty of SMA

The uncertainty inherited in SMA compromises different types during the process steps. The low spatial resolution of Landsat MSS image used in this study (79m*79m) prohibited the detection of features that have sizes smaller than MSS pixel size. The low spectral resolution of MSS (4 bands) enforced the study to select only four endmembers since number of endmembers should be equal to or less than the total band number (Adams *et al*., 1993; Roberts *et al*., 1993). The difference in pixel size between MSS, TM and ETM hinders the best registration of the used datasets during the selection of endmembers. Neither spectral library nor field spectrometer were available, thus pure spectra endmembers were selected from imagery. Selection of endmember from image constitutes a huge task, taking a long time and in addition requiring for long experience and knowledge of different land cover in the study area. Thus the study used all information (bands) of MSS, TM and ETM+ to determine the selected endmembers dependably. Existence of two types of soil, sand soil and salt soil with very high albedo affected the process of selecting endmembers. Salt and sand soils represented dominate materials in the data and suppressed detecting of other surface materials in the study area. Topographic features, especially isolated distributed hills in northern part, increased the dominant of shade endmember fraction. The open canopy of the study area inhibited the normalisation of shade. The mathematical nature of SMA especially with use of an unconstrained method comes out with negative fraction values of some endmembers. SMA requires careful attention to atmospheric correction and careful selection of image endmembers used for identifying land cover change in the study area.

CHAPTER 7: CONCLUSIONS OF FINDINGS AND RECOMMENDATIONS

7.1 Conclusions

Spatial data and multitemporal analysis of remote sensing data were allocated to understand the phenomena of desertification processes in North Kordofan State. SMA technique was adopted to map and analyse the desertification processes using the above mention data. Combinations of multispectral mixture analysis of Landsat imagery and field observations as well as climatic data examined and enlightened the nature and causes of desertification processes in the study area in the years 1976, 1988 and 2003. North Kordofan State, like many semi-arid regions, is characterised by a sign of heterogeneity of land use/land cover. The relationships between man, animal, vegetation, soil and climate, as determinant factors for dynamics of desertification in the study area, were analysed and discussed. SMA results show a noticeable significant decrease in vegetation fraction in 1976, 1988 and 2003, respectively. Meanwhile, sand fraction was rapidly increasing during the same periods. This concludes that desertification can be recognised by reduction of total vegetation cover and exposure of bare sand soil. The results emphasized the phenomena of sand encroachment from the northern part to the southern part following the wind direction in the addressed periods. Increasing of wind speed during the dry season is mainly attributed to increasing of sand encroachment in the study area. Accordingly, the enquiry stated by this study about the extent and direction of sand encroachment could be verified. The results generated from SMA of Landsat imagery prove the viability of such method in monitoring desertification processes in relation to mismanagement of land use in the study area. This concludes that SMA applied to Landsat imagery such as MSS, TM and ETM+ is an efficient technique in mapping and monitoring desertification processes in the study area and its results can be generalized successfully to semi-arid lands. Statistical analysis of SMA results shows high significant difference in shade, green vegetation, sand and salt soil fractions through out the addressed periods (1976, 1988 and 2003). Mapping of the surface vulnerability to wind erosion using EMI highlights the efficiency of multispectral data in detecting the most risky areas with regard to wind erosion in the study area. CVA maps the desertified areas and proves the increase of such areas from 1976 to 1988 as well the decrease of them from 1988 to 2003. Meanwhile, the results of CVA analysis show different pattern of increments in re-growth areas coupled with reduction in desertified areas form 1988 to 2003 compared to SMA results. On the other hand CVA results show an increase in persistence areas during the addressed periods. Interpretation of ancillary data and field observations emphasizes the role of human impacts in the temporal change in both vegetation cover and sand soil. Furthermore, it is well

argued that human activities such as over-grazing, over-cultivation and tree cutting contribute highly to the desertification processes in the study area. The results of SMA and visual interpretation supported by the field observations characterised and mapped the extension of increase cultivated areas and over-grazing pressure. The ongoing results also prove that degradation is remaining localised around villages' peripheries and watering points. These findings verified and answered the enquiry raised by this study about the efficiency of SMA in detecting and mapping desertification processes in the study area. Depending on findings and the arguments raised by the applied parameters (SMA, field observations, statistical analysis …etc) the study reached to the following conclusions:

- SMA is a powerful technique in characterisation and mapping of desertification processes in the study area by providing direct measurements to different land cover.
- SMA provides a valuable tool in detection and mapping of desertification process by offering more detailed information at sub-pixel level.
- SMA distinguishes the role of human activities in accelerating desertification.
- EMI is a useful index to generate an easy and practical method for analysing and mapping the vulnerability of soil to wind erosion.
- CVA allows for further detection and quantification of desertification processes. Its results are evidence for the increase in desertified areas from 1976 to 1988, as well as the increase in re-growth areas from 1988 to 2003 periods. Unlike the more reliable results obtained by the SMA fraction in classing land cover, CVA gives less reliable data in such context.
- Application of multi-temporal (MSS, TM and ETM+) remote sensing data offer an effective opportunity for mapping desertification processes in the study area as well as in arid and semi-arid lands at relatively low cost.
- Descriptive statistics of the fractions using analysis of variance ANOVA and multiple comparison procedure provide a qualitative précised trend of increase and/or decrease of endmembers fractions during the addressed periods.
- Increase of desert encroachment during the addressed periods especially from northern to southern part follows the wind direction in the study area.
- The study indicators show a drastic reduction of vegetation cover from 1976 to 1988 compared to slightly one from 1988 to 2003.
- All indicators obtained by the study argue the increasing of desert encroachment at different levels during the addressed periods.

7.2 Limitations of the study

Some limitations were experienced by this study can be summarised as follows:

- Low quality of the used MSS image.
- Lack of reference endmembers as well as of a spectral library of different land cover in the study area.
- Lack of spectrometer device for field measurement of spectral signature of different land cover materials in the study area.
- Limitation in the total number of endmembers, especially in MSS due to the bands of Landsat.
- Time factors in term of selection of pure image endmembers .
- Inaccessibility and security unrest in some locations of the study area during field surveys.
- Lack of secondary data such as climatic data (rainfall and wind direction), agricultural statistics and some other socio-economic data.

7.3 Recommendations

Intensive land use in fragile ecosystems, such as in North Kordofan State, obviously accelerates desertification and land degradation processes. The decrease in vegetation cover simultaneously with increasing exposure of soil surface will certainly increase the wind erosion and sand encroachment in the study area. Despite of this severe problem, efforts should be exerted to study and assess desertification processes in north Kordofan as well as in arid and semi-arid regions in order to mitigate this problem. Based on the findings under the above mentioned limitations the study reached to the following recommendations:

- Application of remote sensing as accurate, low-cost and safe techniques to assess and monitor desertification processes in semi-arid areas provides valuable information on suitable land use/land cover management to conserve the natural resources in the study area.
- Training and raising of building capacity of researchers in application of remote sensing in natural resource management.
- Application of remote sensing in extensive focus (*in situ*) desertified areas is more effective than widespread global one.
- Using of high resolution and more advanced remote sensing data as hyperspectral one for monitoring desertification and land degradation.

- Integration of topographic correction to improve the classification accuracy with special regard to shade endmembers.
- Establishment of more extensive regional monitoring network to collect baseline data relevant to all aspects of desertification specifically in the study area and Sudan in general.
- Establishment of shelterbelts and windbreaks by cultivating suitable species such as *Maerua crassifolia, Leptadena pyrotechnica* and *Acacia tortilis* to avoid the wind erosion and to protect the study area from desert encroachment.
- To reduce impact of human activities on vegetation, restoration and re-vegetation programs around the settlements is well recommended especially in the areas which are subjected to sever agricultures activities.
- To resolve farmer-nomads tension, integration of rural communities in management of agricultural projects.
- Rationalization of policies towards more conservation programs for rehabilitation of desertified areas.
- Improvement and management of the grazing activities.
- Construction and maintenance of watering points in rural areas.
- Enhancement of rehabilitations programs by forest administration and agricultural sector to protect the natural forest in the area with more emphasis on community participation.

7.4 Further studies

SMA tool used by this study is considered as a fruitfully adopted remotely sensing technique for monitoring arid land environments. Accordingly, the present study applied such techniques for spatial analysis to resolve problems of desertification in north Kordofan. No doubt, further and extended research efforts are needed to identify and maintain cheap and accurate methods for monitoring desertification in such areas. High resolution and more advanced remote sensing data such as hyperspectral imagery and spectrometry, can widely support in this context and increase the accuracy of monitoring drylands. The suggested scientific efforts should address and integrate geographic information systems with some socio-economic parameters to map and interpret the dynamics desertification particularly in areas of resource conflicts between resident farmers and animal herders. The concentration animals around the villages aggravate the problems due to narrow routes to watering points.

The studies can also help in mapping animal routes to water and range sources and hence avoid some bloody conflicts between tribes. Further studies could support a better understanding and can give clear diagnosis of desertification processes as well as the related land cover changes. Moreover, there is an urgent need for establishing centre for networking for regional monitoring and mapping and hence detecting the long term trends of desertification processes. Establishment of an “early warning systems” in such areas is urgently needed. Early warning could be capable to estimate the amount and duration of rainfall based on the statistical records, assess the soil moisture situation, detect change and provide information on trends of vegetation development in arid regions.

References

Adams, J.B., Smith, M.O., and Johnson, P.E. (1986). Spectral mixture modelling: a new analysis of rock and soil types at Viking Lander 1 site. Journal of Geophysical Research, 91:8098-8812.

Adams, J.B., Sabol, D.E., Kapos, V., Filho, R.A., Roberts, D.A., Smith, M.O., and Gillespie, A.R. (1995). Classification of multispectral images based on fractions of endmembers: application to land covers change in the Brazilian Amazon. Remote Sensing of Environment, 52, pp. 137-154.

Adams, J.B., Smith, M.O., and Gillespie, A.R. (1993). Imaging spectroscopy: Interpretation based on spectral mixture analysis. In: C.M. Pieters, and P.A.J. Englert (Eds). Remote geochemical analysis elemental and mineralogical composition. Press Syndicate of University of Cambridge, Cambridge, England, pp. 145-166.

Ahlcrona, E. (1988). The impact of climate and man on land transformation in the central Sudan, Lund University Press, 140 pp.

Archer, S. (1994). Woody plant encroachment into south-western grasslands and savannas: rates, patterns and proximate causes. In: M. Vavra, W. Laycock and R. Pieper, R. (Eds), Ecological implications of livestock herbivory in West society for range management, Denver, Colorado, USA, pp. 13-68.

Ardö, J. and Olsson, L. (2002). Assessment of soil organic carbon in semi-arid Sudan using GIS and the century model. Journal of Arid Environments, 54:633-651.

Asner, G.P., Bateson, C.A., Privette, J.L., Elsaleous, N. and Wessman, C.A. (1998). Estimating vegetation structure effects on carbon uptake using satellite data fusion and inverse modelling. Journal of Geophysical Research- Atmospheres, 103: 28839-28853.

Atkinson, P.M., Cutler and Lewis, M.E.J. (1997). Mapping sub-pixel proportional cover with AVHRR imagery. International Journal of Remote Sensing, 18:917-935.

Babaev, A.G. (1999). Introduction. In: Babaev, A.G. (Ed). Desert problem and desertification in central Asia. Springer-Verlag, Berlin, 1-3.

Bateson, A. and Curtiss,B. (1996). A method for manual endmember selection and spectral un-mixing. Remote Sensing of Environment, 55: 299-243.

Baumer, M.C. Tahara T. (1979). Report on the mission to Sudan. 14 May - 22 June 1979 FAO, ecological management of arid and semi-arid rangelands, FAO/UNEP/ EMASAR/P phase 11 projects.

Beinroth, F.H., Eswaran, H., Reich, P.F. and Van Den Berg, E. (1994). Land related stresses in agroecosystems. In: Stressed ecosystems and sustainable agriculture, (Eds). S.M. Virmani, J.C. Katyal, H. Eswaran, and I.P. Abrol. New Delhi: Oxford and IBH.

Bell, J.F., Farrand, W.H., Johnson, J.R., and Morris, R.V (2002). Low abundance materials at the Mars Pathfinder landing site: An investigation using spectral mixture analysis and related techniques. Icarus, 158: 56-71.

Blum, W.E.H. (1998). Basic concept, degradation, resilience and rehabilitation, in method for assessment of soil degradation. Press, New York, 1-16.

Boardman, J.W. (1993). Automated spectral un-mixing of AVIRIS data using convex geometry concepts. In : Summaries of the fourth JPL ariborne geosciences workshop, JPL publication 93-26, Jet Propulsion Laboratory, Calif, USA , pp.11-14.

Boardman, J.W., F.A. Kuruse and R. O. Green (1995). Mapping target signature via partial un-mixing of AVIRIS data. In: Summaries of the fifth JPL airborne earth sciences workshop, JPL publication 93-26, Jet Propulsion Laboratory, Calif, USA, pp.23-26.

Boardman, J.W. and Kuruse, F.A. (1994). Automated spectral analysis: A Geologic example using AVIRIS data, north Grapevine Mountains, Nevada: In Proceedings tenth thematic conference on geologic remote sensing, environmental, Research Institute of MICGIGAN; Ann Arbor, MI,pp. 1-418.

Campbell, B.J. (1996). Introduction to Remote Sensing (Second Edition). Taylor and Francis, London.

Campbell, B J. (2002). Introduction to remote sensing (Third Edition). The Guolford Press, New York, N.Y.

Chavez, P.S. (1992). A change detection technique to identify differences in multi-temporal remotely sensed image data: Example detecting dust storms and vegetation changes in Southwestern United States. American society of photogrammetry and remote sensing annual conference, Albuquerque, New Mexico, March 1992.

Chen Z., Elvidge C.D., and Groeneveld D. P. (1998). Monitoring seasonal dynamics of arid land vegetation using AVIRIS data. Remote Sensing of Environments, 65:255-266.

Cochrane, M.A., and C.M. Souza (1998). Linear mixture model classification of burned forests in the eastern Amazon. International Journal of Remote sensing, 19: 3433-3440.

Cracknell, A.P. (1998). Synergy in remote sensing- what´s in a pixel? International Journal of Remote Sensing, 19:2025-2047.

Green, R. O. and J. W. Boardman, (2000). Exploration of the relationship between information content and signal-to-noise ratio and spatial resolution in AVIRIS spectral data, 2000. Proceedings from the airborne earth science workshop. JPL, publication.

Cross, A.M., Settle, J.J., Drake, N.A. and Paivinen, R.T.M. (1991). Sub-pixel measurement of tropical forest cover using AVHRR data. International Journal of Remote Sensing, 12: 1119-1129.

Darkoh, M.K. (1995). The deterioration of the environment in Africa’s drylands and river basins. Desertification Control Bulletin, 24, 35–41.

DECARP, (1976). Sudan desert encroachment control and rehabilitation program. Prepared jointly by the central administration for Natural Resources Ministry of Agricultural Council, National Council for Research in collaboration with UNEP and FAO, Khartoum, Sudan.

DeFries, R.S., J.R.G, Townshend and M.C. Hansen (1999). Continuous field of vegetation characteristics at the global scale at 1 km resolution. Journal of Geophysical Research, 104:16911-16925.

Dennison, P.E., Roberts, D.A. and Regelbrugge, J. (2000). Characterizing chaparral fuels using combined hyperspectral and synthetic aperture radar. Proceedings of the ninth JPL airborne earth science workshop. Jet Propulsion Laboratory, Pasadena, CA, pp. 119-124.

Doka, A. M. A. (1980). Remote Sensing for monitoring soil resources and areas affected by desertification in central Sudan. Proceeding of Sudan symposium and workshop on remote sensing. Vol. 2, October 1980. Visiting international scientist programm, Remote Sensing Institute. SDSU. USA.

El Smmani, M.O. and Abdel Nour H.O. (1986). North Kordofan a collection papers on desertification and drought impact and related issues. Institute of Environmental Studies (IES), University of Khartoum,81-125.

Elmore, A. J., Mustard, J.F., Manning, S.J. and Lobell, D.B. (2000). Quantifying vegetation change in semiarid environments: Precision and accuracy of spectral mixture analysis and Normalized Difference Vegetation Index. Remote Sensing of Environment, 73:87-102.

Elmqvist, B. (2004). Land use assessment in dry lands of Sudan using historical and recent high resolution satellite data. PhD. Thesis Lund University, Centre of Sustainability.

Elvidge, C. D. and Lyon, R. J. P. (1985). Influence of rock-soil variation on the assessment of green biomass. Remote Sensing of Environment, 17:265–279.

Elvidge, D., Tomoaki, M.,Walley, T., Jansen, D., Groeneveld, P. and Christopher, J.R. (1999). Monitoring trends in wetland vegetation using a Landsat MSS time series 1999. Remote sensing change detection. Environmental monitoring methods and application. Edited by Ross S.

Engvall , J.L. J.D. Tubbs, and Q.A. Holmes (1977). Pattern recognitions of land sat data based upon temporal trend analysis. Remote Sensing of Environment, 6:303-314.

ENVI, (2002). ENVI user´s Guide. Research System Inc., Bounlder, Colorado, 930.

Escfadel R. and Huete A.R. (1991). Improvement in remote sensing of low vegetation cover in arid regions by correcting vegetation indices for soil “noise”. C.R. Academie des Sciences Paris, 312:1385-1391.

Finkel, H.J. (1986). Semi-arid and water conservation. CRC press, Boca Raton, Florida, USA, 126pp.

Fisher, P. (1997). The pixel: A snare and delusion, International Journal of Remote Sensing, 18:679-685.

Garcia, M. and Ustin, S.L. (2001). Detection on interannual vegetation responses of climatic variability using AVHRR data in costal Savanna in California. IEEE Transaction on Geosciences and Remote Sensing, 39: 1480-1490.

Garcia-Haro F.J., Gilabert M.A. and Meliam J. (1996). Linear spectral mixture modelling to estimate vegetation amount from optical spectral data. International Journal of Remote Sensing. 17:3373-3400.

Gillespie, A.R., Smith, M.O., Adams, J.B., Willis, S.C., Fischer, A.F. and Sabol, D.E. (1990). Interpretation of residual images: Spectral mixture analysis of AVIRIS images, Owens Valley, California. Proceeding of second ariborne imaging spectrometer data analysis conference. Jet Propulsion Laboratory, Pasadena, CA, pp. 243-270.

Graetz, R. D. (1991). Desertification: A tale of tow feedbacks. Eco-system Experiments, H.A. Mooney et al., Eds., Wiley, 59-87.

Green, A.A., Berman, M., Switzer, P. and Craig, M .D. (1988). A transformation for ordering multispectral data in terms of image quality with implications for noise removal: IEEE Transaction on Geosciences and Remote Sensing, 26, no.1, 56-74.

Haboudane, D., Bonn, F., Royer, A., Sommer, S. and Mehl, W. (2002). Land degradation and erosion risk mapping by fusion of spectrally-based information and digital geomorphometric attributes. International Journal of Remote Sensing, 23: 3795-3820.

Hall, F.G., Shimabukuro, Y.E. and Huemmrich, K.F. (1995). Remote sensing of forest biophysical structure using mixture decomposition and geometric reflectance models. Ecological Applications, 5: 993-1013.

Harrison, M.N and Jackson, J.K (1958). Ecological classification of vegetation cover of Sudan.

Hellden, U (1978). Evaluation of Landsat-2 imagery for desertification studies in Northern Kordofan, Sudan. Lund University, Department of Geography, report nr 38.

Hellden, U. (1988). Desertification monitoring: Is the desert encroaching? Desertification Lund University, Department of Geography, control Bulletin 17: 8-12.

Huete A.R. and Jackson R.D (1987). Suitability of spectral indices for evaluating vegetation characteristics on arid rangelands. Remote Sensing of Environment, 23:213-232.

Huete A.R. and Tucker C.J (1991). Investigation on soil influences in ABHRR red and near-infrared vegetation index imagery. Remote Sensing of Environment, 12: 1223-1242.

Huete A.R., Jackson R.D., and Post D.F. (1985).Spectral response of plant canopy with different soil backgrounds. Remote Sensing of Environment, 17:37-53.

Huete, A.R. (1985). Soil and atmosphere influences on the spectra of partial canopies. Remote Sensing of Environment, 25:89-105.

Huete, A.R. (1986). Separation of soil plant spectral mixtures by factor analysis. Remote Sensing of Environment, 19: 237-251.

Huete, A.R. (1988). A soil-adjusted vegetation index (SAVI). Remote Sensing of Environment, 25: 295- 309.

Hulme, M. (2001). Climatic perspectives on Sahelian desiccation: 1973-1998. Global Environmental Change, 11: 19-29.

IFAD, (2004). Environmental assessment study. Main report of republic of Sudan, western Sudan resource management programme. Part 1: Greater Kordofan. Near East and North Africa Division Project Management Department.

IIED/IES, (1990). Gum Arabic rehabilitation project in the republic of Sudan: Stage 1 report, IIED, London.

Jansinki, M.F. (1996). Estimation of sub-pixel vegetation density of natural regions using satellite multispectral imagery. IEEE Transaction on Geosciences of Remote Sensing, 34, 804-813.

Jensen, J.R. (1986). Digital image processing. Prentices-Hall. New Jersey.Jansinki, M.F., (1996). Estimation of sub-pixel vegetation density of natural regions using satellite multispectral imagery. IEEE Transaction on Geosciences of Remote Sensing, 34, 804-813.

Johnson P.E., Smith M.O. and Adams J.B. (1985). Quantitative analysis of planetary reflectance spectra with principal components analysis, J. Geophys. Res. 90, C805-C810.

Kameyama, S., Yamagata, Y., Nakamura, F. and M. Kaneko (2001). Development of WTI and turbidity estimation model using SMA–application to Kushiro Mire, eastern Hokkaido, Japan. Remote sensing of Environment, 77: 1-9.

Kennedy, P.J. (1989). Monitoring the phenology of Tunisian grazing lands. Remote Sensing, 835-845.

Lal, R. (1994). Tillage effects on soil degradation, soil resilience, soil quality, and sustainability. Soil Tillage Research, 27, 1–8.

Lambin, E.F. and Strahler,A.H. (1994b). Change vector analysis in multispectral space. A tool to detect and categorized land cover change processes using high temporal resolution satellite data. Remote Sensing of Environment, 48, 231-244.

Lampery, H.F (1975). Report on the desert encroachment reconnaissance in northern Sudan, 21 Oct to 10Nov, 1975. UnESCO/UNEP. 16p.

Le Houerou, H.N (1996). Climate change, drought and desertification. J. Arid Environment. 34, 133-185.

Li, L. and J.F. Mustard (2003). Highland contamination in Iunar mare soils: Improved mapping with multiple endmember spectral mixture analysis (MESMA). Journal of Geophysical Research- Planets.

Lillesand, T.M. and Kiefer, R.W. (2000). Remote Sensing and Image Interpretation, 4th Edition, John Wiley and sons, New York.

Lorena, R.B., Santos J.R., Shimabukouro Y.E., Brown I.F and Kulx H.J.H. (2002). A change vector analysis techniques to monitor land use/land cover in SW Brazilain Amazon: Acre state in: PECORA- 15 integrated remote sensing at global regional and local scale, Denver, Colorado/USA, 8-15.

Ludwig J.A. and Tongway, D.J.(1995). Spatial organization of landscapes and its function in semi-arid woodlands, Australia. Landscape Ecology 10, 85-94.

Malila, W.A (1980). Change vector analysis: an approach for detecting forest changes with Landsat . Proceedings of the 6th annual symposium on machine processing of remotely Sensed data. Purdue University, West Lafayette, IN , pp, 326-335.

McGwire K., Minor T. and Fenstermaker L. (2000). Hyperspectral mixture modelling for quantifying sparse vegetation cover in arid environments. Remote Sensing of Environment. 72: 360-374.

Metrological Department of North Kordofan State, (2003). Annual rainfall report of *Bara* Province, North Kordofan, Sudan.

Metrological Department of North Kordofan State, (2005). Annual rainfall report of *Sheikan* and *Bara* Provinces, North Kordofan, Sudan.

Metternicht, G.I. and Fermont, A. (1998). Estimating erosion surface features by linear mixture modelling. Remote Sensing of Environment, 64: 254-265.

Ministry of Agriculture, and Animal Wealth, North Kordofan, (2003). Annual report of the livestock North Kordofan, Sudan

Ministry of Agriculture, and Animal Wealth, North Kordofan, (2005). Annual report of the main crops production in North Kordofan, Sudan

Mustard, J.F. and Head, J.W. (1996). Buried stratigraphic relationships along the south western shores of oceanus procellarum-implication for early Iunar volcanism. Journal of Geophysical Research-Planets, 101: 18913-18925.

Mustrad, J.F and J.M. Sunshine (1999). Spectral analysis for earth science: investigations using remote sensing data. In: Remote Sensing for the Earth Sciences: manual of remote sensing (Eds3), Rencz. A.N., John Wiley and Sons, New York, pp. 251-307.

Nicholson, S.E. (1994b). Desertification. Encyclopaedia of climate and weather, S.H.

Okin, G.S. Murray B. and Schlesiner W.H (2001a). Degradation of sandy arid shrubland environments, observation, process modelling, and management implications. Journal of Arid Environment. 47:123-144.

Okin, G.S., Roberts, D.A., Murray, B. and W.J. Okin (2001b). Practical limits on hyperspectral vegetation discrimination in arid and semi-arid environments. Remote Sensing of Environment, 77:212-225.

Olsson, K. (1985). Remote Sensing for fuel wood resources and land degradation studies in Kordofan, The Sudan. Ph.D Thesis, Lund, Lund University. 182 pp.

Olsson, L (1985). An integrated study of desertification, the University of Lund Dep of Geography.

Olsson, L. and J. Ardö (2002). Soil carbon sequestration in degraded semi-arid agro ecosystem- perils and potentials. Ambio, 31,471-477.

Painter, T.H., Roberts, D.A., Green, R.O. and Dozier, J. (1998). The effect of grain size on spectral mixture analysis of snow-covered area from AVIRIS data. Remote Sensing of Environment, 65:320-332.

Painter, T.H.J., Dozier, D.A., Roberts, R.E., Davis, and R.O.Green (2003). Retrieval of sub-pixel snow-covered area and grain size from imaging spectrometer data. Remote Sensing of Environment, 85:64-77.

Peddle, D.R., Brunke, S.P. and Hall, F.G. (2001). A comparison of spectral mixture analysis and ten vegetation indices for estimating boreal forest biophysical information from airborne data. Canadian Journal of Remote Sensing, 27: 627-635.

Peddle, D.R., Hall, F.G. and LeDrew, E.F. (1999). Spectral mixture analysis and geometric-optical reflectance modelling of boreal forest biophysical structure. Remote Sensing of Environment, 67: 288-297.

Phinn, S.M., Stanford P., Scarth A.T. Muurray and P.T Shyy (2002). Monitoring the composition of urban environments based on the vegetation-impervious surface-soil (VIS) model by sub-pixel analysis techniques, International Journal of remote Sensing. 23:4131-4153.

Pickup, G., Chewings, V.H. and Nelson, O.J. (1993). Estimating changes in vegetation cover over time in arid rangelands using Landsat MSS data, Remote Sensing of Environment-vol.43, pp. 243-263.

Pinet, P.C., Shevchenko, V., Cheverl, S.D., Daydou, Y. and Rosemberg, C. (2000). Local and regional Iunar re-growth characteristics at reiner gamma formation: Optical and spectroscopic properties from Clementine and earth- based data. Journal of Geophysical Research- Planets, 105: 9457-9475.

Price, J.C. (1997). Spectral band selection from visable-near infrared remote sensing. Spectral spatial resolution tradeoffs. IEEE Trans. Geosciences Remote Sensing 35:1277-1285.

Puigdefabregas, J. (1995). Desertification: stress beyond resilience, exploring a unifying process structure. Ambio, 24, 311-313.

Ray, T. W. (1995). Remote sensing of land degradation in arid/semiarid regions. PhD, California Institute of Technology.

Ray, T.W. and Murray, B.C. (1996). Non-linear spectral mixing in desert vegetation. Remote Sensing of Environment, 55: 59-64.

Riano, D., Chuvieco, E., Ustin, S., Zomer, R., Dennison, P., Roberts, D. and J. Salas (2002). Assessment of vegetation regeneration after fire through multitemporal analysis of AVIRIS images in Santa Monica Mountains. Remote Sensing of Environment, 79: 60-71.

Robert, D.A. Gardner, M. Church, R. Ustin S. Scheer, G. and Green, R.O. (1998). Mapping chaparral in the Santa Monica mountains using multiple endmember spectral mixture models. Remote Sensing of Environment, 65:267-279.

Robert, D.A., Green, R.O. and Adams J.B. (1997b). Temporal and spatial patterns in vegetation and atmospheric properties form AVIRIS. Remote Sensing of Environment, 44:255-269.

Roberts, D. A., Getulio, T., Batista, Jorge, L.G., Pereira, Eric, K., Waller, and Bruce, W. (1999). Change identification using multitemporal spectral mixture analysis: Application in

eastern Amazonia: in Ross S. Lunetta and Chistopher D. Elvidge; Remote Sensing Change Detection for Environmental Monitoring Methods and Application, 1999.

Roberts, D.A., Dennison, P.E., Gardner, M., Hetzel, Y.L., Ustin, S.L. and Lee, C. (2003). Evaluation of the potential of hyperion for fire danger assessment by comparison to the Airborne Visible Infrared Imaging Spectrometer. IEEE Transaction on Geosciences and Remote Sensing.

Roberts, D.A., Dennison, P.E., Ustin, S.L., Reith, E. and Morais, M.E. (1999). Development of a regionally specific library for the Santa Monica mountains using high resolution AVIRIS data. Proceedings of the eight AVIRIS earth science workshop, Jet Propulsion laboratory, Pasadena, CA, pp. 349-354.

Roberts, D.A., Smith, M.O. and Adams, J.B. (1993). Green vegetation non-photosynthetic vegetation and soil in AVIRIS data. Remote Sensing of Environment, 44: 255-269.

Rogan, J., Franklin, J. and D.A. Roberts (2002). A comparison of methods for monitoring multitemporal vegetation change using Thematic Mapper imagery. Remote Sensing of Environment, 80: 143-156.

Sadowski, and S. Ruttenberg (1994). The 1 km resolution global data set: Needs of the international geosphere biosphere programme. International Journal of Remote Sensing, 15, 3417-3441.

Schlesinger, W.H., Reynolds, J.F., Cunningham, G.L., Huenneke, L.F., Jarell, W.M.,Virginia, R.A. and Whitford, W.G. (1990). Biological feebacks and global desertification. Science 247, 1043-1048.

Schmidt, H. and Karnieli, A. (2000). Remote sensing of the seasonal variability of vegetation in a semi-arid environment. Journal of Arid Environments, 45, 43-59.

Schweik, Charles M. and Glen M. Green. (1999). The use of spectral mixture analysis to study human incentives, actions, and environmental outcomes. Social Science Computer Review, 17(1):40–63.

Settle, J.J. and Drake N.A. (1993). Linear mixing and the estimation of ground cover proportion. International Journal of Remote Sensing, 14:1159-1177.

Small, C. (2001). Multiresolution analysis of urban reflectance. Remote sensing data fusion over urban areas, IEEE/ISPRS Joint Workshop 2001 IEEE, Rome, Italy, pp 15-19.

Small, C. (2002). Multitemporal analysis of urban reflectance. Remote Sensing of Environment, 81: 427-442.

Small, C. (2004). The Landsat ETM+ spectral mixing space. Remote Sensing of Environment, 93, 1-17.

Smith, M.O., Adams, J.B. and Gillespie, A.R. (1990). Reference endmembers for spectral mixture analysis, 5th Australian Remote Sensing Conference., vol. 1, 331-340.

Smith, M.O., Ustin S.L., Adams, J.B. and Gillespie, A.R. (1990a). Vegetation in deserts: I. A regional measure of abundance from multispectral images, Remote Sensing of Environment. 31, 1-26.

Smith, M.O., Ustin S.L., Adams, J.B. and Gillespie, A.R. (1990b). Vegetation in deserts: II. Environmental influences on regional vegetation, Remote Sensing of Environment, 31, 27-52.

Smith, M.O., Johnson, P.E. and Adams, J.B. (1985). Quantitative determination of mineral types and abundances from reflectance spectra using principal components analysis. Journal of Geophysical Research, 90: C797-804.

Stocking, M. (1995). Soil erosion and land degradation. In: O'Riordan, T. (Ed) Environmental science for environmental management. London, Longman, 233-243.

Tobias , H. (2004). Analysing environmental change in semi-arid areas in Kordofan, Sudan. PhD thesis, Lund university, Geobiosphere Science Centre.

Tongway, D.J. and Ludwig, J.A. (1996). Restoration of landscape patchiness in semi-arid rangelands, Australia. In: Processing of the fifth international rangeland congress, Townsville, Australia, pp. 563-564.

Townshend, J.R.G., Justice,C.O., Skole, D., Malingreau, J.P., J. Cihlar, Teillet; P., Sadowski, F. and Ruttenberg, S. (1994). The 1 km resolution global data set: Needs of the international geosphere biosphere programme. International Journal of Remote Sensing, 15, 3417-3441.

Tucker C. J., Newcomb W. W. and Dregne, H. E. (1994). AVHRR data sets for determination of desert spatial extent. International Journal of Remote Sensing, 15: 3547-3565.

Tucker C.J. and Miller L.D. (1977). Soil spectra contributions to grass canopy spectral reflectance". Photogrammetric Engineering and Remote Sensing, 43 (6): 721-726.

Tucker, C.J. (1979). Red and photographic infrared linear combinations for monitoring vegetation. Remote Sensing of Environment, 20: 127-150.

Tucker, C.J. (1986). Maximum normalized difference vegetation index images for sub-Saharan Africa for 1983-1985. International Journal of Remote Sensing, 7: 1383-1384.

Tucker, C.J., Dregen, H.E. and W.W. Newcomb, (1991). Expansion and contraction of Sahara desert from 1980 to 1990. Science, 253, 299-301.

Tucker, C.J. Townshend, J.R.G. and Goff, T.E. (1985). African land covers classification using satellite data. Science, 227: 369-375.

Tucker, C.J., Vanpraet, C., Boerwinkel, E. and Gaston, A. (1983). Satellite remote sensing of total dry matter production in the Senegalese Sahel. Remote Sensing of Environment, 13: 461-474.

Tueller, P.T. and S.G. Oleson. (1989). Diurnal radiance and shadow fluctuations in a cold desert shrub plant community. Remote Sensing of Environment 29:1–14.

UN Starbase Report, (2003). Sudan transition and recovery database, report on North Kordofan State. Office of UN resident and humanitarian coordinator for Sudan, 27 June 2003.

UNCCD, (1994). Status of ratification and entry into force. United Nations Convention to Combat Desertification, Paris, 14 June 1994.

UNEP, (1992). World Atlas of Desertification. Edward Arnold, London, 69pp.

UNEP, (1993). Good news in the fight against desertification. Desertification Control Bulletin, 22, 3.

UNEP, (1994). Land degradation in South Asia: Its severity, causes and effects upon the people. INDP/UNEP/FAO. World Soil Resources Report 78. Rome: FAO.

Ustin S.L., Adams, J.B., Elvidge, C.D., Rejmanek, M., Rock, B.N., Smith, M.O., Thomas, R.W. and Woodward, R.A. (1986). Thematic Mapper studies of semi-arid shrub communities. Bio-Science.36:446-452.

Ustin, S.L., Smith, M.O. and Adams, J.B. (1993). Remote sensing of ecological processes: A strategy for developing ecological models using spectral mixture analysis. In J. Ehleringer and C. Field (Eds.) Scaling Physiological Processes: Leaf to Globe. Academic Press, p.339-357.

Van der Meer, F.D and S.M.de Jong (2000). Improving the results of spectral un-mixing of Landsat Thematic Mapper imagery by enhancing the orthogonality of endmembers. International Journal of Remote Sensing, 21, pp. 2781-2797.

Verbyla, D. L. (1995). Satellite remote sensing of natural resources. Boca Raton, FL: Lewis.

Warren, A. (1996). Desertification. The physical geography of Africa, W. M. Adams, A.S. Goudie , and A.R. Orme, (Eds)., Oxford University Press, 342-355.

Weltzin, J.F. Archer, S. and Heitschmidt, R.K. (1997). Small mammal regulation of vegetation structure in temperate savanna. Ecology 78, 751-761.

Westing, A.H. (1994). Population, desertification and Migration. Conserve21, 109-114.

Westoby, M. Walker, B. H. (1998). Opportunistic management for ranglands not at equilibrium. J. Range Manage. 42, 266-274.

Williams, M.A.J. and Balling, R.C.: (1996). Interactions of desertification and climate, Edward Arnold. London,

Yagub, A.M., Babiker . F. and Alwayia, A. (1994). Indication of recovery in biomass production and soil orgainic matter of Sudanese Sahel region: A case study North Kordofan. In Dryland husbandry in the Sudan. Workshop report, p. 57-77. OSSREA, Addis Ababa (Ethiopia). OSSREA DHP Publications Series. 1996. no. 1.

Appendices

Appendix 1: Name and locations of the villages in the study area

Long	Latut	Villages name
30°.19' 91.6"	13°.82' 19.4"	*Eledabiss*
30.°19' 02.7"	13°.80' 80.5"	*Elbashiri*
30°.20' 25.6"	13°.77' 08.3"	*Elyaawa*
30°.18' 91.6"	13°.69' 91.6"	*Elrayad*
30°.19 ' 13.8"	13°.65' 44.4"	*Umkadaada*
30°.18 27.7"	13°.64' 66.6"	*Um assal*
30°.10' 77.7"	13°.62' 69.4"	*Um sayala*
30°.06' 69.4"	13.69' 11.1"	*Um sharradi*
30°.06' 36.1"	13°.71' 80.5"	*Um saadown elshraif*
30°.08' 80.5"	13°.72 33.3"	*Um debkrrat*
30°.05' 80.5"	13°.73' 88.8"	*Elmorra*
30°.08' 91.6"	13°.82' 69.4"	*Elrroda*
30°.19' 11.1"	13°.83' 86.1"	*Abu gaidda*
30°.21' 08.3"	13°.90' 52.7"	*Abu dalaam aama*
30.15' 55.5"	14°.00 69.4"	*Twaal*
30°.16' 86.1"	14°.05' 30.5"	*Um baggowm*
30°.13' 94.4"	14°.06' 52.7"	*Umkharrian*
30°.13 ' 75.00"	14°.06' 91.6"	*Umkharrian*
30°.15' 74.9"	14°.14' 55.5"	*Damirat eltom*
30°.17' 58.3	14°.27' 11.1"	*Albania*
30°.18' 61.1"	14°.31' 47.2"	*Shrrshar*
30.10' 55.5"	14°.32' 19.4"	*Majlada*
30°.06' 80.5"	14°.23' 11.1"	*Umbalak*
30°.05' 72.2"	14°.19' 66.6"	*Algbshan*
30°.00' 02.7"	14°.25 22.2"	*Alagaa*
30°.13' 05.5"	13°.99' 88.8"	*Um bagshium*
30°.12' 05.5"	13°.93' 25.5"	*Elbadda*
30°.08' 55.5"	13°.90' 83.3"	*Alshigala*
30°.05' 63.8"	13°.92' 25.9"	*Umtasswa*
30°.02' 05.5"	13°.92' 47.2"	*Abu alwaan*
30°.01' 66.6"	13°.91' 38.8"	*Taybaa*
29°.87' 77.7"	14°.02' 86.1"	*Um higelga*
29°.85' 33.3	14°.00' 11.1"	*Um hajar*
29°.84 38.8"	13°.97' 19.4"	*Alrakeeb*
29°.88' 80.5"	13°.89' 13.8"	*Umgreaa*
29°.90' 33.3"	13°.83' 94.4"	*Alhaj eluen*
29°.88' 80.5"	13°.81' 66.6"	*Mushaheeda*
29°.84' 25.6"	13°.76' 83.3"	*Um sheeriti*
29°.82' 05.00"	13°.74' 30.5"	*Algabeer*
29°.80' 88.8"	13°.68' 11.1"	*Umkreeadum*
29°.85' 00.5"	13°.68' 55.5"	*Alzoom*
29°.89' 88.8"	13°.70' 08.3"	*Umnaala*
29°.95' 86.1"	13°.70' 22.2"	*Jradaua*
30°.01' 33.3"	13°.72 ' 16.6"	*Alhumaowy*

30°.11' 44.4"	13°.75' 86.1"	*Umkhrwaa*
30°.22' 41.6"	13°.82' 22.2"	*Alhamrra*
30°.14' 25.00"	14°.16' 52.7"	*Damerat abdu*
29°.99' 36.1"	13°.79' 13.8"	*Um marrad*
29°.82' 41.6"	13°.64' 08.3"	*Karraa*
29°.45'.00.0"	13°.44' 44.4"	*Umsarrea*
29°.40' 25.9"	13°.50' 94.4"	*Jub bshraa*
29°.35' 94.4"	13°.53' 16.6"	*Aldaleel*
29°.31' 55.5"	13°.62' 02.7"	*Khaliul yossif*
29°.29' 52.7"	13°.82' 25.0"	*Umgaffal*
29°.31' 16.6"	13°.89' 02.7"	*Almazrub*
29°.31' 83.3"	13°.89' 27.7"	*Um kamar*
30°.36' 75.0"	13°.70' 11.1"	*Bara*
30°.16' 583.3"	14°.03' 52.7"	*Um aood*
29°.87' 52.7"	13°.91' 08.3"	*Elzreega*

Appendix 2: Analysis of variance between sand soil in 1976, 1988 and 2003

Source of Variation	DF	SS	MS	F	P
Between sand soil Treatments	2	64.665	32.333	27.874	<0.001
Error	8524	9887.365	1.160		
Total	8526	9952.030			

Appendix 3: Analysis of variance between salt soils in 1976,1988 and 2003

Source of Variation	DF	SS	MS	F	p
Between Treatments	2	35.892	17.946	16.214	<0.001
Residual	8524	9434.644	1.107		
Total	8526	9470.536			

A**ppendix 4**: Analysis of variance between vegetation treatments in 1976, 1988 and 2003

Source of Variation	DF	SS	MS	F	P
Between Treatments	2	35.892	17.946	16.214	<0.001
Residual	8524	9434.644	1.107		
Total	8526	9470.536			

Appendix 5: Analysis of variance of shade treatment in 1976, 1988 and 2003

Source of Variation	DF	SS	MS	F	P
Between shade treatments	2	7.627	3.814	8.293	<0.001
Error	8524	3920.083	0.460	-	-
Total	8526	3927.711	-	-	-

Appendix 6: Analysis of variance of RMS in 1976,1988 and 2003

Source of Variation	DF	SS	MS	F	P
Between endmembers	2	0.00587	0.00293	0.00292	0.997
Error	8524	8549.921	1.003		
Total	8526	8549.927			

Appendix 7: Annual rainfall in North Kordofan State from 1960-2004. (IFAD 1999)

	Rainfall in mm		
Years	Bara	Elobeid	Sodari
1960	255	317	
1961	353	446.7	
1962	412	511.8	
1963	167	315.8	
1964	304	544.3	
1965	192	358.9	
1966	192.5	217.4	
1967	234.5	267.4	
1968	212	189.9	
1969	131	164.2	
1970	185	261.4	
1971	175.8	332.7	
1972	383.5	336.9	
1973	129.3	193.5	
1974	207.5	346.6	
1975	235.5	201.6	
1976	247	432.6	
1987	312	303.6	
1978	345	468.2	
1979	304	284.4	
1980	213	364.9	
1981	286	312.3	
1982	311	291.9	
1983	187	351.8	
1984	115	161.7	
1985	74	218.6	
1986	152	375.6	
1987	167	226.3	
1988	238	346	
1989	161	267.8	
1990	115	170.6	
1991	194	204.1	0
1992	167	492.8	0
1993	133	344.3	0
1994	269	543	242
1995	322	326	149
1996	180	356	169

1997	157	352	0
1998	272	315	109
1999	651	618	0
2000	266	324	190
2001	310	315	179
2002	112	216	114
2003	411	400	178
2004	281	290	82

Appendix 8: Total cultivated areas in *Bara* from 1989-2000

	Crops			
Years	millet	sorghum	seasame	groundnuts
1989	21498	0	20501	0
1990	0	0	0	0
1991	324352	11116	25550	1433
1992	81082	77326	199252	0
1993	59779	9511	108230	84368
1994	112424	130368	144597	0
1995	30374	64129	113686	0
1996	420809	135032	125222	0
1997	933381	34040	122050	0
1998	793868	17070	68678	0
1999	1192713	128751	269916	62519
2000	514790	191480	92120	13835

Appendix 9: Total cultivated areas in *Sodari* from 1989-2000

	Crops			
Years	millet	sorghum	sesame	groundnuts
1989	159285	6391	0	0
1990	0	0	0	0
1991	40222	6323	1202	0
1992	39844	40946	307	0
1993	12983	9355	3583	0
1994	580534	32278	664745	0
1995	369661	24912	3786	1800
1996	246027	20229	378	0
1997	353203	5933	0	0
1998	445761	5270	348	0
1999	49778	3305	2400	0
2000	71341	2746	0	0

(Ministry of Agriculture and Animal Wealth, 2005)